STRESS IN SEDIMENTARY BASINS SEMINAR

J. S. BELL

Geological Survey of Canada
Open File Report No. 2140

STRESS IN SEDIMENTARY BASINS SEMINAR

Text prepared for Petro Canada
May 12th, 1989.

J. S. Bell

Institute of Sedimentary and Petroleum Geology, 3303 33rd St. N.W., Calgary, Alberta T2L 2A7. Tel: 403-284-0110.

CONTENTS

* most feasible approaches to use in sedimentary basins.

FOREWORD TO OPEN FILE REPORT

These notes were prepared to accompany a seminar presented to Petro Canada over a period of three hours by J. S. Bell and P. R. Price. The seminar included exercises in deriving stress magnitudes from hydraulic fracture records and in obtaining horizontal principal stress directions from unprocessed 4-arm dipmeter logs. Examples of the exercises and the seminar schedule are included as Appendices at the end of this report.

These course notes contain some significant unpublished material. Recent improvements in methods for deriving stress magnitudes from leak-off tests are described. The new approaches give more accurate values and have been made possible by improvements in how leak-off tests are recorded and reported. Estimates of subsurface tensile strengths can also be made when appropriate data suites are available. New maps of breakout orientations in Western Canada are included, with those breakouts affecting Paleozoic rocks being separated from those measured in the Mesozoic section. In the case history section, compositing stress magnitude profiles is described, using measurements in the Garrington area of Alberta as an example. The stress regime of the Scotian Shelf is also described here in more detail than elsewhere, although a comprehensive report is being submitted for publication in the Proceedings of the "Rock at Great Depth" Symposium to be held at Pau, France, in August 1989. This latter report will also include the innovations in leak-off pressure interpretation referred to above. Because of the new information contained herein, which has not yet been formally submitted for publication, it was thought that it would be useful to release these course notes as an Open File Report at this time.

Much of the new work reported here, as well as the earlier GSC studies of stress in sedimentary basins, has been supported by funds from the Frontier Geoscience Program. This program has funded a series of contractual studies involving breakout analyses and interpretation of leak-off tests in basins in offshore Eastern Canada, that were undertaken between 1985 and 1988. I would also like to express my gratitude to many colleagues in the Geological Survey for sharing their knowledge of particular areas with me, so that the stress information could be interpreted in its geological context.

PREFACE

These course notes have been written to introduce you to the subject of in-situ stresses in sedimentary basins. I have attempted to make them "user friendly" but appreciate that, in so doing, there will be sections that will seem overly simple and naive to readers who really know what is going on and are acquainted with specific procedures. I review here some methods with which I have no first-hand experience, and I have included some unpublished material, especially on estimating stress magnitudes. Most of the latter comes from ongoing studies, and I cannot promise you that you are receiving a "preprint" of what will eventually be published. Also, I haven't concealed my opinions. Thus, there is an excellent chance that some of the things you read here will not be completely correct and will, perhaps, "benefit from a different approach"! So "Buyer beware", and please don't hesitate to point out errors or to offer better case histories. Furthermore, I would like to know if you find these notes useful and, if not, why not.

There has been a deliberate attempt to include as many Canadian examples and case histories as possible.

METHODS OF STRESS MEASUREMENT - INTRODUCTION

Many exploration and exploitation problems can benefit by being considered in the context of the physical setting of the rocks under investigation. It is now quite customary in the oil industry to be concerned about subsurface temperatures, both those of today and those that existed in the past, because it is appreciated that the thermal treatment rocks receive affects their ability to generate hydrocarbons (if they are source rocks) and their ability to retain them (if they are reservoirs). Less emphasis has been placed on the non-fluid pressure regime, in part because its role in controlling organic maturation appears to be insignificant, and also, perhaps, because stress is quite frequently thought of as something which happened in the past. Former stress regimes are assumed to have been anisotropic, that is to say, the compression in one direction was greater than in another. This is true today over most of the Earth's crust. Information on the wide occurrence of stress anisotropy has become focussed over the last decade by the large amount of research on in-situ stress that has been undertaken, much of it in North America. This has led to a renewed appreciation that how a rock behaves depends in large part on its own inherent properties and on the far field stresses to which it is subjected. Therefore, it is becoming harder to ignore the stress regime if one wishes to understand how best to explore for and exploit subsurface resources.

Measuring in-situ stress in the subsurface involves undertaking procedures which will show how much and in what direction the rocks are being squeezed. Stress at a point can be fully described by the magnitude and orientation of three orthogonal principal stresses. defined as the smallest, largest and intermediate stresses.

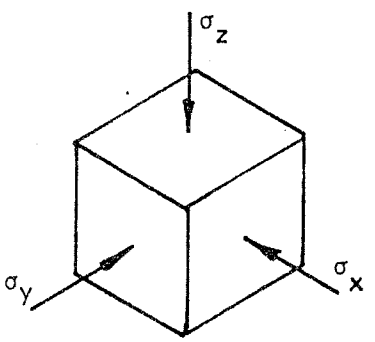

Fig. 1. Principal stress vectors acting at a point.

If a free surface is present, such as the interface between the Earth's surface and the Atmosphere, one of the principal stresses will be oriented normal to that surface. Therefore, since most sedimentary basins have essentially flat tops, one principal stress will be close to vertical in orientation. Even if there is some surface relief, at depths below several hundred metres its effect will be minimal in terms of deflecting the principal stresses, and the generalisation that one principal stress is vertical will hold. This being the case, stress analysis in sedimentary basins involves determining the magnitude of the vertical stress and the magnitudes and orientations of the two horizontal principal stresses.

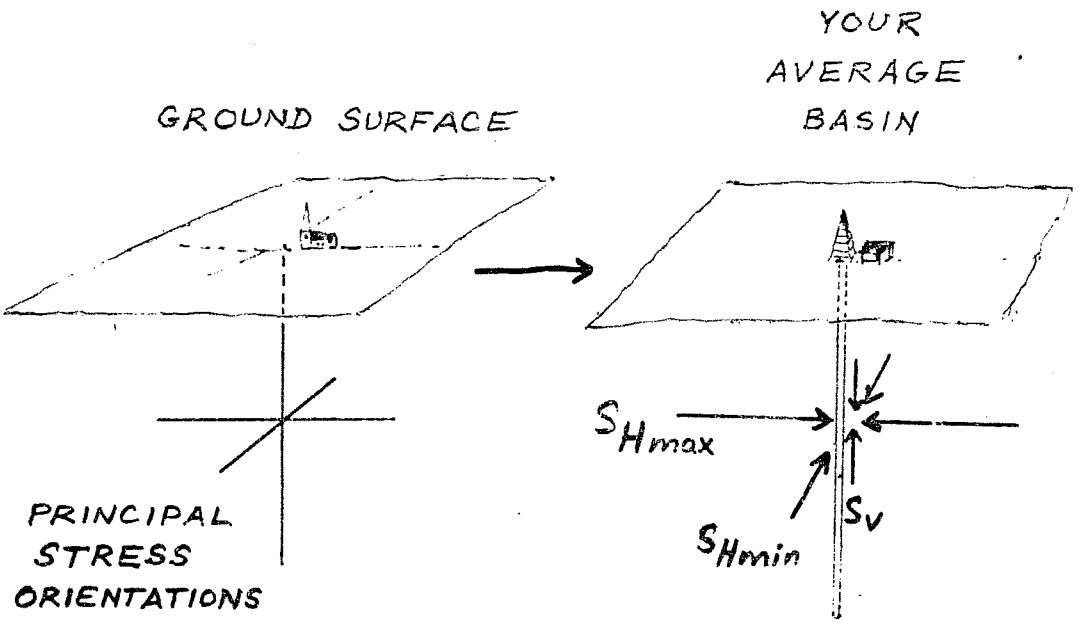

Fig. 2. Principal stress orientations in sedimentary basins.

If money and time were no object, we could undertake an elaborate array of borehole experiments to provide a three-dimensional network of information to describe the stress regime in considerable detail. In practice, we are almost always in a hurry and loath to spend any more money than we have to, so we have to compromise. What is discussed below is how this can be done reasonably quickly and cheaply. Ideally, we shall be using information already gathered for other purposes and, moreover, information that other companies probably paid for!

First, however, we will review the various methods of stress measurement which can be used in sedimentary basins.

MEASURING STRESS MAGNITUDES IN BOREHOLES

Stress measurements are very sensitive to where they are made. For example, many measurements made in mines close to excavations give a picture of the stress field that is distorted by the opening. In other words the opening itself is controlling what is being measured. Now this may be exactly what a mining engineer requires, but exploration and production geologists are usually interested in far field or "regional" stresses because they are planning activities at some distance from the point of measurement. It is, therefore, important to make a measurement, or use information, that is revealing something about the far field stress and is not just giving a local borehole response.

OVERBURDEN CALCULATION

As noted above, we assume that one of the principal stresses will be vertical and aligned with wells that have been drilled. We also assume that this vertical stress will be equal in magnitude to the weight of the overburden at the point of measurement. It could be slightly higher if a large load, such as an ice sheet, has recently been removed. Although it cannot be "proved", empirical evidence tends to suggest that large remanent stresses are best retained by crystalline rocks that have a fabric of interlocking grains. Measurements in rocks in the Canadian Shield imply that, locally, the vertical stress can exceed the calculated weight of today's overburden. However, in sediments, there appears to be much less ability to retain significant remanent stresses. The rock fabrics are such that the rocks can relax quickly once the pressures on them are reduced. Empirically, we have evidence that this occurs when we observe cores expanding and cracking after they are removed from the core barrel. In one spectacular case in my experience, a calcareous shale core recovered from several thousand metres split itself axially with such precision that the examining geologists initially assumed that it had already been slabbed! Hoek and Brown (1980) have compiled information to support the contention that Sv, the vertical principal stress, corresponds to the overburden load.

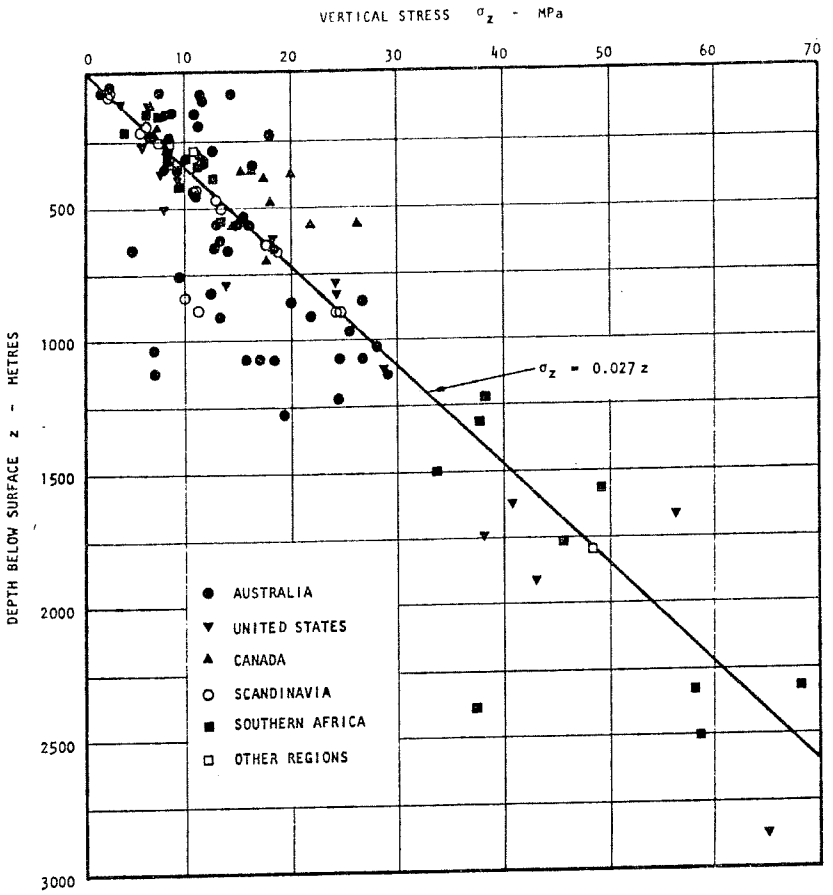

Fig. 3. Plot of vertical stresses against depth (Figure 40, from Hoek and Brown, 1980).

In the past, various mean densities have been used to estimate Sv in Western Canada. Kry and Gronseth (1982) used 2.5, McLellan (1988) integrated density logs in the Wapiti area of Alberta and found 2.43 was an appropriate figure. In reality, a mean value will not give a precise estimate since density varies vertically and, overall, increases with depth. A straightforward approach is to integrate the density log after making corrections for any thick sections of coal or evaporites (Tittman and Wahl, 1965) and after making sure that the values from heavily caved intervals are adjusted appropriately. If the logs are digitised, they can be scanned, corrected and summed mechanically. Alternatively, this can be done by hand (see Scotian Shelf case history). Whatever procedure is followed, it is likely that there will be an interval of several hundred metres, behind surface casing, which has not been logged and for which density values will have to be interpolated. This should not be a problem, since it only involves extrapolating the deeper data to the surface. In an offshore well, one would also add the weight of the seawater column.

HYDRAULIC FRACTURING

Hydraulic fracturing has proved to be a very reliable method for obtaining measurements of the magnitude and orientation of the smallest principal stress acting on rocks at significant depths in boreholes.

The method involves packing off an interval in a well, building up the fluid pressure in the borehole by surface pumping, fracturing the formation, injecting fluid into the fracture, then stopping the pumping and allowing the fracture to close and the fluid to dissipate slowly into the formation. The pressure required to just hold the fracture open is defined as the smallest principal stress, so the object of the exercise is to determine the pressure when the fracture closed. This is easier said than done. All we have are the pressure/time records, but not an independent method to check when the fracture actually closed. Figure 4 is a schematic pressure/time record of a hydraulic fracture experiment.

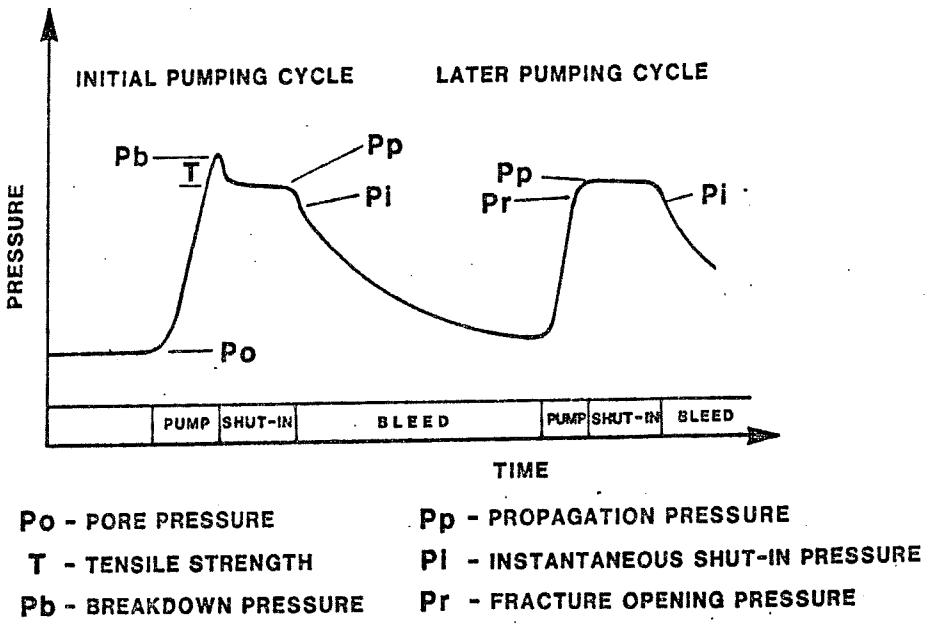

Fig. 4. Schematic Pressure/time record of a hydraulic fracture experiment.

In Figure 4, we start out with a well containing fluid at formation pressure. By pumping we increase the pressure so that it builds up across the open hole interval selected for fracturing. Initially, build up is linear and rapid. The pressure build up drops off as the formation is fractured and "breakdown" occurs. This happens

when the fluid pressure has been increased sufficiently to overcome the tensile strength of the rock and split it apart. Once this has occurred, less pressure is required to propagate the fracture so, although pumping continues, "breakdown" pressure levels are not maintained, and the fracture is advanced through the surrounding rocks at a lower pressure than was needed to initiate it. At this point pumping is terminated and a decline in pressure sets in. At first pressure drops rapidly. This is because fluid can leak away, or "bleed off", into the surrounding rock through the sides of the fracture as well as through the wall of the borehole. The pressure soon begins to decline much more slowly and this is because the fracture has now closed and the only remaining escape route for the fluid is through the borehole wall. On our idealised pressure/time record there is a clearcut change in the slope of the pressure decline curve, which marks the moment at which the fracture closed. This inflection point is known as the ISIP (Instantaneous Shut-In Pressure) and it is equated with the magnitude of the least principal stress by many investigators.

Recently, the Closure Pressure (Nolte, 1982), recognised by an inflection point slightly lower than the ISIP, has also been used by many researchers as a measure of the least principal stress. In these notes, Closure Pressure will not be discussed further, not because it may not have merit, but because using it introduces no new principles and could be confusing. Readers who want more information are referred to Nolte (1982) as well as McLennan and Roegiers (1982).

Some pressure/time records are easier to interpret than others. Very permeable rocks are not likely to have well developed inflection points simply because there is no marked change in bleed off rate as a fracture gradually closes. "Tight" formations, on the other hand, may exhibit marked differences. To reduce uncertainty, fractures are often reopened and closed several times and repeated pressure/time records obtained so that several ISIPs can be interpreted and compared. This method should produce good results. Rocks will vary in their tensile strengths and it will require higher breakdown pressures to fracture some than others, but the minimum pressure needed to hold a fracture open should be a measure of the external far field stress that is pressing on the rock.

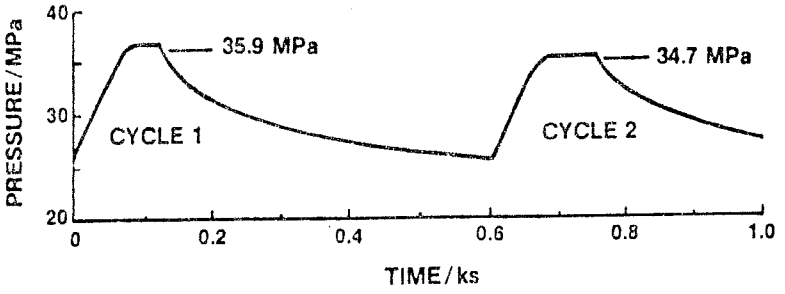

Fig. 5. Pressure/time record of opening an induced hydraulic fracture twice during stress determination in a deep gas well. The ISIPs are indicated.

In practice, fractures can be induced in a number of situations. They can be propagated from open hole at the base of a well if the lowest part is packed off. They can be initiated between packers in open hole or between packers through perforations. The "wall" conditions will probably influence the breakdown pressure magnitudes, but should not affect the pressure at which the fractures close.

The smallest principal stress magnitude at a particular depth should be compared to the corresponding vertical principal stress. In most basins, below depths of a few hundred metres, this value will be less than Sv and, therefore, the stress measured must be the smaller horizontal principal stress. The larger horizontal principal stress cannot be directly measured by hydraulic fracturing, but it can be inferred.

For homogeneous isotropic rock, Hubbert and Willis (1957) showed that:

$$SHmax = 3SHmin - Pb - Pp + T$$

where Pb is the breakdown pressure, Pp is the pore pressure and T is the tensile strength. This equation can be used for pressure data gathered during the first opening and closing of a hydraulic fracture. If the fracture is being reopened, the following relationship applies:

$$SHmax = 3SHmin - Pr - Pp$$

where Pr is the reopening pressure. This is because the rock now has zero tensile strength. In other words,

$$T = Pb - Pr .$$

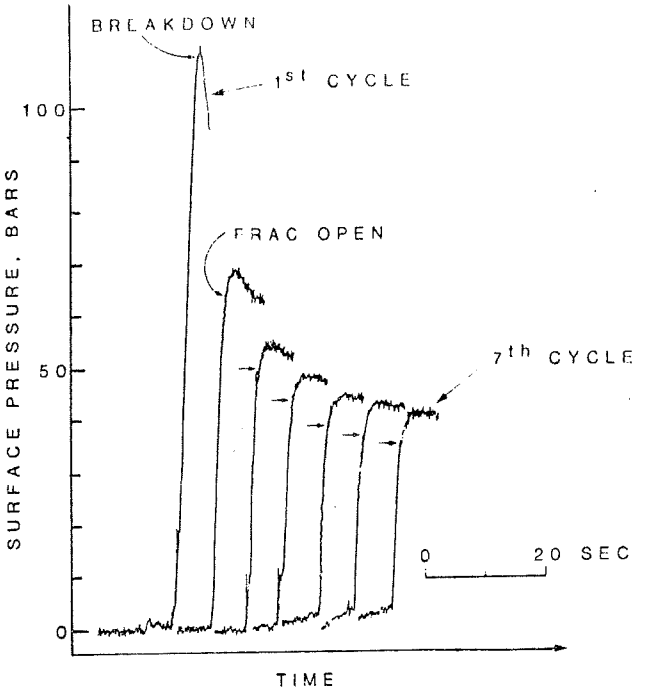

Fig. 6. The beginnings of seven fracture opening cycles performed in a well at Monticello, South Carolina. Note the decrease in opening pressure in each cycle. The difference between the breakdown pressure and the final fracture reopening pressure is a measure of the tensile strength of the rocks (from Hickman and Zoback, 1983).

It can be seen that the equation will not allow SHmax to become as large as twice the magnitude of SHmin. This is reasonable because such stress ratios could not be reached before the rock mass failed by faulting (Brace and Kohlstedt, 1980). (This is a point worth emphasising because lack of contemporary fault activity does not imply that present day stresses are not anisotropic. The quiescence is just a sign that principal stress ratios have not become great enough to cause faulting.)

ANELASTIC STRAIN RECOVERY

When cores are cut at significant depths in a well and raised to the surface they expand due to stress release. This stress release can generate micro cracks through differential expansion of adjacent grains according to Nur and Simmons (1970). The strain resulting from this stress release or, to be more precise, the relaxation of stored strain energy, generally consists of two parts: an instantaneous elastic component and a time-dependent (anelastic) component. If the time dependent component can be measured, it is possible to estimate the in-situ stress state

(Voight, 1968). However, this has to be done quickly as most of the anelastic recovery occurs within 48 hours of removing the core from the well.

Ideally, oriented cores are used and placed in a strain cell designed to measure the expansion of the core as it relaxes from its subsurface stress state to zero stress (Teufel, 1983). A record of such strain recovery is shown below. In this case, strain relief monitoring began 7 hours after the core was cut (Teufel and Warpinski, 1984).

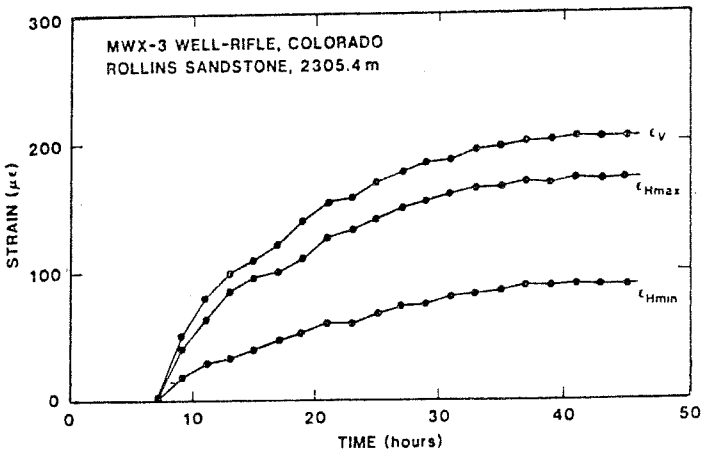

Fig. 7. Strain recovery/time curves of the temperature corrected principal strains (from Teufel and Warpinski, 1984, Fig 1).

In addition to the strain recovery measurements, mechanical properties and pore pressures of the rocks in question are needed to calculate stress magnitudes. The former can be obtained from triaxial compression tests and the latter can usually be inferred fairly precisely in oil industry wells from drilling mudweights and formation tests. Blanton (1983) and Blanton and Teufel (1983) use a viscoelastic model to calculate the principal horizontal stress from the following formulae:

$$\sigma_{Hmax} = \sigma_{Ve}\frac{(1-\nu)\Delta\epsilon_{Hmax} + \nu(\Delta\epsilon_{Hmin} + \Delta\epsilon_V)}{(1-\nu)\Delta\epsilon_V + \nu(\Delta\epsilon_{Hmax} + \Delta\epsilon_{Hmin})} + \alpha P_P$$

$$\sigma_{Hmin} = \sigma_{Ve}\frac{(1-\nu)\Delta\epsilon_{Hmin} + \nu(\Delta\epsilon_{Hmax} + \Delta\epsilon_V)}{(1-\nu)\Delta\epsilon_V + \nu(\Delta\epsilon_{Hmin} + \Delta\epsilon_{Hmax})} + \alpha P_P$$

where the principal strains are (ϵ_{Hmax}, ϵ_{Hmin}, ϵ_V, Poisson"s ratio. is (ν), the effective overburden stress, (σ_{Ve}) is the total overburden stress less the pore pressure and the pore pressure is αP_P.

This method has not been widely used in Canada. It appears to be quite promising and is not expensive to undertake. Some results have been questionable, but other users, such as McLellan (1988) at Wapiti, report results that are compatible with those obtained by other techniques.

DIFFERENTIAL STRAIN ANALYSIS

Differential strain analysis complements anelastic strain recovery. It assumes that a core expands due to the creation or enlargement of microcracks when removed from its former stress regime. These cracks will be aligned in the plane of the maximum and intermediate principal stresses. and they should be volumetrically proportional to the corresponding in-situ stress magnitude.

The method consists of artificially reversing the core expansion under hydrostatic pressure. The contraction of the rock should be proportional to the original stress exerted on it. Montgomery and Ren (1983) prepared cubes 4 cm square from oriented core samples and instrumented them with rosette strain guages as shown and the entire assemblage was placed in a flexible jacket. The specimens were then loaded into a pressure vessel and subjected to increasing hydrostatic pressure that was raised to levels of 16,000 - 18,000 psi (110.4 - 124.1 MPa) and held at such pressures until the strain guage readings stabilised. This took from 5 to 10 minutes.

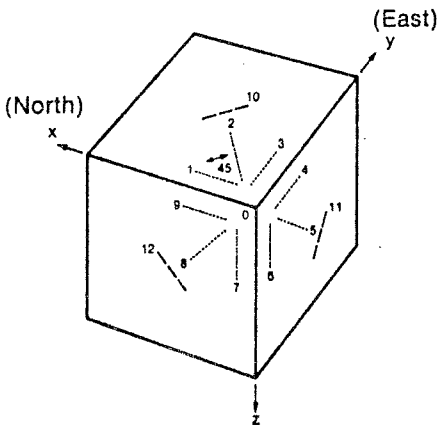

Fig. 8. Cube Guage pattern (from Montgomery and Ren, 1983, Fig 1).

The results of this particular investigation were interpreted in terms of the ratio between horizontal principal stresses rather than absolute values of their magnitudes so, in this case, an independent estimate of one horizontal principal stress magnitude would have been required.

The advantage of Differential Stress Analysis is that it can be applied to old core samples, provided they have been carefully handled. Its handicaps are the starting assumptions. If compression of the core causes the collapse of openings which were not formed during stress release, erroneous results will be obtained. In some cases, preexisting vugs have collapsed and given overestimates of former confining stress magnitudes.

Again, this is a technique which has not been widely applied. It appears to be worth using in situations where a large number of measurements can be made, especially when they can be compared to stress magnitude values obtained by other methods.

BOREHOLE HOLOGRAPHY

This is an experimental technique which is not yet available for use in boreholes. Development is presently underway, so it is summarised here from Schmitt (1989). The method uses double exposure optical holography, which is a sensitive technique for recording micron scale displacements. A holographic camera is used to record the stress relief displacement field induced by drilling a small hole (1 cm diameter) perpendicularly into a borehole wall. This is achieved by taking holographic exposures on the same piece of film before and after the hole is drilled. The film's emulsion contains two slightly different holograms that interfere with one another when the holograms are viewed. The observer sees a three-dimensional holographic image with a series of superimposed dark fringes which form an assymetric "butterfly" pattern centred on the small hole in the wall of the well. The configuration of these dark fringes is related to the magnitude and direction of the stress displacement field and can be used to determine the stresses that exist at the borehole wall by comparison with numerical simulations. The technique can also be used to measure the elastic modulus of the rocks.

Borehole holography has the capability of measuring all three of the principal stresses. This could prove enormously beneficial and it will be especially interesting to learn how close is the vertical stress to the measured weight of the overburden at various depths in wells.

LEAK-OFF TEST ANALYSIS

Leak-off tests are run during drilling to measure the maximum mud weight a well can sustain. It is essential to know this when drilling into high pressured seqwences to avoid blow outs (Dickey, 1986) The tests are run below casing. After casing has been cemented and the casing shoe drilled out, the well is deepened a few metres and the mud pressure increased by surface pumping. Pressure is built up until the formation starts to fracture and "leak-off" occurs. Pressure is built up slowly by pumping in a few barrels of mud in small increments.

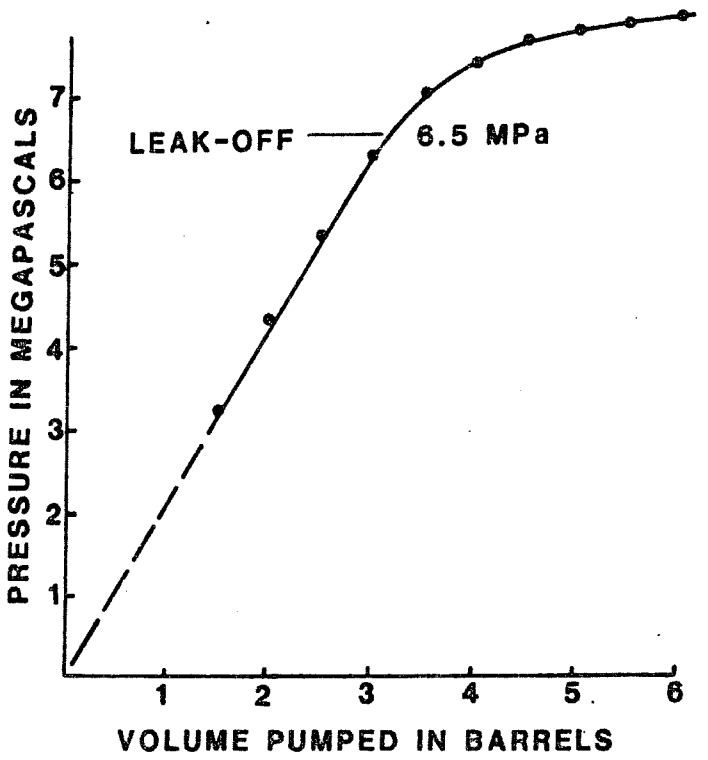

Fig. 9. Mud-volume/Pressure plot of a leak-off test run at the Hare Bay E-31 well on the Labrador Shelf.

Initially, pressure build up is linear as the mud is compressed against the casing and the open borehole wall. At the point where pressure build up ceases to be linear, leak-off is interpreted to have occurred through formation breakdown. In effect, a small fracture has been initiated in the open borehole wall. If the open interval is short, the depth at which this occurs can be well constrained. As soon as leak-off can be diagnosed, pumping ceases because the test

is designed to measure the strength of the formation, and the last result the drillers want is a formation greatly weakened by having a huge fracture propagated through it.

Usually leak-off test results are merely reported as a single pressure, though some well history reports give the actual mud volumes pumped and the corresponding pressures measured, so that one can make an independent interpretation. Very occasionally, pressure decline information is also provided. Such records are extremely interesting because they can be treated like hydraulic fracture pressure/time plots and used to infer breakdown pressures and ISIPs or smallest principal stress magnitudes.

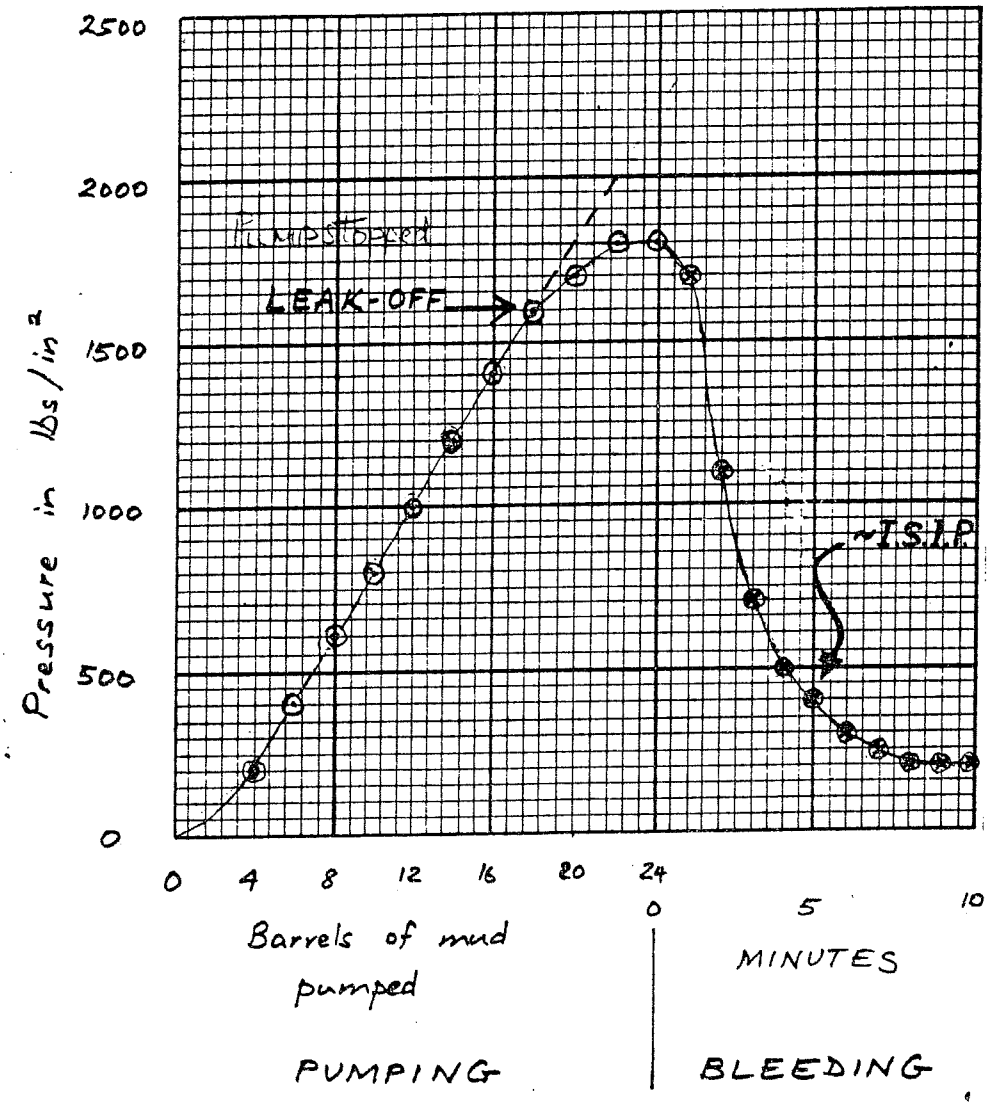

Fig. 10. Leak-off test record from well 4-29-45-14W5, Alberta (obtained from the ERCB).

Figure 10 is a record of pumping and bleed-off for a leak-off test run over an 8 metre open interval below surface casing at 246.5 metres below ground surface. Leak-off occurred at a surface pump pressure of 1600 psi. Pressure decline was initially rapid but the pressure began to decrease much more slowly at some point between 3 and 6 minutes after bleed off started. If we interpret the inflection point at 5 minutes and 400 psi, this means that the ISIP, or least principal stress, is 400 psi (2.76 MPa) greater than the mudweight pressure. The mud pressure gradient was 9.9 kPa/m, which at a depth of 251m K.B., amounts to a bottomhole pressure of 2.48 MPa. Thus the least principal stress at that depth calculates as 5.24 MPa corresponding to a gradient of 21.3 kPa/m. Since this is less than the overburden gradient, the figure represents the smaller horizontal principal stress.

The significance of this particular test is the very large difference between the leak-off pressure and the inferred ISIP. The former occurred at a surface pressure of 1600 psi (11.03 MPa) , or a sub casing shoe pressure of 13.51 MPa, which corresponds to a gradient of 53.8 kPa/m! Breakdown pressure was very much greater than fracture closing pressure in this case, and it illustrates how high the tensile strength was for this particular rock interval. (It is even possible that the cement was never properly drilled out and the test measured the tensile strength of the cemented formation!).

Figure 11 illustrates a similar record of a leak-off test run to test a shale interval below 2653 m depth in the Glooscap C-63 well on the Scotian Shelf. Leak-off occurs at a surface pressure of 3140 psi which, once mud pressure is added, gives a downhole leak-off pressure of 48.2 MPa. The bleed-off pressure decline record exhibits a marked change in rate at 2940 psi surface pressure which, at depth, corresponds to 46.9 MPa, not a great deal less than the leak-off pressure. In fact, the latter is only 2.8% greater than the inferred ISIP that, in this case, is the smaller horizontal principal stress.

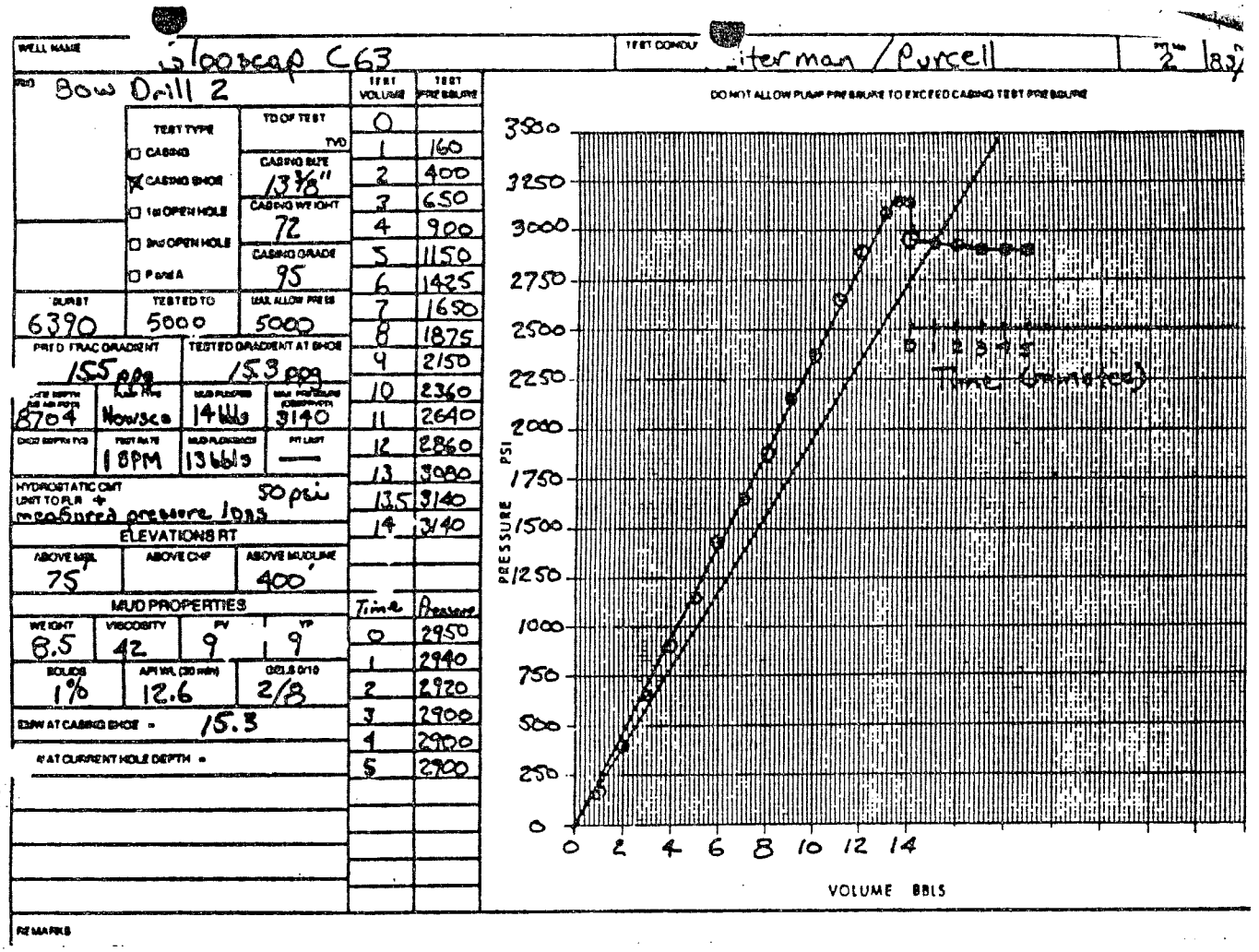

Fig. 11. Glooscap C-63 Leak-off Test run below casing at 2653 m. K.B.

This example indicates that, where tensile strengths are low, leak-off tests can give a close estimate of the magnitude of the smaller horizontal principal stress. Assuming the leak-off test is giving us the breakdown pressure required to initiate a fracture, it is clear that this will always be greater than the minimum stress required to hold the same fracture open. However, if the tensile strength is negligible or zero (as with a rock containing preexisting cracks), the breakdown pressure will not be very much larger than the fracture closing pressure. Breckels and Van Eekelen (1981) showed this empirically when they compared leak-off pressures to ISIPs derived from hydraulic fractures in wells in the Gulf Coast. When plotted against depth the "lower-bound" leak-off data coincided with the hydraulic fracturing data (Fig. 12).

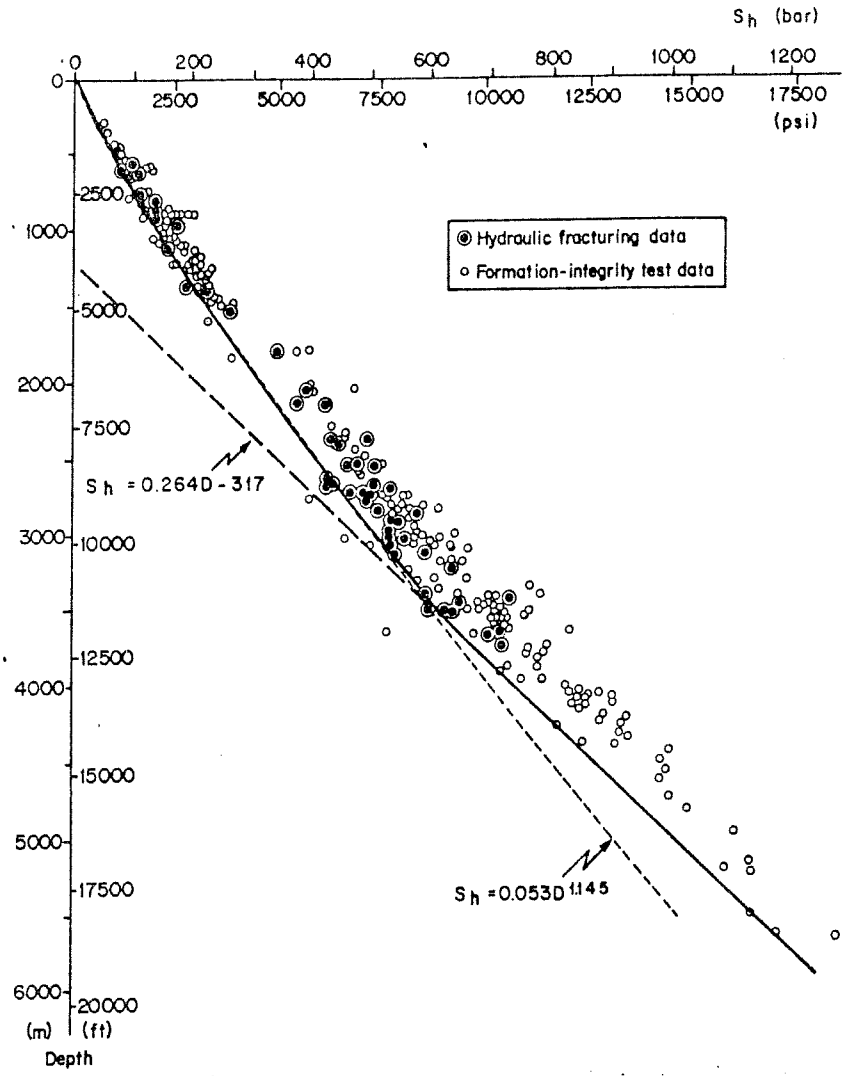

Fig. 12. Minimum horizontal stress versus depth in the U. S. Gulf Coast (from Breckels and Van Eekelen, 1981, Fig. 2). Note the coincidence of the "lower bound" leak-off pressures (here called Formation Integrity Tests) and the ISIPs determined by hydraulic fracturing.

From this, one can conclude that leak-off pressures can be used to constrain estimates of the least principal stress (usually horizontal), but that it is advisable to have enough test results to be able to identify the population with the lowest values and to use these to infer stress magnitudes. The problem is that you will never know whether the higher pressures in a population are being measured in rocks with zero tensile strength and, thus, giving a reasonable estimate of stress magnitude, but one can be reasonably sure that the low values come from rocks of minimal strength. Experience suggests that this is generally true for clastics, but not always for carbonates.

In certain instances one can estimate tensile strength, if repetitive leak-off tests are run over the same interval. An example of such tests comes from the Venture B-43 well, drilled by Mobil on the Scotian Shelf (Ervine and Bell, 1987).

Test	Open interval	Leak-off Pressure
1	1.0m	103.4 MPa
2	58.0m	101.7 MPa
3	113.0m	100.5 MPa
4	152.0m	100.5 MPa

Table 1. Sequential leak-off tests run in Venture B-43 below casing set at 4781m K.B. (obtained from well history report).

The tests were run below casing at a depth of 4781m with successive open intervals of 1m, 58m, 113m and 152m. We assume that in each case the leak-off test opened the same fracture. For the first test, 103.4 MPa was required for leak-off. This dropped to 101.7 for the second test and for tests 3 and 4, which were presumably reopening an established fracture, only 100.5 MPa pressure was needed to promote leak-off. We have a case here of the initial breakdown pressure of the first test being followed by reopening pressures 2.9 MP lower. That difference is believed to represent the tensile strength of the shale below casing. This type of information is not often available, but it does support the thesis that tensile strengths of clastic rocks, particularly shales, can be very low.

We have seen that leak-off tests can give good estimates of the least principal stress and that this is usually the smaller horizontal principal stress in sedimentary basins. We can obtain the vertical principal stress from density logs; what about the larger horizontal principal stress?

Bredehoeft et al. (1976) showed that, for isotropic rocks:

SHmax = 3(SHmin) - Reopening pressure - Pore pressure

This equation can be used when more than one leak-off test has been run below the same casing shoe and pressure decline has been recorded as shown in Fig. 11. The West Chebucto K-20 well on the Scotian Shelf had two leak-off tests run below casing at 3822.2 m K. B. The first test gave the following results:

Pore Pressure:	38.9 MPa (from a Repeat Formation Test)
Leak-off Pressure:	69.1 MPa (interpreted from a pressure build up record as in Fig. 11)
I. S. I. P.	62.6 MPa (interpreted from a pressure decline record as in Fig. 11)

A second test was run with 1305.8 m of open hole. Leak-off occurred at 67.1 MPa. Assuming the same fracture was opened, this value can be interpreted as a fracture reopening pressure, so that:

SHmax = 3(62.6) - 67.1 - 38.9, which amounts to <u>81.8 MPa.</u>

Ideally, it would have been better if the second leak-off test had been run with a far shorter open hole interval, so that one could be that much surer that the same fracture had been opened on both occasions. Nevertheless, this approach is the best way to get reliable SHmax estimates from leak-off pressure records.

If a second leak-off test was not run, but the single test has a suitable pressure decline record, the next best approach is to substitute the leak-off pressure itself for the reopening pressure, as follows:

SHmax = 3(ISIP) - Leak-off Pressure - Pore Pressure

This equation will underestimate SHmax, especially if the rock interval has significant tensile strength, but it is likely to give reasonable results for shales.

If there is no pressure decline record available, and all that has been reported is a leak-off pressure, we can make the simplifying assumption that the leak-off pressure is of similar magnitude to the reopening pressure and the instantaneous shut in pressure for rocks with minimal tensile strengths, so that the Bredehoeft at al. (1976) relationship becomes:

SHmax = 2(Leak-Off Pressure) - Pore Pressure.

This equation offers a means of making a crude estimate of the magnitude of the larger horizontal principal stress (Ervine and Bell, 1987). Since the leak-off pressure will inevitably be larger than the smaller horizontal principal stress, it will overestimate SHmax. This overestimation can, however, be reduced by using the lowest reliable leak-off pressure of a series, if more than one test has been conducted below the same casing shoe. In other words, the relationship is:

SHmax = 2(lowest Leak-off Pressure of a series) - Pore Pressure.

In many cases, these latter two equations offer the only way of estimating SHmax. However, the results may may be accurate enough to determine the ratio between the three principal stresses, as discussed later in the Scotian Shelf stress regime case history.

BOREHOLE BREAKOUT SHAPE

Now that breakout shape can be recorded fairly accurately, at least in terms of surface morphology, by borehole televiewers there is considerable incentive to see if they will yield information on stress magnitudes. Hydraulic fracturing is expensive and setting packers to contain the high pressures required at great depth is extremely difficult, so any method which promises reliable results from passive measurements by logging tools is obviously worth trying to develop. So far this has not occurred, although Zoback et al. (1985) suggested it might be possible to estimate the ratio between the horizontal principal stresses from measurements of breakout radius and depth. Their analysis was based on modelling breakouts as single-cycle phenomena, whereas they must be self-propagating to some extent, and it also suffered from our current inability to determine whether or not a breakout has completely caved. However, this was a first attempt and refined attacks on the problem are underway. For more information, readers should consult Zoback et al. (1985) and read Haimson and Herrick (1986).

3. MEASURING STRESS DIRECTIONS

HYDRAULIC FRACTURING

A hydraulic fracture will expand the rock in a direction perpendicular to the direction of least compression (smallest principal stress) and will therefore extend within the plane formed by the largest and the intermediate principal stresses (Hubbert and

Willis, 1957). Therefore, if we can measure the direction of a fracture, we can obtain the orientation of the least principal stress and the plane in which the other two stresses lie. There are various ways of doing this. The most widely used is the oriented impression packer that is inflated against a borehole wall after fracturing to obtain a physical impression of the crack and to record its orientation. Another approach is to scan the fractured interval with a borehole televiewer to identify the newly created fracture and establish its orientation.

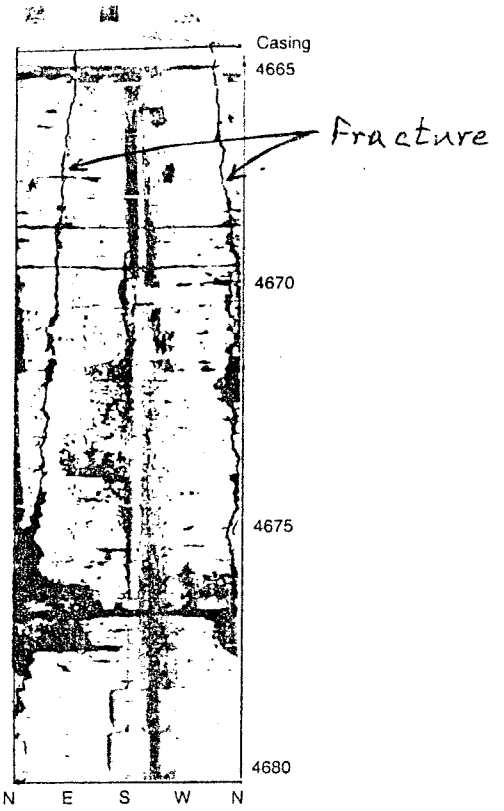

Fig. 13. BHTV record of an induced hydraulic fracture (from Wiley, 1981).

Alternatively, the job could be done with a formation microscanner. In addition, it is possible to recover the fracture itself! Daneshy et al. (1986) have described inducing hydraulic fractures at the bottom of wells by packing off the basal drilled interval and increasing the mud pressure. This induces a fracture, opens it and fills it up with mud. An oriented core is subsequently recovered containing the fracture, which can easily be identified because it will be lined with drilling mud!

All these methods assume that the fracture leaves the well at the same angle at which it propagates into the surrounding rock. This need not be the case, especially if the stress field immediately around the well differs from the far-field regime. There are some spectacular examples of such situations. Interested readers should examine Gronseth and Kry's (1987) description of fracturing at Norman Wells, where vertically-oriented fractures split off from a well and became horizontal once they had extended beyond its influence.

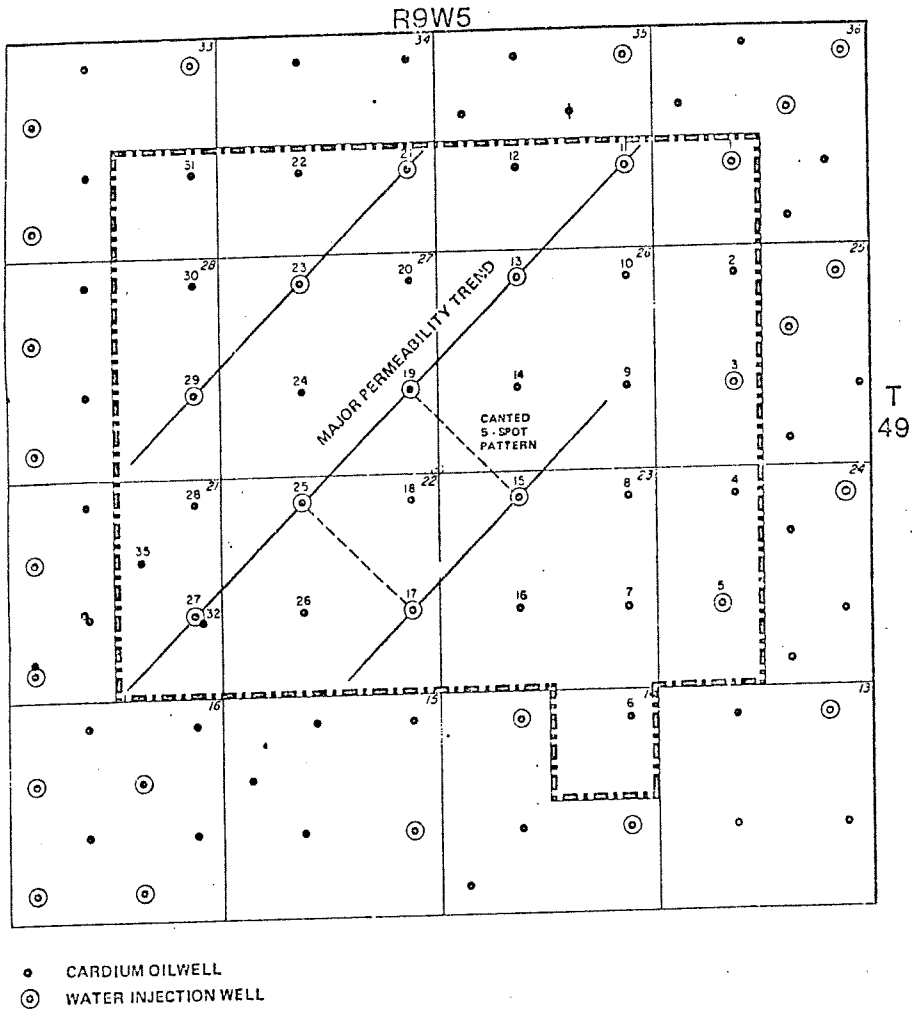

Fig. 14. NE-SW "permeability trend"(direction of induced hydraulic fractures) produced by waterflooding the Pembina J lease (from McLeod, 1977).

To be sure of determining a fracture's orientation you need to be able to map the fracture. This can be done either by tracking it or by monitoring some effect related to its propagation. In waterflooding operations, hydraulic fractures can be induced and their extent and direction can be followed when water injected in one well flows out of another. This happened in the Cardium Sandstone in the Pembina Field in Western Canada (McLeod, 1977; Hassan, 1982). Some of the early waterfloods were injected at pressures well above the fracture gradient (and even, in some cases, above the overburden gradient!), with the result that wells NE and SW of the injection wells watered out rather rapidly and a "preferred permeability" was established that limited the recovery of oil. NE-SW trending hydraulic fractures had been induced in the direction of the larger horizontal principal stress and perpendicular to the smaller horizontal principal stress, and these could be mapped by the fluid connections.

Some of the operators of heavy oil and tar sand properties have induced fractures by injecting hot fluids under pressure and then have attempted to map the fractures by temperature logging adjacent wells. Depending on the level of control, this can be effective. Fracture advancement has also been monitored seismically. In recent years, tiltmeter arrays have been used to map fractures (Wood, 1978). The theory is that the induced fracture will deflect the ground surface by a very small amount and that, if this deflection can be mapped precisely, the orientation and extent of the fracture can be documented. While all of this is not always possible, tiltmeter arrays appear to be capable of identifying fracture directions quite well, although the procedure can be costly.

A commercial fracture identification log is available which derives its data from the 4-arm dipmeter tool (Brown, 1979). It uses breakout criteria to identify fractured zones, which is probably not justified, and confirms the presence of fractures by resistivity anisotropy, which may be justified. In favourable situations, it is claimed that the log will identify the quadrant cut by the fracture, so it could.represent a crude method of obtaining stress orientation data. I am not aware of any systematic attempts to derive induced fracture orientations from these logs in this way, so I cannot advise on how worthwhile such an approach might be.

In conclusion, induced fracture orientations are good indicators of in-situ stress directions, but the more information one has the more reliable the interpretation is likely to be.

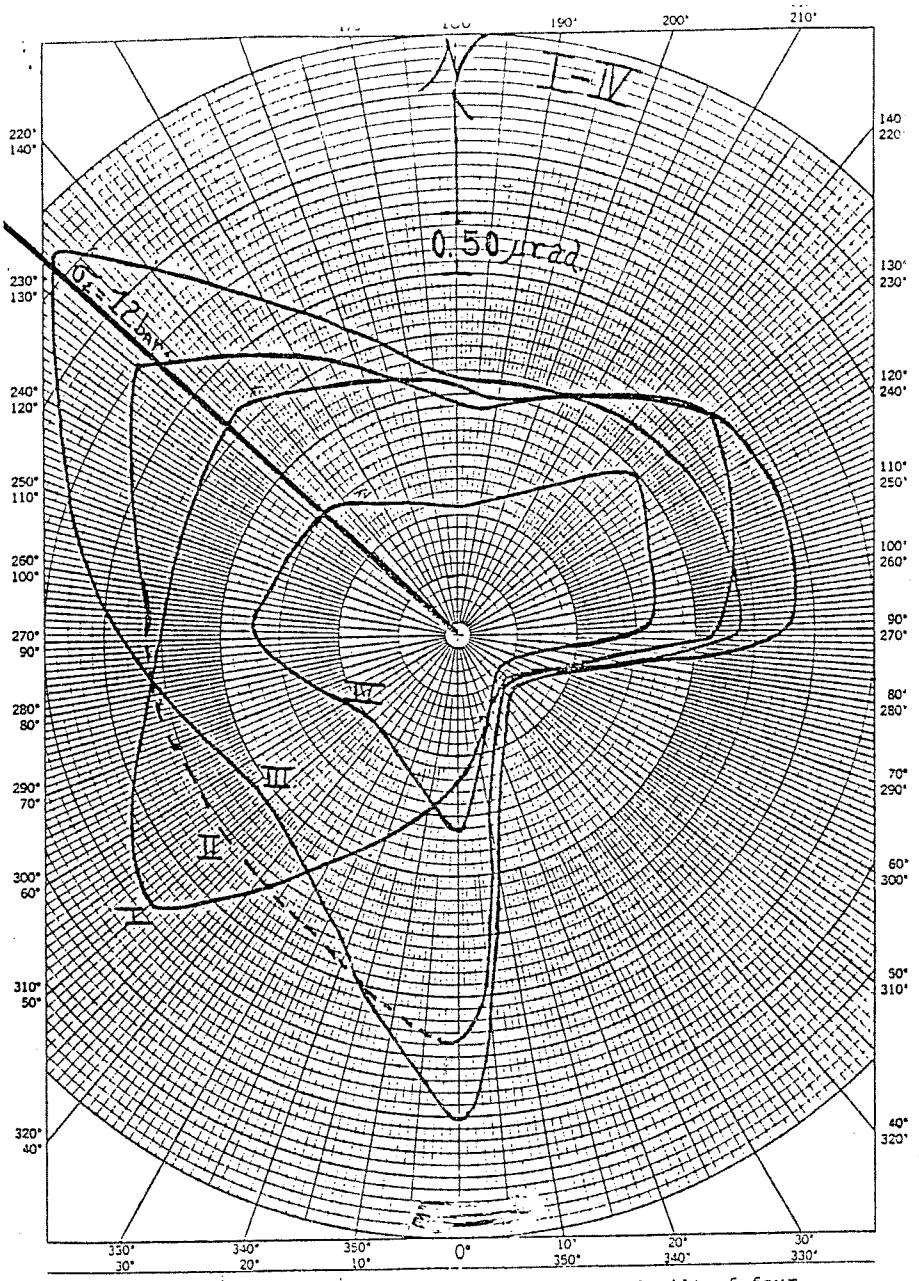

FIGURE 13 - Composite plot of the recorded tilt of four horizontal hydraulic fractures.

Fig. 15. Tiltmeter maps made of ground warping caused by four hydraulic fractures (from Wood, 1978).

ANELASTIC STRAIN RECOVERY

Anelastic strain recovery appears to be quite a good reconnaissance method for obtaining principal stress orientations. When oriented cores are placed in a strain cell, the direction of greatest expansion will correspond to the larger horizontal principal stress axis. McLellan (1988) obtained a large spread of azimuth values (N11E-N48E) from 5 samples in a well in the Wapiti area. The mean stress orientation was within 5 degrees of directions obtained by other methods. Other investigators have obtained more consistent results, but anelastic strain recovery does not appear to be capable of giving very precise stress directions at this stage of its development. However, it is relatively cheap and easy to do at a wellsite and could provide useful information in sections where other indicators cannot be measured.

DIFFERENTIAL STRAIN ANALYSIS

Much the same comments can be made about Differential Strain Analysis. An oriented core is presumed to contract most in the direction it expanded most, namely the direction of the largest principal stress. Results on oriented samples cut from oriented cores tend to be rather variable McLellan (op. cit.) obtained an azimuth range of N10E-N55E from 6 samples from a well in the Wapiti area. Montgomery and Ren (1983) measured an even larger scatter (N81E to N35W) on eight samples from a well in the Caroline area. Again, if nothing better is available, it looks as though differential strain analysis could give a gross idea of stress directions.

As mentioned earlier, the technique can be used on oriented cores that have been collected previously, so it should be considered if stress orientation information is required in an area for which such samples are available. One problem in Alberta is that, although the ERCB Core Storage Facility records oriented cores in their data files (and scribe lines can be identified on them), the actual records of orientation are currently kept by the operators. In other words, for oriented cores, the orientations are not publically available.

BOREHOLE BREAKOUTS

In the last ten years, borehole breakouts have emerged as the single most accurate indicator of far field. stress orientations.in sedimentary basins.

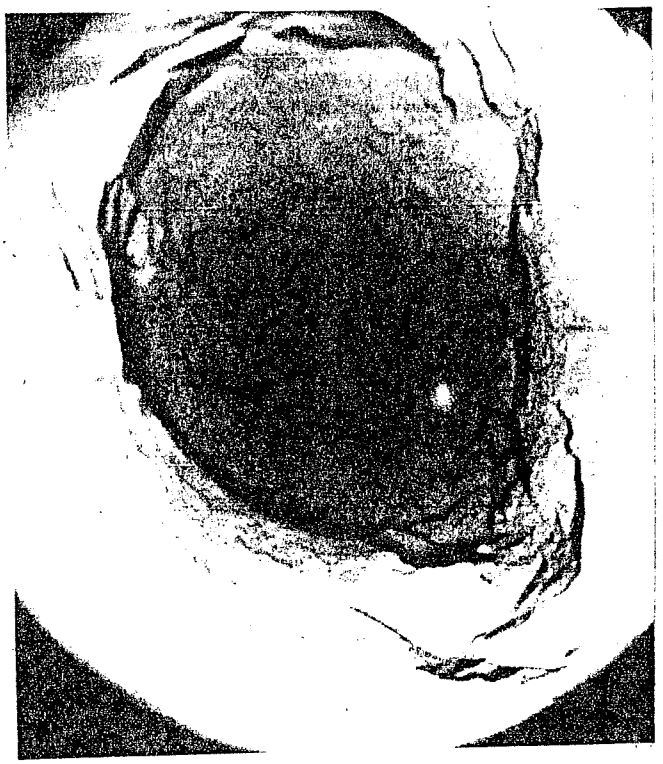

Fig. 16. A breakout zone in tuff at the Nevada Test Site, U. S. A. A downhole view (photograph provided by J. E. Stringer).

When a borehole is drilled through stressed rock, the stresses are amplified around the borehole wall to levels which may exceed the cohesive strength of the rock. If this occurs shear fractures are formed and the sides of the borehole can fall away. This is the basic cause of caving. If stresses are isotropic in the plane normal to the direction of the borehole, in other words if the two horizontal principal stresses are of the same magnitude , the far-field stresses will be doubled all round the borehole wall. Should this doubling exceed the rock strength, fractures will form and caving may occur, but it will be evenly distributed around the hole wall and simply enlarge the hole evenly in all directions.

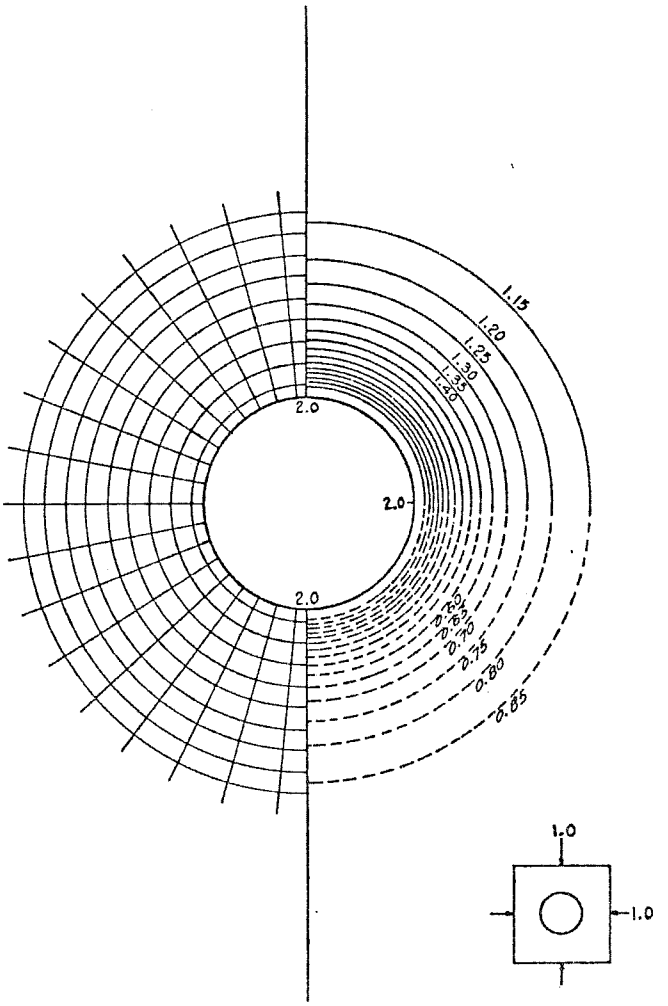

Fig. 17. Stress amplification around a borehole where SH=Sh. The stress magnitude is doubled all around the hole wall (from Hoek and Brown, 1980).

On the other hand, if the horizontal principal stresses are not equal, stress amplification will be greater on some parts of the borehole wall than on others. The greatest tangential stresses will be exerted on the side of the borehole wall that coincides with the axis of the smaller horizontal principal stress (Fig. 18).

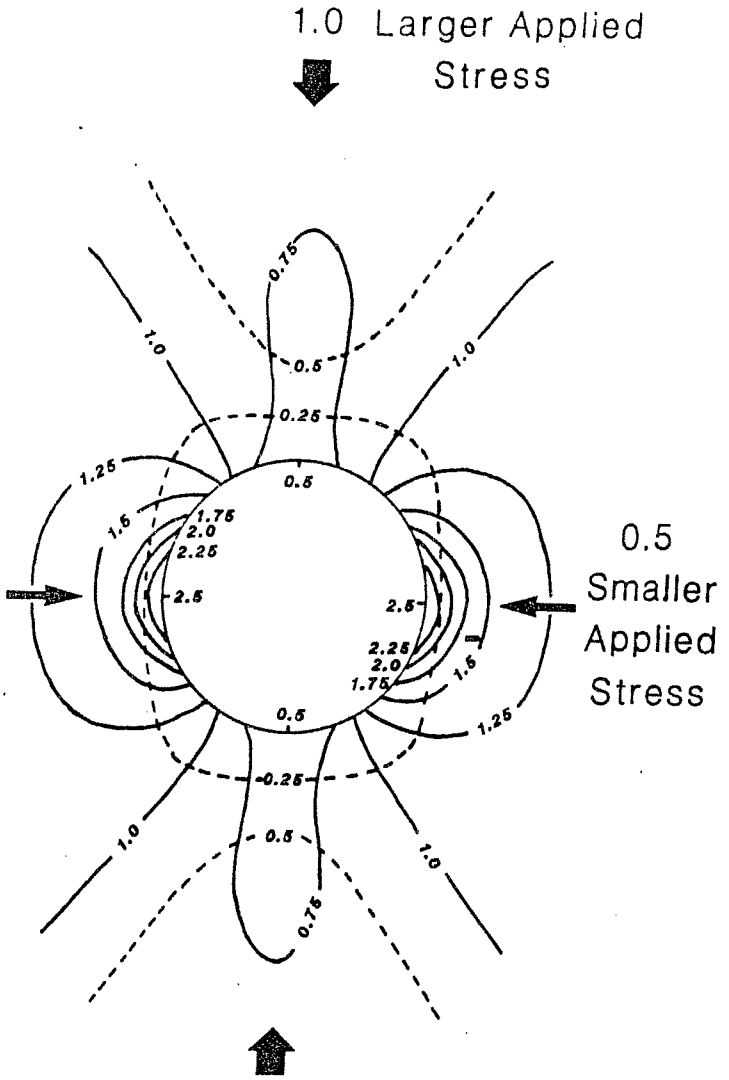

Fig. 18. Stress amplification around an anisotropically stressed borehole , where the far field stress ratio is 1 : 0.5 , derived from Hoek and Brown (1980). Note how the contrast in principal stress magnitudes varies areally around the hole. Shear fractures are most likely to occur where this is greatest, within the lunate arcs bounded by SHmax amplifications of 2.

As a result, tangential shear fractures will occur more extensively there and the borehole will tend to cave unevenly. Caving will produce boreholes with semi-elliptical cross sections with the long axes oriented parallel to SHmin. A map of stress amplification around an anisotropically stressed borehole shows where the stress contrast is greatest and thus where shear failure is most likely.

As will be discussed later, in the section on borehole stability, breakout size is a function of stress contrast and rock strength. There are also certain situations when breakouts occur with their long axes aligned with the larger horizontal principal stress (Woodland, 1987), but these are encountered rarely, so will not be discussed here.

The best way to study breakouts and map their orientations is to identify them with the borehole televiewer. Unrolled 360 degree borehole wall images illustrate them well.

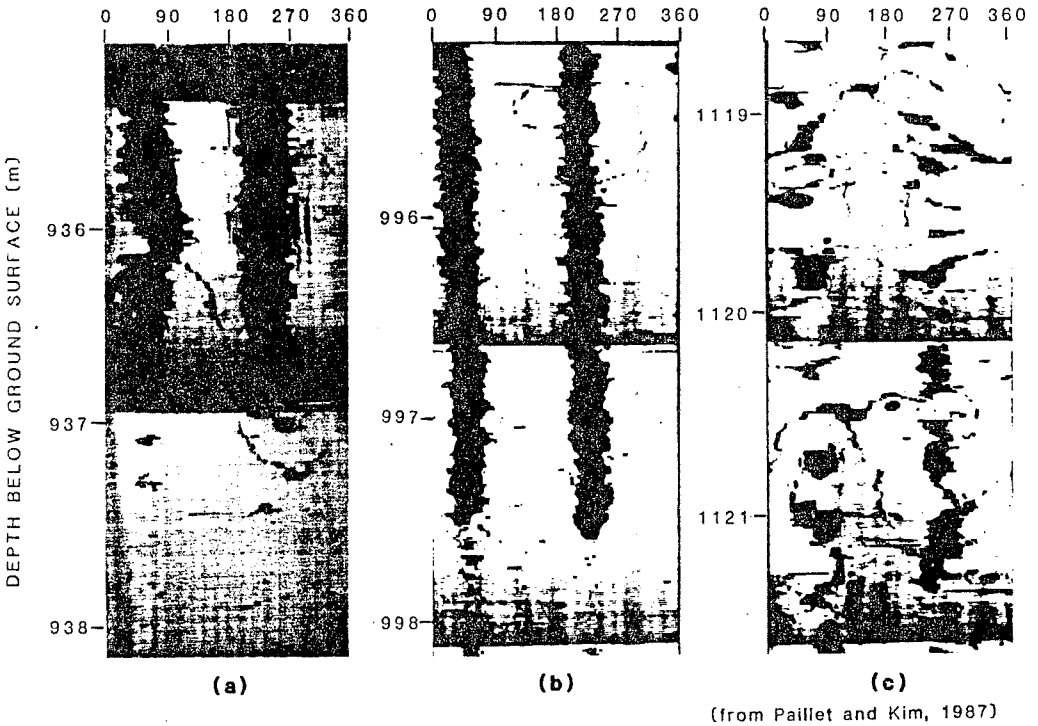

Fig. 19. Borehole televiewer images of (a, b) continuous and (c) discontinuous breakouts published by Paillet and Kim (1987). The breakouts occur in Columbia River basalts in Washington State, U. S. A. Image (a) also contains a sinusoidal trace of a steeply dipping natural fracture which crosses the wellbore at right angles to the long axis of the breakout.

"Wedding ring" printouts of borehole circumferences, created by superimposing the traces of several televiewer passes, also give a good picture of the breakout shape and orientation.

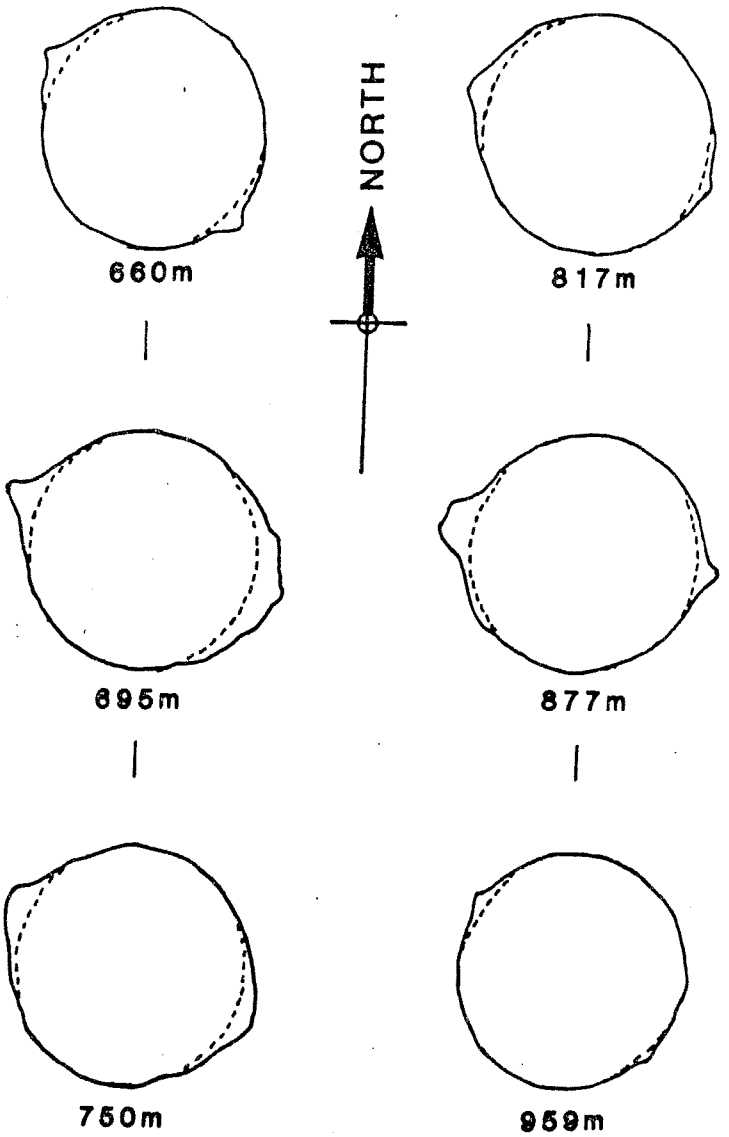

(from Newmark and others, 1984)

Fig. 20. Cross sectional images of borehole breakouts in basalts identified in DSDP hole 504B by the borehole televiewer (from Newmark et al. (1984). These cross sections were created by superimposing several borehole circumference images.

Another way of illustrating breakout morphology in three dimensions is with simulations of interior molds of boreholes.

For most hard-pressed explorationists such luxury isn't an option, because borehole televiewers are very expensive and slow to run. Formation microscanners give almost as much information and can be raised up a hole as fast as a 4-arm dipmeter tool (c. 10m/minute), but have only become widely available recently. They are the tool of the future for breakout analysis.

Fortunately, the 4-arm dipmeter tool is excellent at identifying breakouts and measuring the orientation of their long axes. These tools have been around since the late sixties and have been used to log thousands of wells in Canada. In the early days, there were only two log formats: the well-known "tadpole" plot giving the dip and strike of the beds, and a rather "busy" log with all the resistivity curves and tool orientation, hole drift information and caliper extension. This "busy" log contains all the breakout information we need, namely, where are the elliptically caved intervals and how are they oriented?

Fig. 21 shows a section of the uncomputed 4-arm dipmeter log run in Paleozoic carbonates in the Nairb Pembina 1-9-50-12W5 well. in the West Pembina area of Alberta. A breakout interval occurs between depths of 9418 ft and 9527 ft. Between these depths the two pairs of calipers are differentially extended. Calipers 1 and 3, shown by the dotted line, record a borehole diameter just over 9 inches, slightly greater than bit size (8.75 inches given in the log header). Calipers 2 and 4, shown by the solid line, record a variable.borehole diameter ranging from 10 to to 11 inches. The borehole is non-circular, probably semi-elliptical, and the largest diameter is parallel to calipers 2 and 4. Below 9527 ft. the extension of both sets of calipers is approximately the same, showing that there the hole is circular. Note that the orientation record for Caliper 1, labelled the No. 1 electrode, shows that the dipmeter tool was rotating clockwise as it was pulled up the well until it reached a depth of 9527ft. At this depth, tool rotation ceased and remained constant at an azimuth of approximately 200 degrees until the tool reached 9418 ft, at which depth rotation resumed. What happened is that the 2 and 4 calipers became trapped in the elliptically oriented breakout, so the torque on the tool cable was no longer able to make the dipmeter rotate as it was pulled up the well. These are the two basic diagnostic features of breakouts: differential caliper extension combined with a cessation of tool

rotation. To obtain the orientation of this breakout interval, we take the 200° for the 2-4 caliper direction, add 25° (Magnetic Declination is +25° , recorded on the log header), subtract 90° (because the trapped calipers were 2 and 4, whereas the 200° azimuth refers to Caliper 1). This gives us 135° , the orientation of the smaller horizontal principal stress.

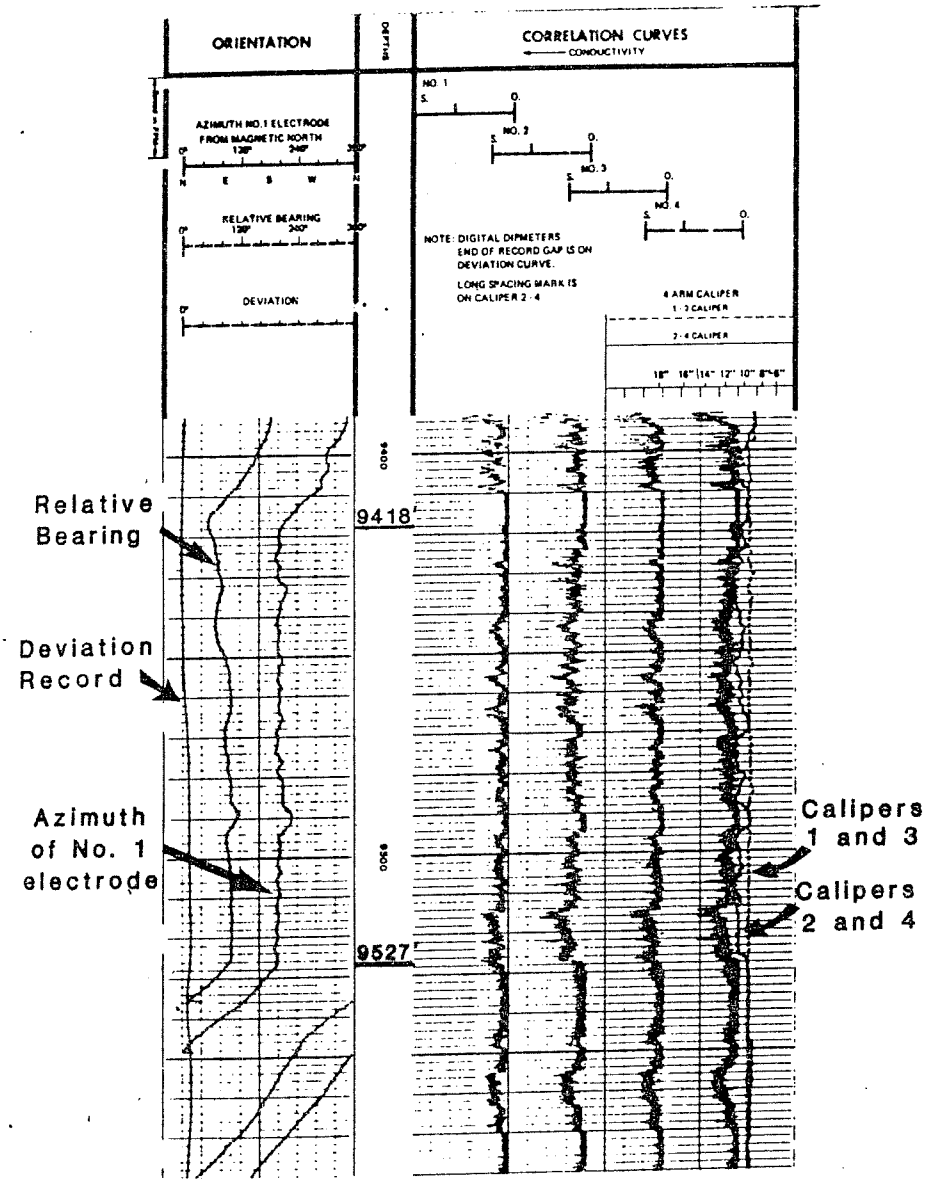

Fig. 21. Unprocessed data display of a section of a low angle four-arm dipmeter log run in the Nairb 1-9-50-12W5 well in Alberta. Interpretation is explained in the text.

This is the simplest format of dipmeter log to analyse for breakouts. If a precise stress orientation is required, it is worth

measuring as many breakouts as possible and measuring each of them at successive intervals. These readings are then averaged. Mardia's (1972) vector mean method is the most rigorous, but arithmetic means are quite adequate and do not give results more than 1% different. One can hardly expect to read the dipmeter log infallibly to the nearest degree, and the calipers are not going to nestle into the breakout so as to give a perfect long axis orientation every time!

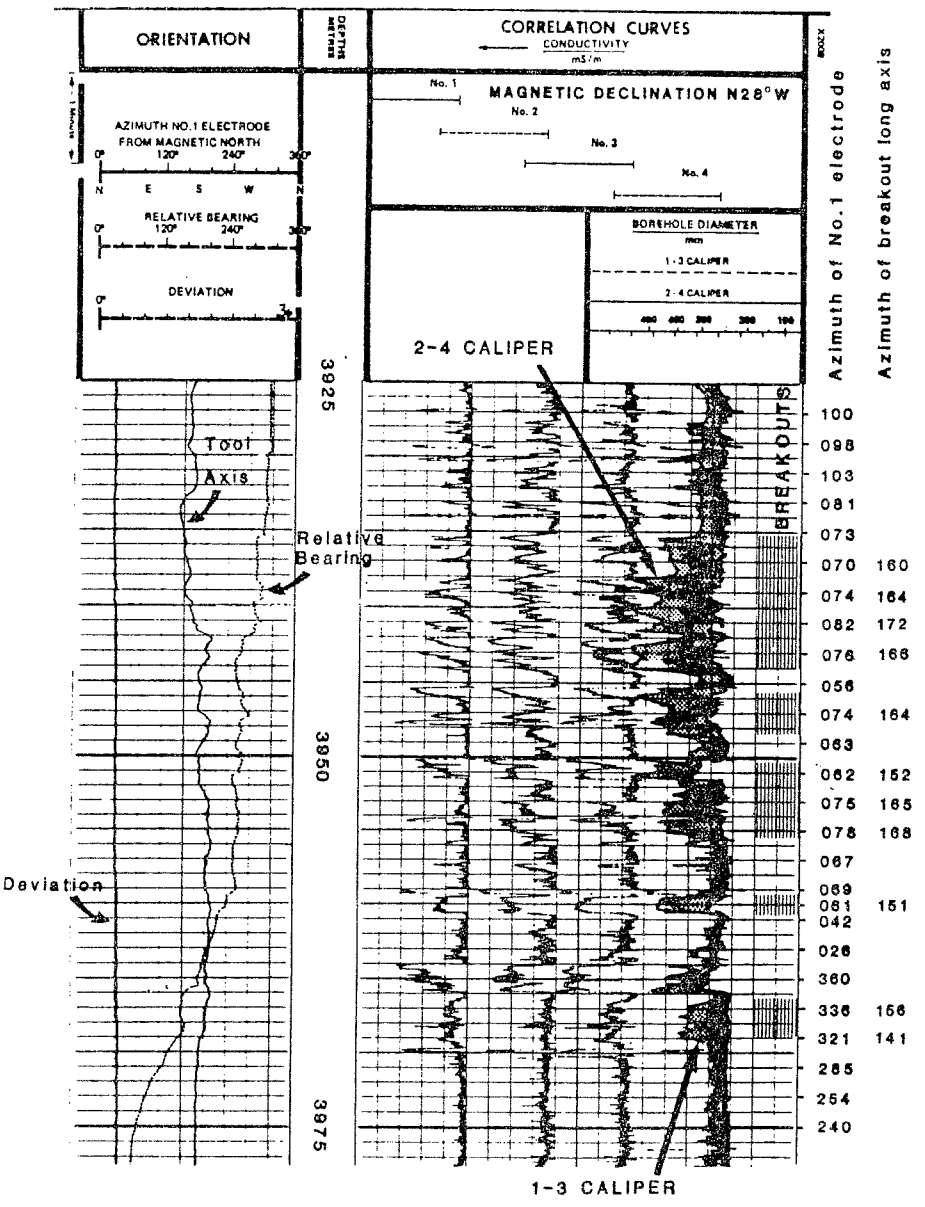

Fig. 22. Section of a typical unprocessed data display of a high angle four-arm dipmeter log. The azimuth of Caliper No. 1 is obtained by summing the angles recorded for the tool axis and the relative bearing and then correcting for magnetic declination.

There are other dipmeter formats. The format for tools fitted with wide-angle inclinometers is compared in Fig. 22 and its interpretation summarised in the caption. It is tedious to analyse by hand and is much better handled by computer with digitised logs. Breakout data can also.be found on Directional Logs, Borehole Geometry Logs, Cement Volume Logs and other variously titled outputs of dipmeter logs. At the present time, no logging company is offering digitally processed breakout analyses, though the software is available (Brereton and Evans, 1987). Data can be summarised in various ways. Some authors favour rosettes, others simply map mean azimuths.

The great advantage in using breakouts to map contemporary in-situ horizontal principal stresses is that there is a lot of free data available which does not take long to process. A remarkably informative map can be made quickly in areas where many logs are available. The Frontier basins of Canada, except on the West Coast, are full of wells in which 4-arm dipmeters have been run.

ELASTIC DEFORMATION OF BOREHOLES

Borehole televiewer records have shown that unequal horizontal stresses can squeeze some wells so that they become very slightly elliptical in cross section. The distortion is very small, the difference in opposite diameters being less than a millimetre, but the orientation is consistent and, in some cases, the shorter diameter coicides with hydraulic fracture traces on the borehole wall. This elastic deformation appears to be real, but is probably feasible to measure only in boreholes drilled through strong, relatively homogeneous, rocks that resist caving or breaking out. To my knowledge, no publications have yet described stress orientations that were obtained in this way.

STONELEY WAVE POLARISATION

It has been observed recently that horizontal particle motions recorded from three-component vertical seismic profile experiments are polarised in the direction of SHmax. Barton and Zoback (I986) have reported this phenomenon in three wells.

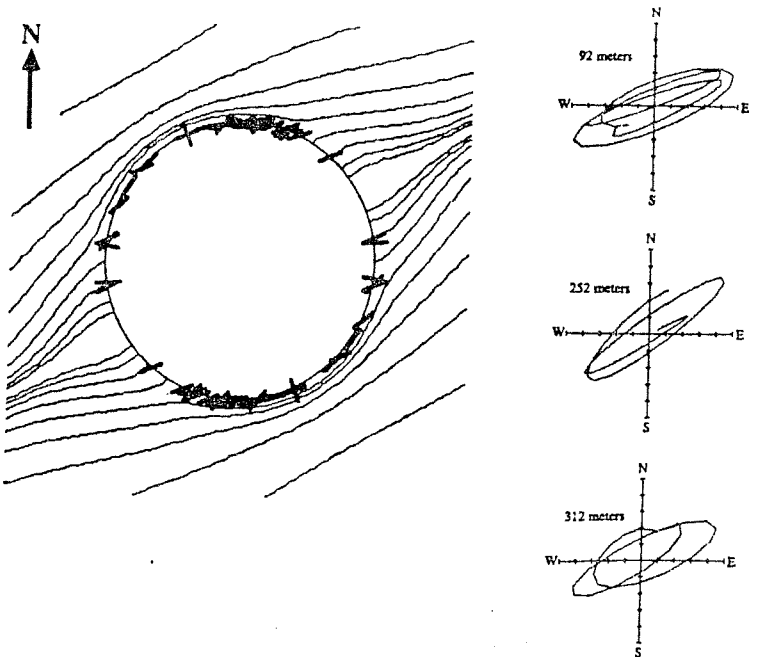

Fig. 23. Stoneley wave particle motion shown with respect to depth for three depths in an Oklahoma well (on right). On the left hand side of the figure, the particle motion polarisations for the Stoneley waves that were recorded at all depths in the hole are projected onto a single borehole cross section and compared to the theoretical SHmax trajectories for the location (from Zoback et al. , 1986).

It appears that the polarisation of these borehole surface waves may be related to elastic anisotropy of the surrounding rock. More analysis and documentation is needed, but the method could prove to be an effective way of determining stress orientation in cased wells, or in boreholes which have no breakouts.

SHEAR WAVE SPLITTING

It can be demonstrated theoretically that cracks in a medium induce a birefringence or anisotropy in the propagation of shear waves through it. This shear wave splitting has now been recognised on three-component seismometer records in many areas and has led investigators, such as Crampin (1987), to hypothesise that much of the upper 10 to 20 kilometers of the Earth's Crust contains fluid-filled microcracks that are aligned with the stress field. In other words, these microcracks parallel SHmax trajectories.

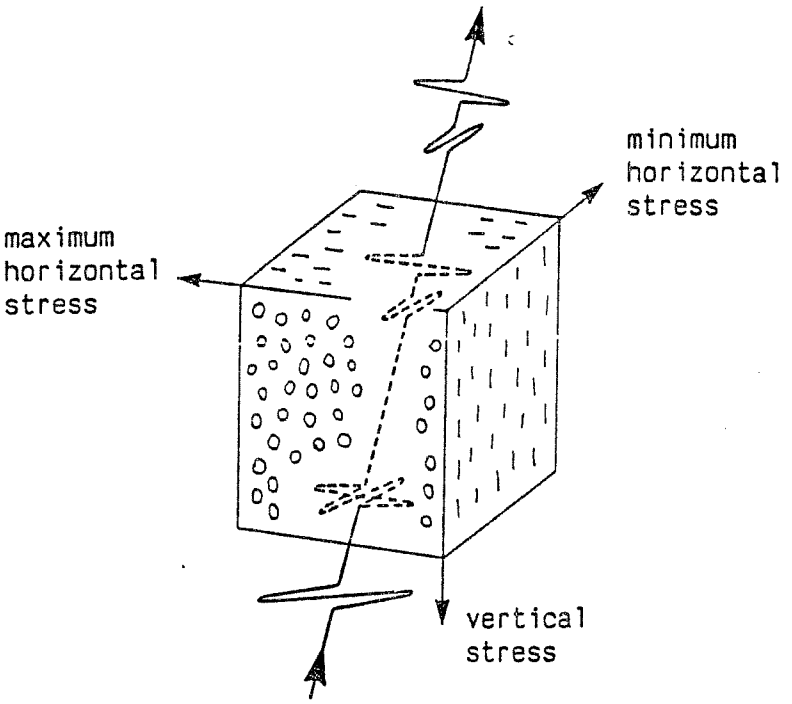

Fig. 24. Relationship of shear wave splitting to the inferred stress aligned fluid-filled microcracks (from preprint by S. Crampin).

If this phenomenon proves to be widespread (Crampin calls it Extensive Dilatancy Anisotropy or EDA), the implications are considerable. Three component VSP surveys could map stress orientations. Perhaps more to the point, analysing split shear waveforms could provide information on the orientation (from polarisation) and the volumetric abundance (from attenuation) of subsurface fractures. Reservoir heterogeneity is currently being mapped in this way by several companies, but I am not aware of any attempts yet to harness the technique as a method for prospecting for naturally fractured reservoirs.

Shear wave splitting appears to have great potential as a means of mapping stress trajectories, but its most exciting contribution may well be documenting the widespread presence of aligned fluid-filled microcracks in the upper crust. If such a fabric proves to exist, there are many significant implications for earth science.

EARTHQUAKE FOCAL MECHANISMS

Hopefully, there will be no major earthquakes that are directly related to your exploration or production activities! However, analysis of the first motions of large earthquakes can indicate principal stress directions.

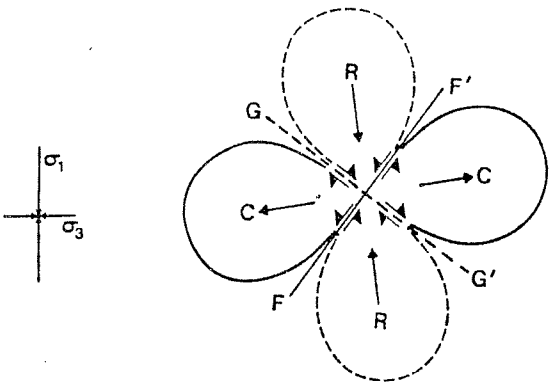

Fig. 25. Source mechanism of a left-lateral strike -slip movement on a vertical fault plane. C - compressive first arrivals, R - rarefactive first arrivals, F-F' - fault plane which ruptures, G-G' - auxiliary plane on which no movement occurs.

An earthquake is caused by failure on a new or existing fracture that is caused by shear stress. In Figure 25, taken from Gough and Gough (1987), F-F' is a fault plane in crustal rocks. Principal stresses σ_1 and σ_3 are so oriented that slip will occur along this plane when the stress contrast builds up to a level sufficient to fracture the rocks. If Figure 25 represents a map view, the movement which occurs on plane F-F' will be left-lateral strike slip. If this occurs suddenly, compressional waves are radiated. Quadrants labelled C receive waves for which the "first motions" are compressional; quadrants labelled R receive initial rarefactions. Distant observatories record first arrivals and their analysis indicates the earthquake mechanism. By convention, the results are plotted as "beach ball" diagrams with the quarter spaces receiving compressional first arrivals blackened, as shown in Figure 26.

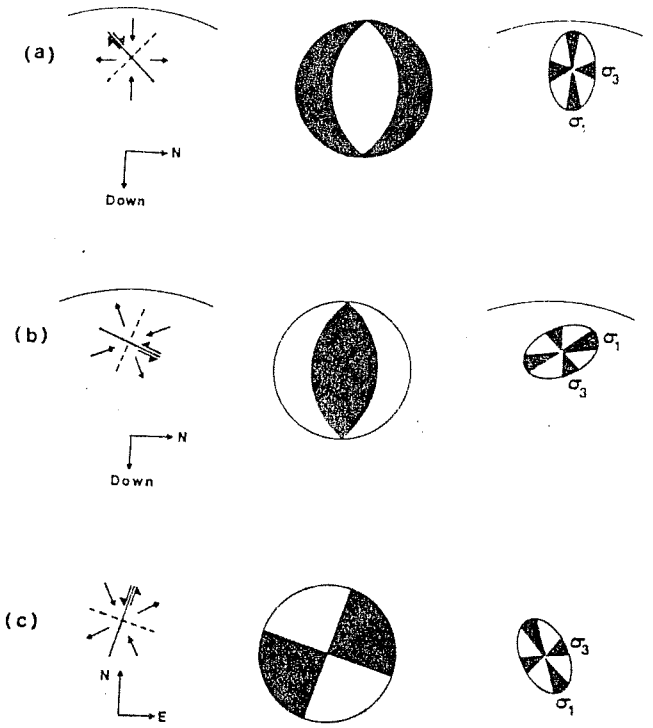

Fig. 26. Fault regimes (left), "beach ball" source mechanism plots (centre) and inferred orientations of the greatest and least principal stresses (right) for (a) a normal-fault earthquake, (b) a thrust fault earthquake and (c) a strike-slip fault earthquake. (From Gough and Gough, 1987).

The largest principal stress lies somewhere in the two quarter spaces receiving rarefactive first motions (white areas of the beach balls) as shown by McKenzie (1969) but, frequently, interpreters assume that the largest principal stress lies along the "P axis" that bisects these quadrants. In practice, this may often be true. Such orientations of SHmax, obtained from deep crustal earthquakes, frequently align with stress directions obtained from other indicators. A classic example is in Eastern Canada (Fig. 27), where similar stress orientations are given by shallow hydraulic fracture experiments and the P axes of deeper earthquakes (Adams, 1987).

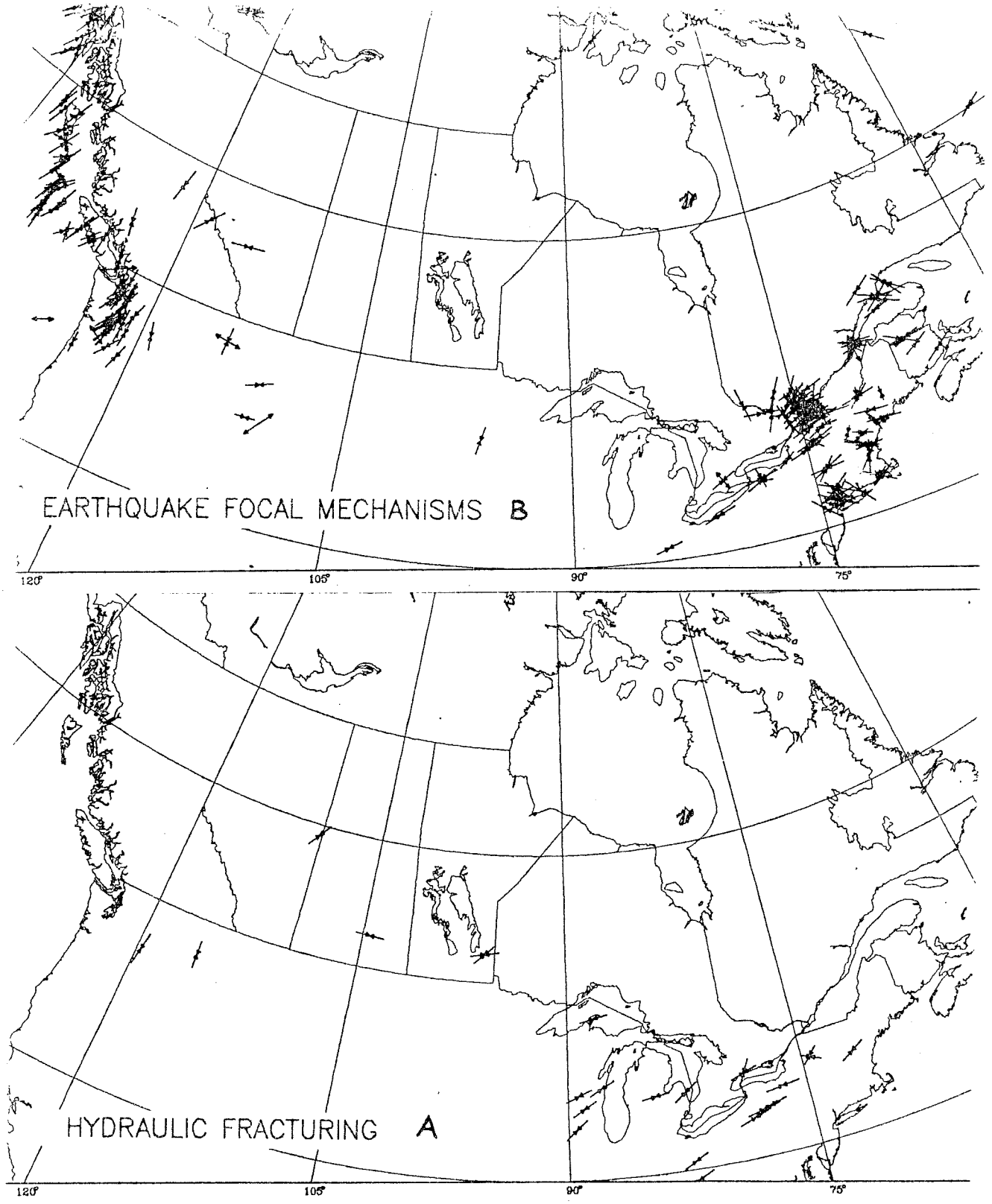

Fig. 27. Maps of SHmax orientations obtained by hydraulic fracturing (Map A) and earthquake focal mechanisms (Map B) from Adams, 1987.

However, it should be appreciated that the plane on which movement occurs is going to determine the spatial geometry of the compressional wave first motions received by distant stations. Rocks are functionally lazy and will choose the path of least resistance in everthing they do. If an old plane of weakness exists that is suitable to relieve the stress, they will use it, and it will not have to be oriented at exactly 45° to the largest principal stress, to allow the P axis to be perfectly diagnostic of that vector's direction! So, beware! On the other hand, fault plane solutions are very useful for indicating the nature of faulting and thus the type of stress regime, and their P axes are likely to be within 30° of the largest principal stress azimuth. Hence, they can be used to check the likely validity of orientations obtained by other methods. Usually, large earthquakes occur naturally at greater depths than stresses can be measured by instruments, so judgement should be used in relating data sets.

GEOLOGICAL INDICATIONS

The contemporary in-situ stress regime can be diagnosed from present day faulting and stress release phenomena. Active faulting can be diagnosed by earthquake activity, offset of a fault's surface traces or can be recognised on seismic reflection records. For example, in many offshore basins, growth faults are present which can be traced to the seafloor on seismic reflection profiles. These are clearly active faults. Since they are growth faults, and their hanging walls are dropping, this indicates that Sv is the greatest principal stress (Anderson, 1951). The mean horizontal trace of the fault on a map (it is likely to be arcuate) will parallel SHmax and SHmin will be perpendicular to the fault trace (Fig. 28). Hence, if we know that a particular fault is currently active and can determine the nature and geometry of its offset, we can estimate the relative magnitudes of the local principal stresses and map their orientation. We can also estimate the stress magnitudes.

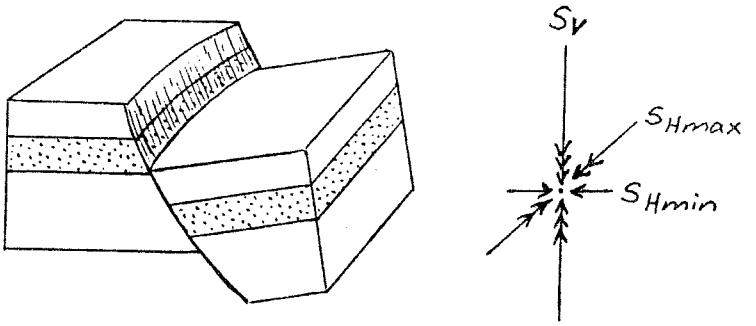

Fig. 28. Block diagram of growth fault showing orientation of principal stresses.

Stress release occurs where principal stress contrasts are great. On limestone quarry floors in Ontario, for example, buckles often occur after rock has been removed. The very high horizontal stresses are relieved in this way (e.g. Adams, 1982). The axes of these buckles have an average orientation perpendicular to the larger horizontal principal stress, so they can be used for stress mapping. If certain simplifying assumptions are made the horizontal stress magnitudes may be estimated (Adams, op.cit.).

With quarry-floor buckling, we have clear indications that slip on bedding planes is occurring in flat-lying rocks. This may be quite a frequent occurrence, but be impossible to document because there are no obvious signs that it has happened. Certain road cuts contain evidence that it has occurred. Vertical holes are often drilled through rock masses and explosives set off at their base to produce a "neat" road cut. This induces a fracture in the plane of the drill holes and, after the outer rock has broken away, half the traces of the borehole remain on the face of the road cut. In the Appalachians and in the Canadian Rocky Mountains (Bell, 1986), these boreholes have been observed to be offset along inclined bedding planes and, moreover, the offsets document uphill movement of rocks after the holes were drilled! The updip slip appears to be a one-time effect that occurred shortly after the road cut was blasted. As such, it is unlikely to be a manifestation of contemporary thrust faulting, but is probably due to stress release. The examples reported so far document movement in the direction of the largest horizontal stress as determined locally by other means.

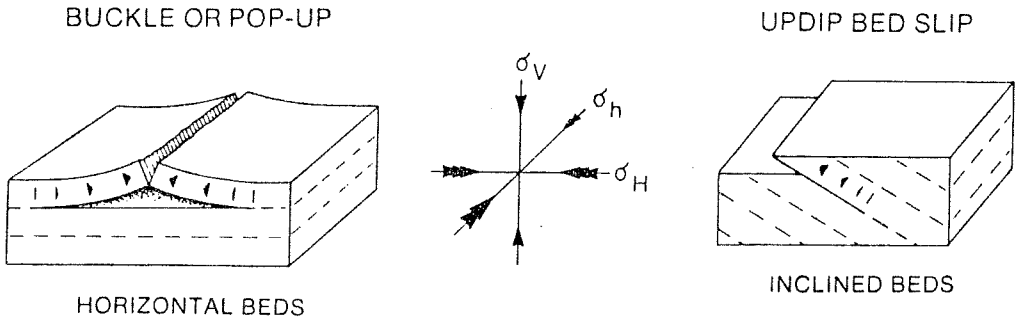

Fig. 29. Surficial stress relief strucures that can form in horizontally-bedded and inclined rocks that are subject to strongly anisotropic near surface horizontal stresses.

Stress release ridges form after ice loads are removed, if horizontal stresses are high. Such post-glacial phenomena have been quite widely reported in eastern Canada and the northeastern United States. Aligned volcanoes have also been cited as evidence of the contemporary stress regime. They are interpreted as being intruded along a major plane of weakness in the crust coincident with the surface trace of the larger horizontal principal stress in the region (Nakamura et al., 1977). Igneous dikes and sills are also intruded along planes perpendicular to the least principal stress, so recent intrusions can help elucidate the contemporary stress regime.

These examples are mentioned to show that it can be well worth compiling suitable geological data, when evaluating the nature of a contemporary stress regime, even though the literature search may not be straightforward. Many of the papers are published in geotechnical journals, and much of the information is not very well labelled at all; it is merely recorded on geological maps and cross sections!

Over the last few years, John Adams of the Geological Survey of Canada has been maintaining an open file compilation of Canadian crustal stress data with source references (Adams, 1987). The IUGG World Stress Map Project has gathered an enormous volume of worldwide stress data, both published and unpublished (Zoback et al., 1989). It is planned to publish a list of sources, and also data summaries, through the U.S.G.S. under the authorship of M. L. Zoback.

4. CASE HISTORIES

STRESS MAGNITUDES IN THE GARRINGTON AREA, ALBERTA, FROM MINI-FRAC RECORDS

Stress magnitudes do not increase linearly with depth. This is fortunate because, if they did, it would be very hard to persuade an induced hydraulic fracture to stay in the formation it was started in, and all sorts of undesirable reservoir connections would occur. There are relatively few wells in which multiple stress measurements have been made at close vertical intervals. Two are illustrated here. In both cases, the smaller horizontal principal stresses appear to vary significantly over short vertical intervals.

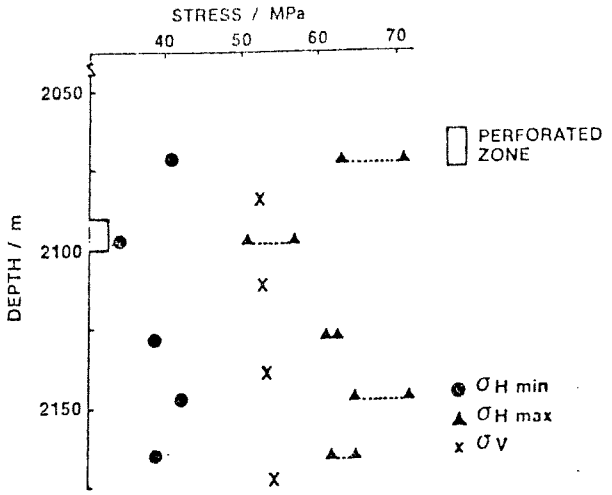

Fig. 30. Stress magnitude variations measured in the Esso Kelly c-16-I 93-P-1 well drilled in the Deep Basin in British Columbia. Merasurements were made by hydraulic fracturing (Kry and Gronseth, 1982).

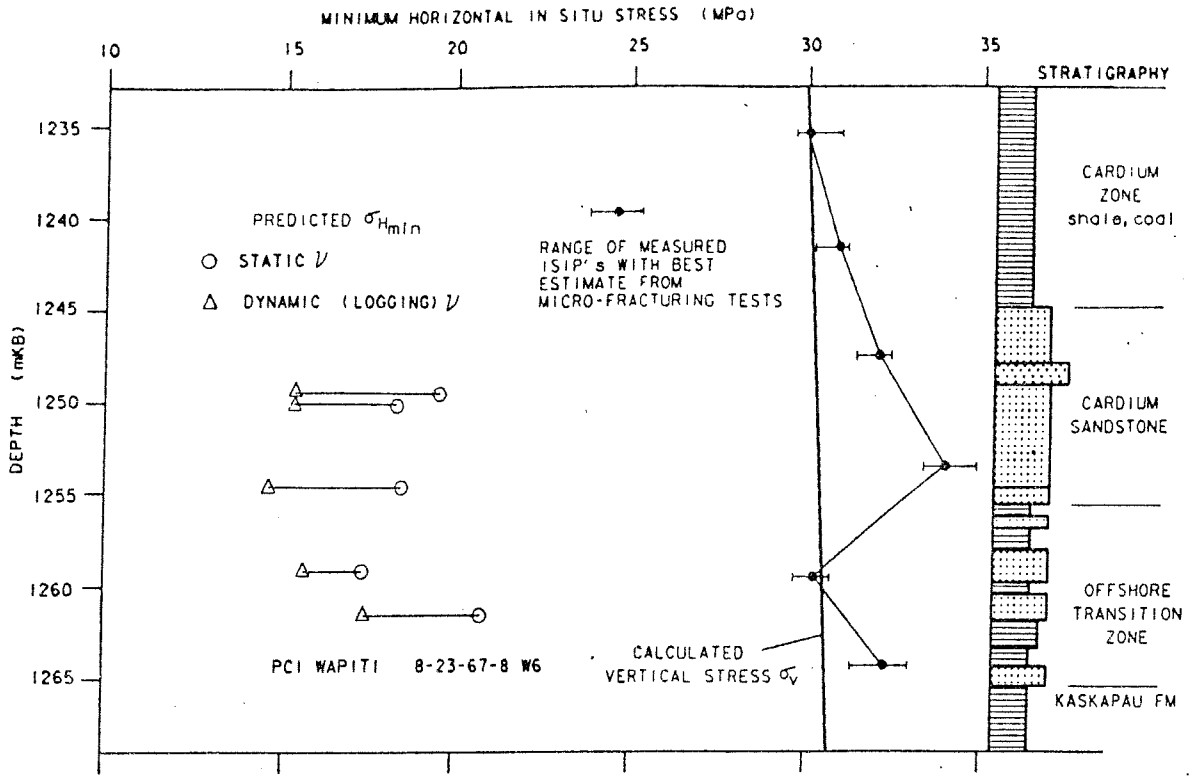

Fig. 31. Measurements of the smaller horizontal principal stresses derived from min-frac tests run in the Petro Canada Wapiti 8-23-67-8W6 well in Alberta (McLellan, 1988).

Knowing that such stress profiles exist should remind us that the "smoothed" stress profiles we construct are, at best, generalisations. They are not tools for predicting fracture containment or even for predicting exactly what stress magnitudes will be measured at particular depths. To get some idea of how stresses vary with depth in an area, one can create a composite profile.

Woodland and Bell (1988) published magnitudes of smaller horizontal principal stresses, as derived from mini-frac tests, from some 115 wells in western Canada. A number of these wells were in the Garrington area of Alberta. The minifrac results from these wells were correlated to the stratigraphic levels at which they were gathered, and then depth normalised to the stratigraphic column of one particular well. The result is shown in Fig. 32, which attempts to show what the stress magnitudes would have been, if they had all been measured in the 16-17-36-5W5 well. Note that the values from the shales below the Second White Specks are relatively lower than those from the Viking Sandstone. The SHmin depth/pressure relationship has been drawn to reflect changes in magnitude reflecting lithologic variation, since it is believed that there is likely to be much more fine-scale vertical variation than indicated by the ten magnitudes shown on this composite section. This particular exercise tells us that it should be possible to contain hydraulic fractures within the Viking Sandstone in this area.

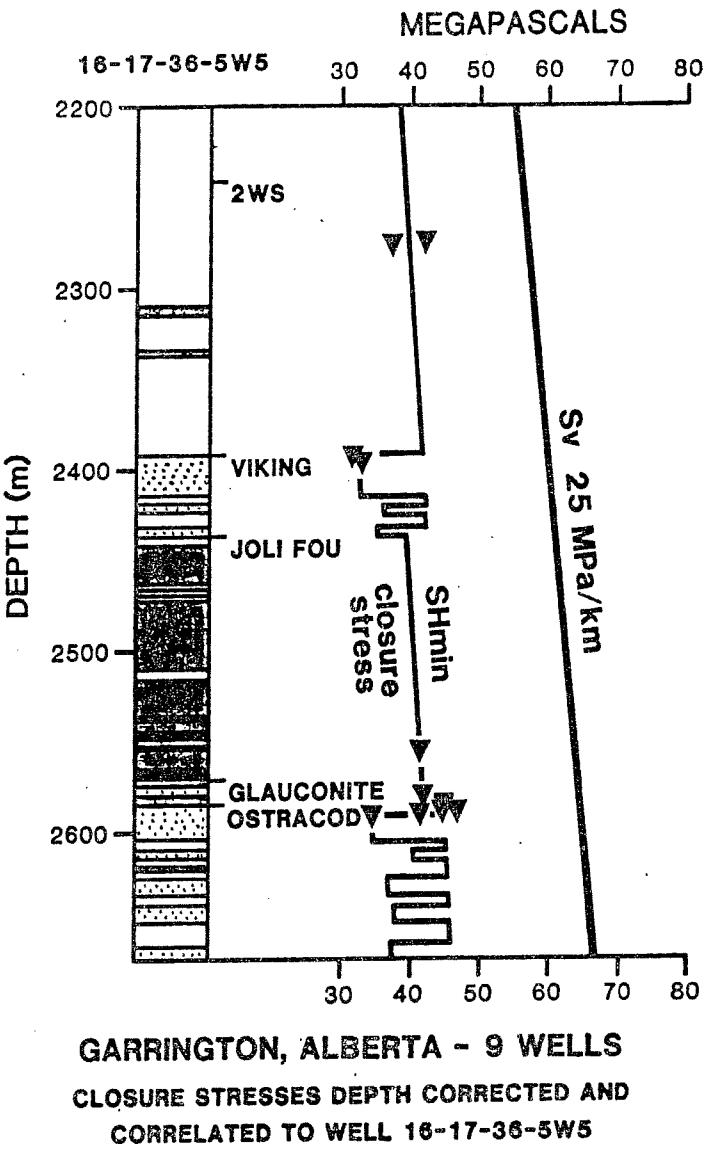

Fig. 32. Composite SHmin profile for the Garrington area (Bell and Price, 1989).

SCOTIAN SHELF STRESS REGIME DETERMINED FROM DENSITY LOGS, LEAK-OFF TESTS AND BREAKOUTS

This case history involves using subsurface information to compile a regional interpretation of the stress regime. We are not going to be able to look in a highly focussed way at stress tensor variation in small volumes of rock.

Stress magnitudes are obtained by integrating density logs with depth, extrapolating values for the unlogged intervals behind surface casing and adding the weights of the water columns. This gives an Sv/depth profile for each well studied. Selected wells are those which have had leak-off tests run below three or more casing shoes. Usually, the information we require is reported in the Well History Report and the mudlogger's report, both of which are released by COGLA in Canada once the confidentiality period has expired. Various pressure units are used. For comparison, 1 megapascal (MPa) = 10 bars = 145 psi = 10.2 kg/cm2.

As an example, we will consider the leak-off test run below intermediate casing at the Olympia A-12 well. The Drilling Summary states that ". . . 473 mm (18 5/8 ") casing was run in and landed at 4956ft (1511m) K.B. The casing was drilled out and a leak-off was conducted to 1980 kg/m3 (16.5 ppg) equivalent mud weight." This test was tabulated in the Well History Report as shown below:

Date	Drill depth	Casing		Mudweight	Surface pressure	F.L.O.T. lb/gal MWE	Total F.L.O.T. pressure
		Size	Depth				
3-6-82	5025 ft 1531.5 m	18 5/8" 473 mm	4956 ft 1510.5 m	9.4 lb/gal 1126 kg/m^3	1800 psi 12.4 MPa	16.4 1968 kg/m^3	4223 29.1 MPa

Table 2. Details of a leak-off test run at the Olympia A-12 well on the Scotian Shelf, eastern Canada. Note the value of the mudweight equivalent pressure in column 7. In the text of the well history report 16.5 is given. One number is wrong!

The data are not quite identical with the written text, but we will assume the table is correct!

The base of the casing is at 4956 ft K.B. (1510.5 m). At the time the leak-off test was run the cement had been drilled out and the well deepened to 5025 ft K.B. (1531.5 m), leaving an unlined "open hole" interval of 69 ft (21 m) at the bottom of the well. A fracture was initiated in this section by the leak-off test. We assume that this occurred at or near the top of the open hole interval and, therefore, assign a depth of 4956 ft K.B. (1510.5 m) to the test.

The mudweight of the drilling fluid was 9.4 lbs/gallon. At the base of the casing it exerted a pressure of (9.4 x 4956 x 0.052) or 2422.5 psi (16.7 MPa) on the rocks surrounding the wellbore. This pressure was then increased by pumping a small additional quantity of mud down the well. The pressure exerted by the rig pump was monitored and increased linearly at first. At a surface pressure of 1800 psi (12.4 MPa), the pressure increase ceased to be linear and "leak-off" occurred. The total bottom hole pressure was (2422.5 + 1800.0) or 4222.5 psi (29.1 MPa). In mudweight equivalent this is (4222.5/4956 x 1/0.052) or 16.4 lbs/gallon.

Lithological descriptions and logs indicate that the 4956-5025 ft (1510.5-1531.5 m) interval consists of moderately indurated shale. This is likely to have a low tensile strength, so that the leak-off test value will be close to SHmin. Thus we can estimate SHmax from the relationship:

SHmax = 2(Leak-off pressure) - Pore fluid pressure

The Well History Report states that, to depths of 14,000 ft in Olympia A-12, pore pressures are hydrostatic and exhibit a normal seawater gradient of 0.465 psi/ft (8.94 lb/gal MWE) or 1073 kg/m3. This is confirmed by the mudweight records. Above 14,234 ft (4338.3 m) K.B., mudweights varied from 8.6 to 9.4 lb/gal, which was adequate to counterbalance the formation pressure. Hence, at 4956 ft (1510.5 m) K.B., pore fluid pressure would have been (0.465 x 4956) or 2304.5 psi (15.9 MPa). At this depth, therefore:

SHmax = (2 x 4222.5) - 2304.5 psi = 6140.5 psi or 42.3 MPa

To obtain Sv, we integrate the density log to 4956 ft K.B. depth, after first ensuring that the well has been drilled approximately vertically. The Directional Survey log confirms that this is the case for Olympia A-12! For this calculation, we are trying to estimate the weight of the overburden, so we only deal with the "rock column" from sea level downwards. So we subtract the Kelly Bushing elevation (131.0 ft) and make our calculation for a depth of 4825 ft (1470.6 m) below sea level.

The interval 0-40 m is assigned seawater density and the unlogged section from seafloor to the base of surface casing (40-472 m) is given a mean density of 2.0. The lower section is assigned densities as indicated below in Table 3. The intervals in column A were selected because they exhibit approximately constant density. Columns B and C contain values read off the density logs, whereas columns D and E and D x E contain values derived from A, B and C. Column F records the running total of the overburden pressure at the base of each interval in the well. Sv at the base of intermediate casing is estimated at 29.5 MPa.

A	B	C	D	E	D x E	F	
Depth Interval m below SL	Bulk Density kg/m^3	Correction kg/m^3	Total Density g/cm	Interval Thickness m	Interval Weight kg/m2	Overburden weight(S_V)	
						kg/m^2	MPa
0-40			1.154	40	46.16	46.16	0.45
40-472			2.000	432	864.00	910.16	8.9
472-992	1950	+50	2.000	520	1040.00	1950.16	19.1
922-1222	2075	+50	2.125	230	488.75	2438.91	23.9
1222-1269	2125	+75	2.200	47	103.40	2542.31	24.9
1269-1342	2175	+75	2.250	73	164.25	2706.56	26.5
1342-1412	2325	+75	2.400	70	168.00	2874.56	28.2
1412-1470.6	2225	+75	2.300	58.6	134.78	3009.34	29.5

Table 3. Intervals of constant density in Olympia A-12 to 1470.6 m below sea level.

In this way, we have obtained estimates of the magnitudes of the three principal stresses at a point 1470.6 m below sae level at the Olympia A-12 well location. The same approach has been used on many other leak-off tests on the Scotian Shelf to expand the coverage, and the results obtained have been examined critically, bearing in mind the approximations involved in their generation. Again, as an example, we will evaluate the stress magnitude estimates we have just obtained.

The values are:

Sv = 29.5 MPa SHmin = 29.1 MPa SHmax = 42.3 MPa

They suggest that: SHmax > Sv > SHmin, that an hydraulic fractures which are induced will be vertical and that, if faulting occurs, the mode will be strike-slip. Are these reasonable conclusions? Is it likely, for example, that the data have misled us and that the true stress regime is one where Sv > SHmax > SHmin? After all, the Scotian Shelf is characterised by listric normal faults around Olympia A-12, is not this what we would expect? The weakest link in the chain of reasoning is the assumption that leak-off pressure is approximately equal to SHmin. Suppose it is Pr, the fracture reopening pressure, in the case just considered. Then the Bredehoeft et al. equation would read:

$$29.1 = 3SHmin - SHmax - 15.9 \quad \text{so that:}$$

$$SHmin = 1/3\ (SHmax + 45)\ MPa$$

If SV > SHmax > SHmin, SHmax would be less than 29.5 MPa, which means, from the above equation, that SHmin would be less than 24.8 MPa. This is 85% of the leak-off pressure. Alternatively,suppose the rocks actually had a significant tensile strength; then the leak-off pressure would be equivalent to Pb, the formation breakdown pressure. In such a situation, the complete Hubbert and Willis (1957) equation: Pb = T + 3SHmin - SHmax - Po, would apply and SHmin would equal 24.8 MPa - 1/3T or less, if Sv was greater than SHmax. Without independent measurements of SHmin, it is a matter of judgement whether one thinks either of these scenarios is probable. In this case, The stress regime is interpreted to be one where SHmax > Sv > SHmin.

As a general rule, we can say that if the SHmax magnitude estimate is only slightly larger than Sv, then it is likely that Sv is the largest principal stress. This is because the assumptions surrounding the interpretation of the leak-off pressure and the equation used to estimate SHmax combine to overestimate the magnitude of the larger horizontal principal stress.

Stress magnitudes have been estimated at many depths in some twenty wells in the manner outlined above. The interpretation for the Venture area in the Sable Sub-basin is shown in Figure 33. This graph portrays measurements and estimates from 4 wells, and interprets a generalised profile of stress magnitude change with depth.

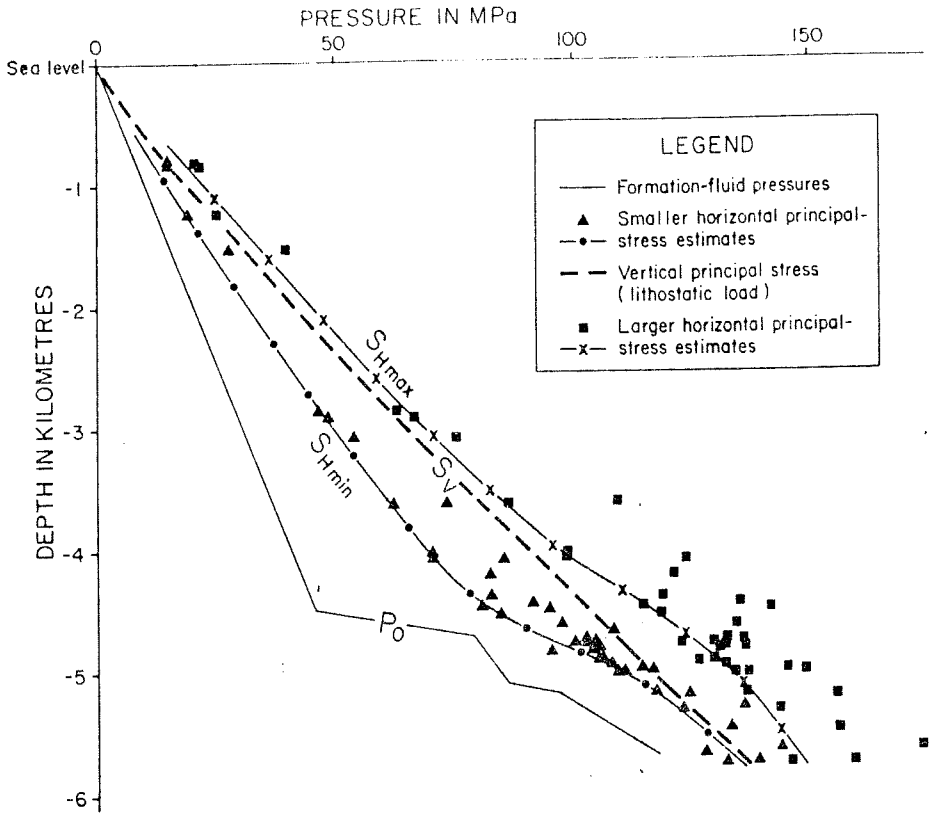

Fig. 33. Pore fluid pressures and stress magnitudes in the Venture area, Scotian Shelf (Ervine and Bell, 1987).

Ervine and Bell (1987) thought that a case could be made for a stress regime with SHmax > Sv > SHmin between subsea depths of 815 and 5773m. This is possible, but not very likely. Above 4000m depth, the estimated magnitude of SHmax is only slightly greater than Sv, and is based on SHmin being equated with leak-off pressures. As we have seen, these are upper limits that inflate SHmax, so it is probable that both SHmin and SHmax are lower than shown, and that SHmax < Sv. Such a relationship is supported by the omnipresence of normal faults, some of which appear to have been active recently. A similar interpretation can be made above 4000m on the Banquereau Bank (Fig. 34).

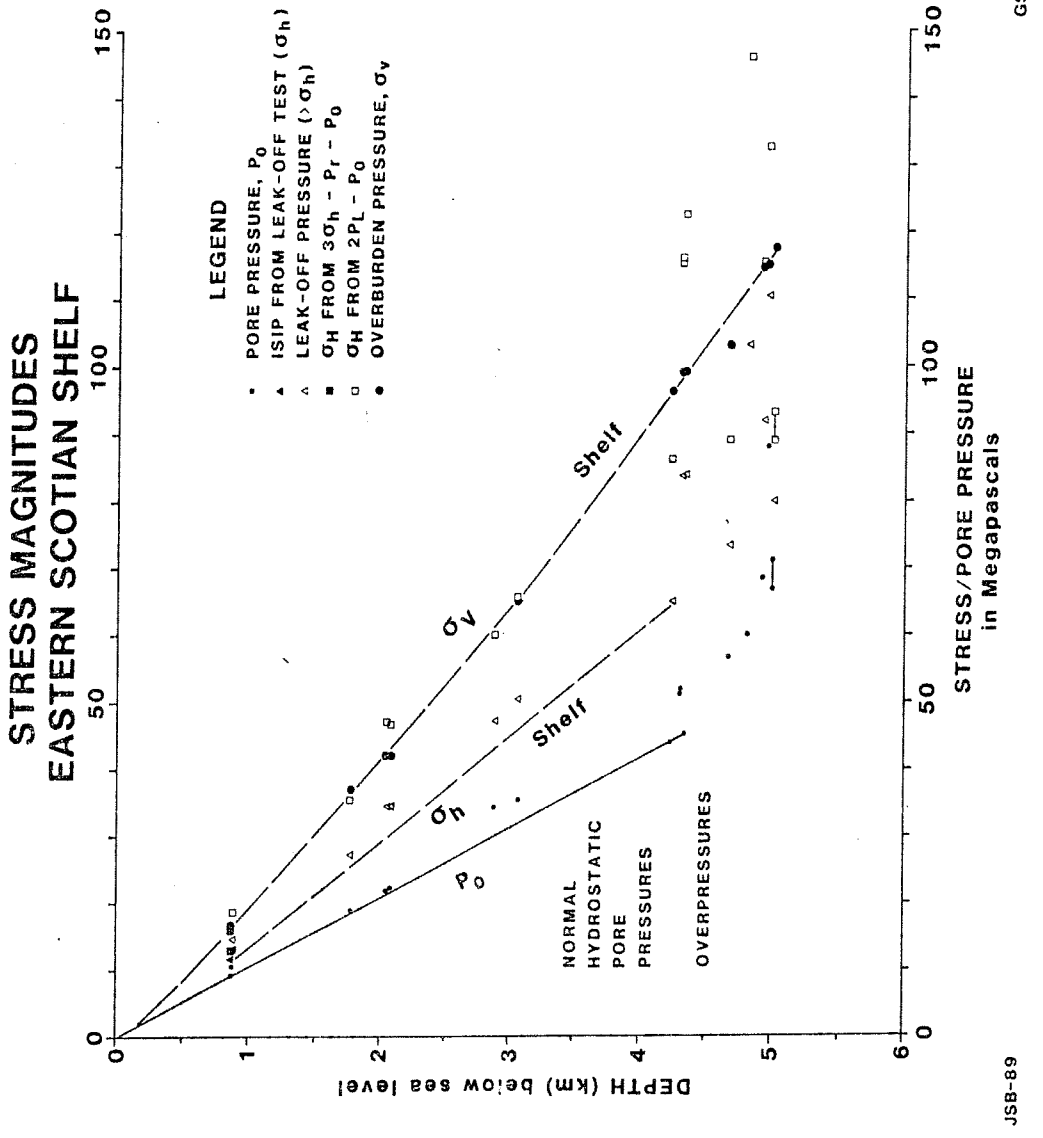

Fig. 34. In-situ stress profile and pore fluid pressures for the Banquereau Bank, offshore eastern Canada, based on pressure data from five wells (Bell, submitted).

In both these areas, overpressures are encountered below 4000m. The overpressures increase leak-off test pressure levels so that they approach the overburden pressure. One stress regime effect is that, within the overpressured sections, around 5000m depth, it is much harder to interpret Sv as greater than Shmax; the converse is more probable. Hence, in the upper part of the overpressured zone a stress regime of SHmax > Sv > Shmin probably exists. As depths of 6000m are approached in the Venture area, leak-off test pressures approach, and occasionally exceed, Sv. The implication is that SHmin is becoming equal to, and possibly greater than Sv. If so, this has important implications. With Sv the smallest principal stress, all induced hydraulic fractures will be horizontal. If such features happened to be produced naturally by rising fluid pressures in the overpressured zone, they would be ideal slip surfaces for the soles of listric normal faults. It is suspected that this is exactly what has occurred.

Our present state of knowledge about the stress regime on the Scotian Shelf, from the standpoint of stress magnitudes, can be summarised as follows:

Depth range	Stress regime	Orientation of induced fractures	Fault Style
0 - 4000/ 4500 m	Sv > SHmax > SHmin	Vertical	NORMAL
4000/4500 - 6000 m	SHmax > Sv > SHmin	Vertical	STRIKE SLIP
below 6000m	SHmax > SHmin > Sv	Horizontal	THRUST

The effective strength of rocks is the pressure required to fracture them. This can be measured as the difference between the fracture gradient and the pore pressure gradient. The former is indicated by leak-off tests; the latter by mudweights, RFTs, DSTs and other indications of formation pressures. In the Venture area, effective rock strength increases with depth to the top of the geopressured section, at which level it declines (Fig. 35)

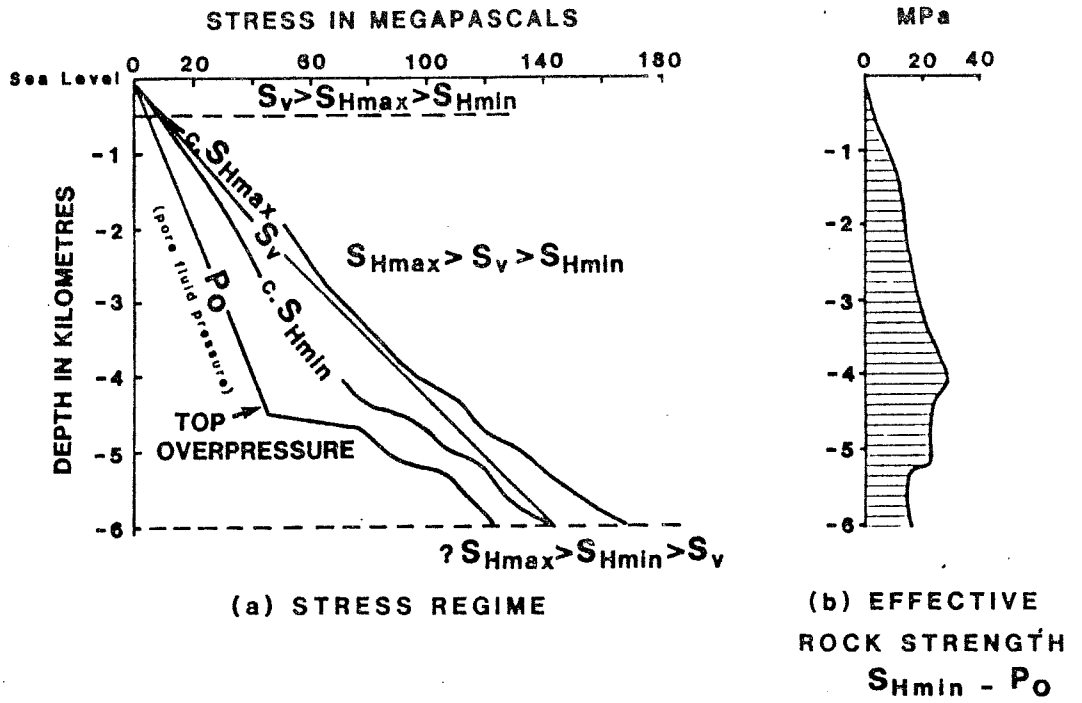

Fig. 35. (a) Variation in principal stress magnitudes and pore fluid pressures with depth in the Venture area. (b) Effective rock strength versus depth for the Venture area. The values shown represent the amount pore pressures have to be raised to initiate hydraulic fractures. Note the decrease in effective strength below 5 kilometers (from Bell, in press).

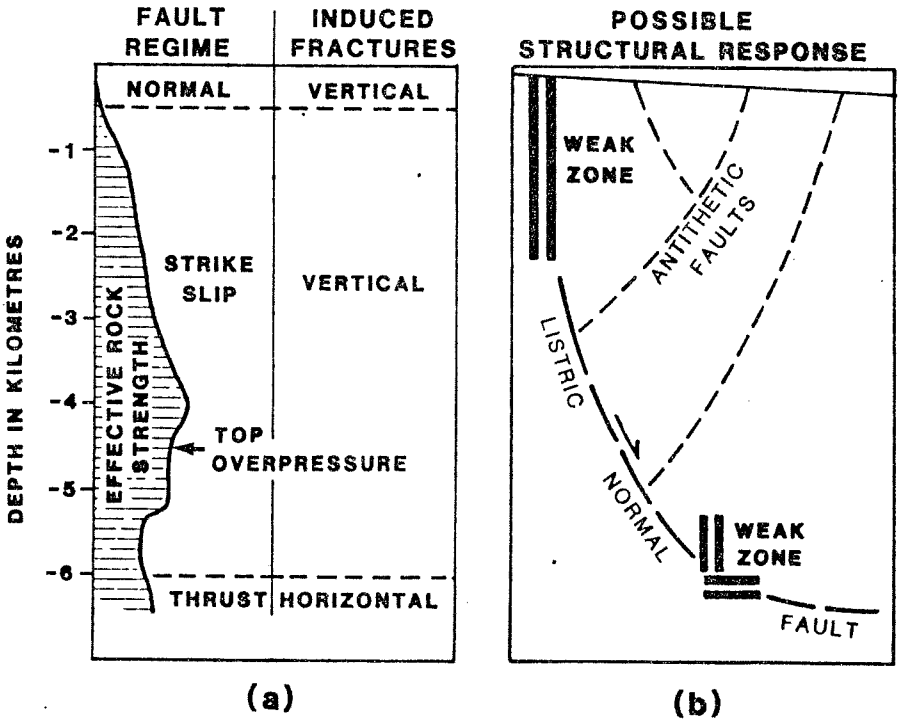

Fig. 36. (a) Relationship between orientations of induced fractures, faulting tendencies and effective rock strength versus depth in the Venture area. (b) Possible structural response if the section was free to undergo extension (which it appears to be).

The consequences of this strength profile are combined with the stress regime inferences summarised above in Fig. 36. This indicates that there are two zones where fracture, or breakdown, can occur most easily: at shallow depths, where fractures will be vertical and at much greater depths, within the geopressured intervals, where fractures may be horizontal. Movement along a surface linking the two zones would be most easily accomplished along an arcuate fracture plane which permitted rotation of the down-slumped block, in other words, through normal growth faulting.

Thus our investigation of the stress regimes in this part of the Scotian Shelf has rationalised the observed recent structural events. We have not yet considered stress orientation. Borehole breakouts have now been logged in some 56 wells and the results augment the original interpretation by Podrouzek and Bell (1985) based on breakouts from 38 wells. Mean orientations are shown below (Fig. 37).

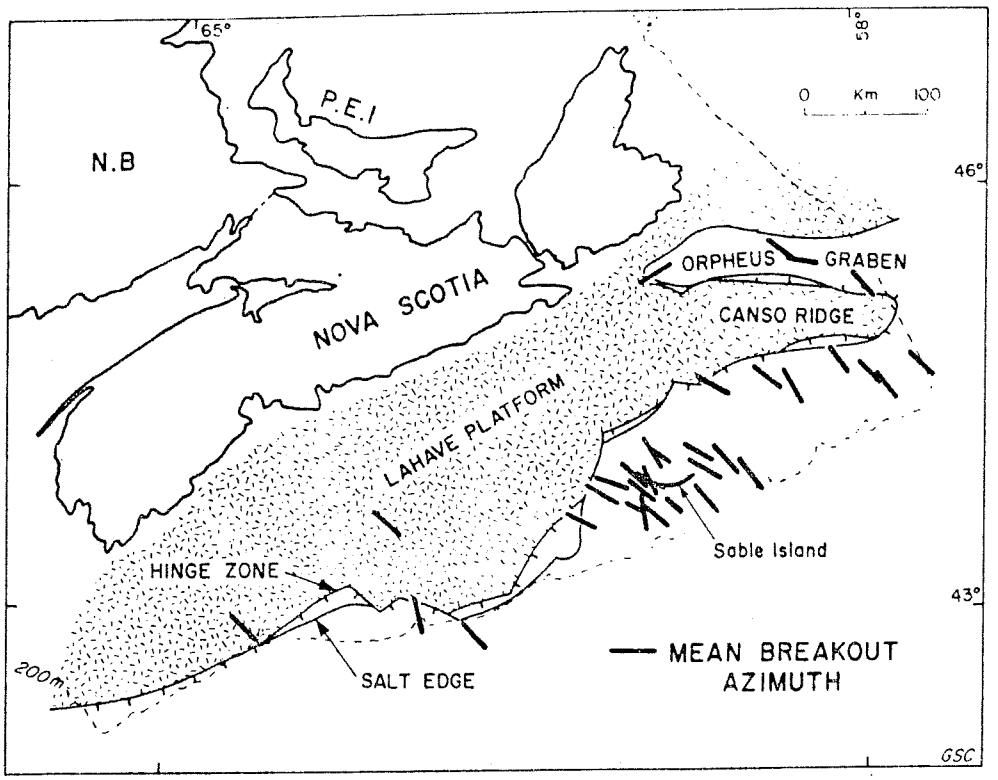

Fig. 37. Mean breakout azimuths from 38 Scotian Shelf wells. Results from closely spaced wells are combined on this figure (Podrouzek and Bell, 1985).

These breakouts show that SHmin is oriented NW-SE, and allow construction of a stress trajectory map (Fig. 38). It predicts that naturally induced hydraulic fractures (or potential fault planes) will be oriented more or less NE-SW, which is a fair approximation of the traces of most of the recently active listric normal faults on the Scotian Shelf.

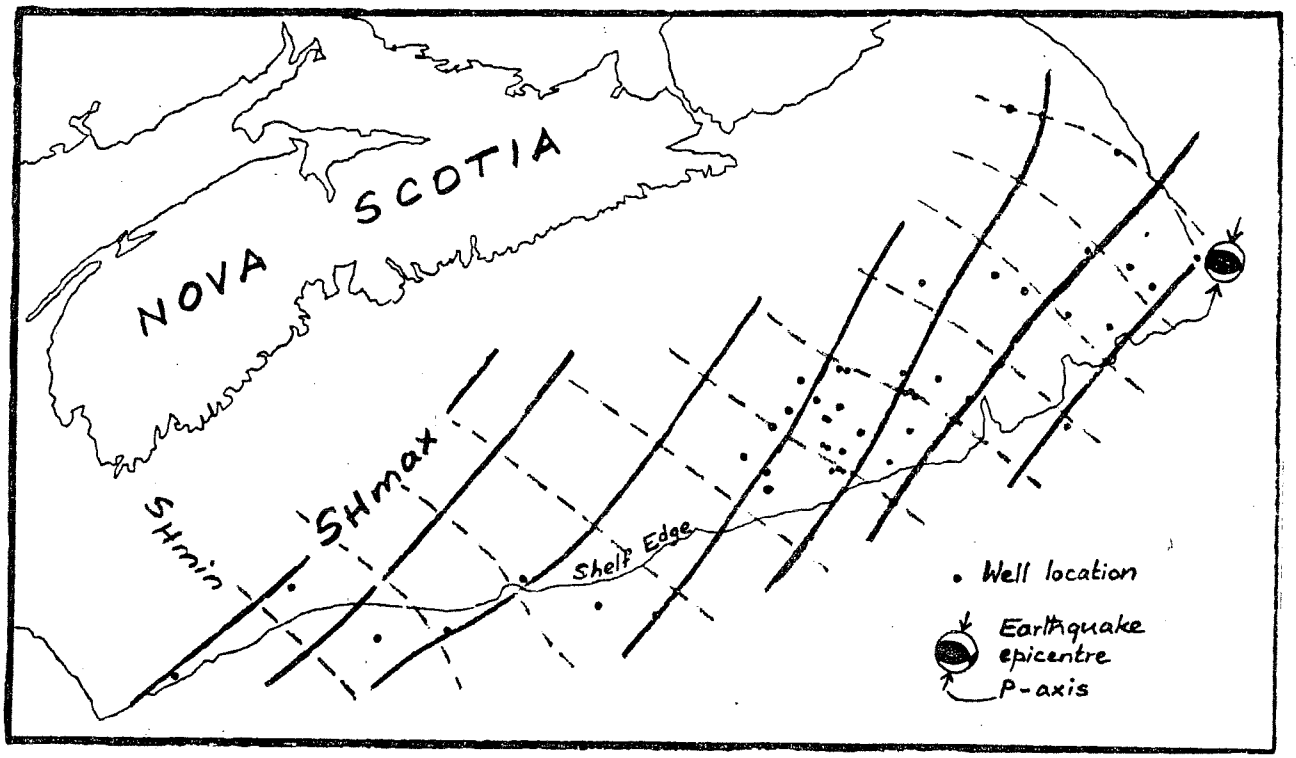

Fig. 38. Stress trajectory map of the Scotian Shelf prepared from breakout data.

STRESS ORIENTATIONS IN THE WEST PEMBINA AREA, ALBERTA AND THE WESTERN CANADIAN BASIN FROM INFERRED HYDRAULIC FRACTURE ORIENTATIONS AND BREAKOUTS

As we have seen, vertical hydraulic fractures that were inadvertently propagated through the Cardium Sandstone in the Pembina area, extended NE and SW of the wells from which they were initiated (Fig. 14). This indicates that the smallest principal stress is oriented approximately NW-SE and is horizontal. However, the information from flow between wells is only as accurate as the grid which sensed it, and it would be beneficial to have a more precise picture of stress orientations.

In the heady days of exploring the West Pembina pinnacle reef play a lot of dipmeter logs were run through the Devonian section. In some cases, when wells needed to be redirected, the information was very welcome. It has also revealed a very consistent orientation of horizontal principal stresses in the area (Fordjor et al. 1983; Bell and Babcock, 1986) as shown below:

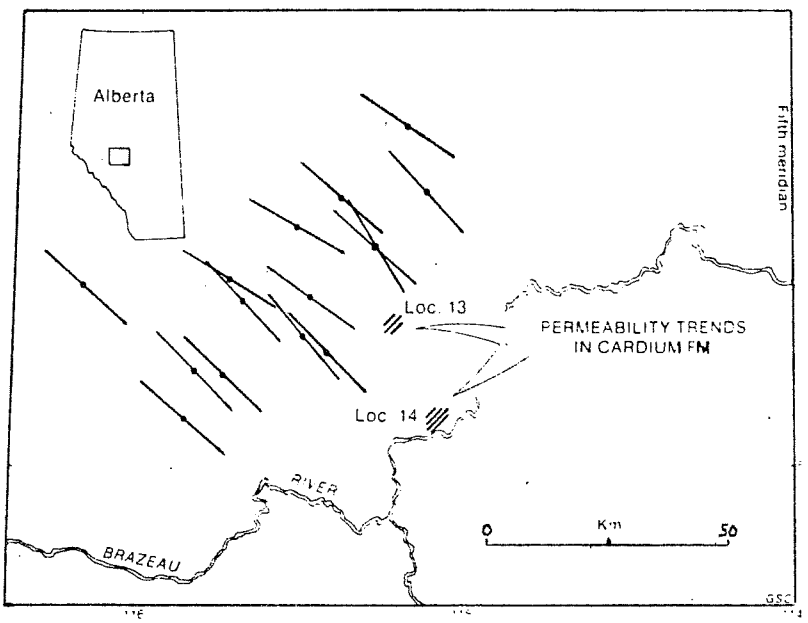

Fig. 39. Consistently oriented mean breakout azimuths from 15 closely spaced wells in the West Pembina area (Bell and Babcock, 1986, Fig. 7).

This approach can be extended across the whole basin, wherever suitable dipmeter logs are available, and stress orientations mapped regionally, as shown in Figs 40 and 41.

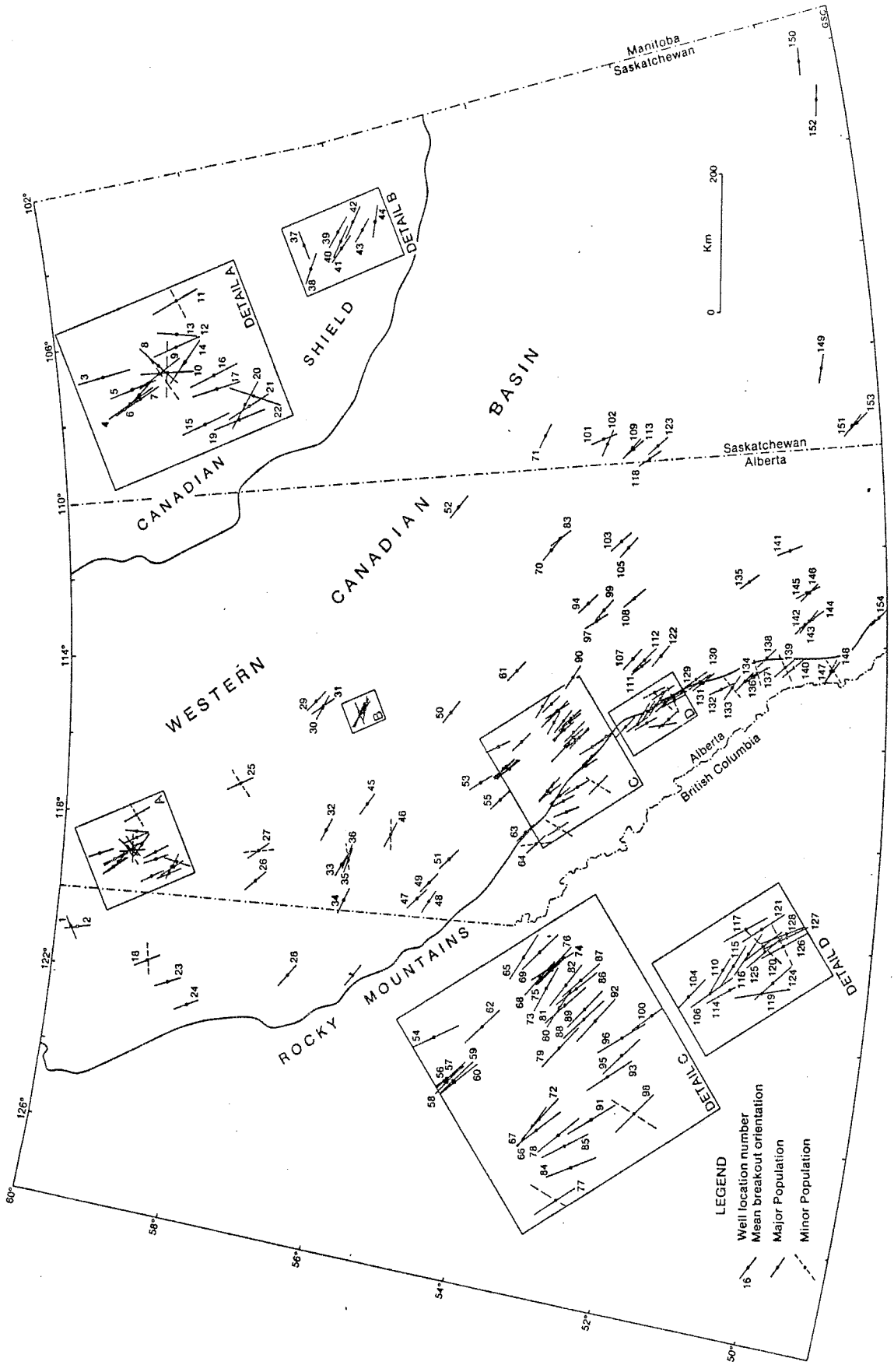

Fig. 40. Mean azimuths of major and minor breakout populations in 154 wells in Western Canada (Bell and Babcock, 1986, Fig. 4).

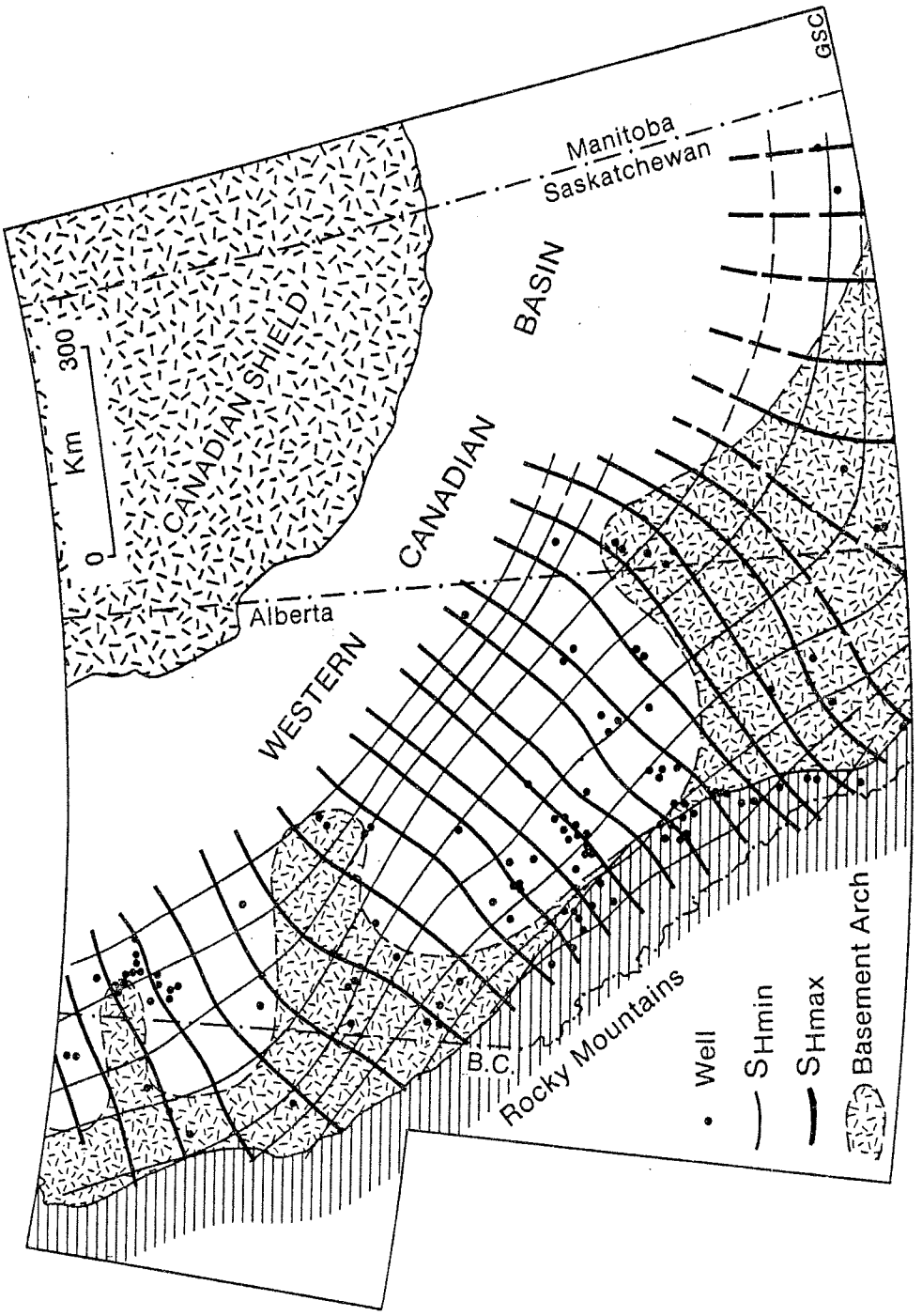

Fig. 41. Stress trajectories inferred from breakouts in the Western Canadian Basin (Bell and Babcock,1986, Fig. 6).

5. LOCAL APPLICATIONS

DIRECTED FRACTURES

In a number of situations it can be advantageous to be able to predict the directions in which hydraulic fractures will propagate away from a well. If the well has missed a target, such as a pinnacle reef, and the reef's location is known, it may be possible to connect the well to this potential reservoir by hydraulic fracturing (Fig. 42). If all evidence points to the reef being close to the well, say within 100 m, this will be a very much cheaper approach than backing off and drilling a redirected well.

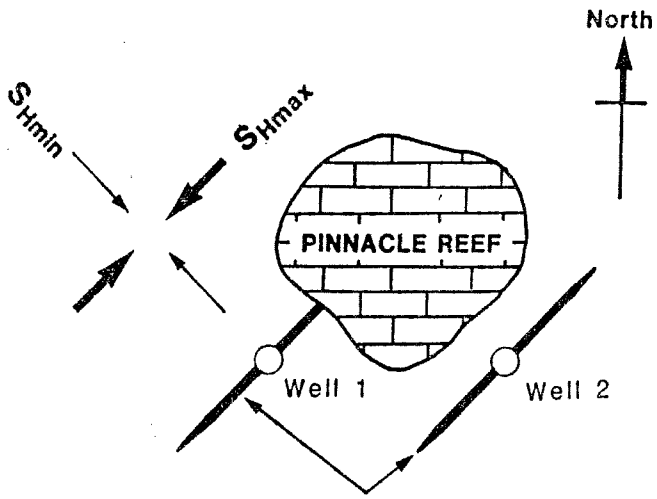

Fig. 42. Prediction of fracture orientation. Horizontal principal stresses derived from breakouts in nearby wells show that hydraulic fractures propagated from Well 1 could intersect the pinnacle reef, whereas fractures generated from well 2 are likely to miss it.

Another possible application, suggested by Hassan (1982), involves controlling wells that have blown out. If a relief well needs to be drilled for the purpose of pumpimg a heavy slurry into the blowout well, it would be worth locating the control well so that any hydraulic fractures emanating from it might intersect the blowout well. If present, natural fractures might have the same trend and such a location would maximise the chance of establishing communication between the two well bores.

Breakouts have given us a good picture of horizontal principal stress orientations in the Western Canadian Basin. The two maps below show stress orientations determined for Paleozoic rocks and for Mesozoic rocks. These maps are suitable for predicting hydraulic fracture directions which will be aligned with SHmax.

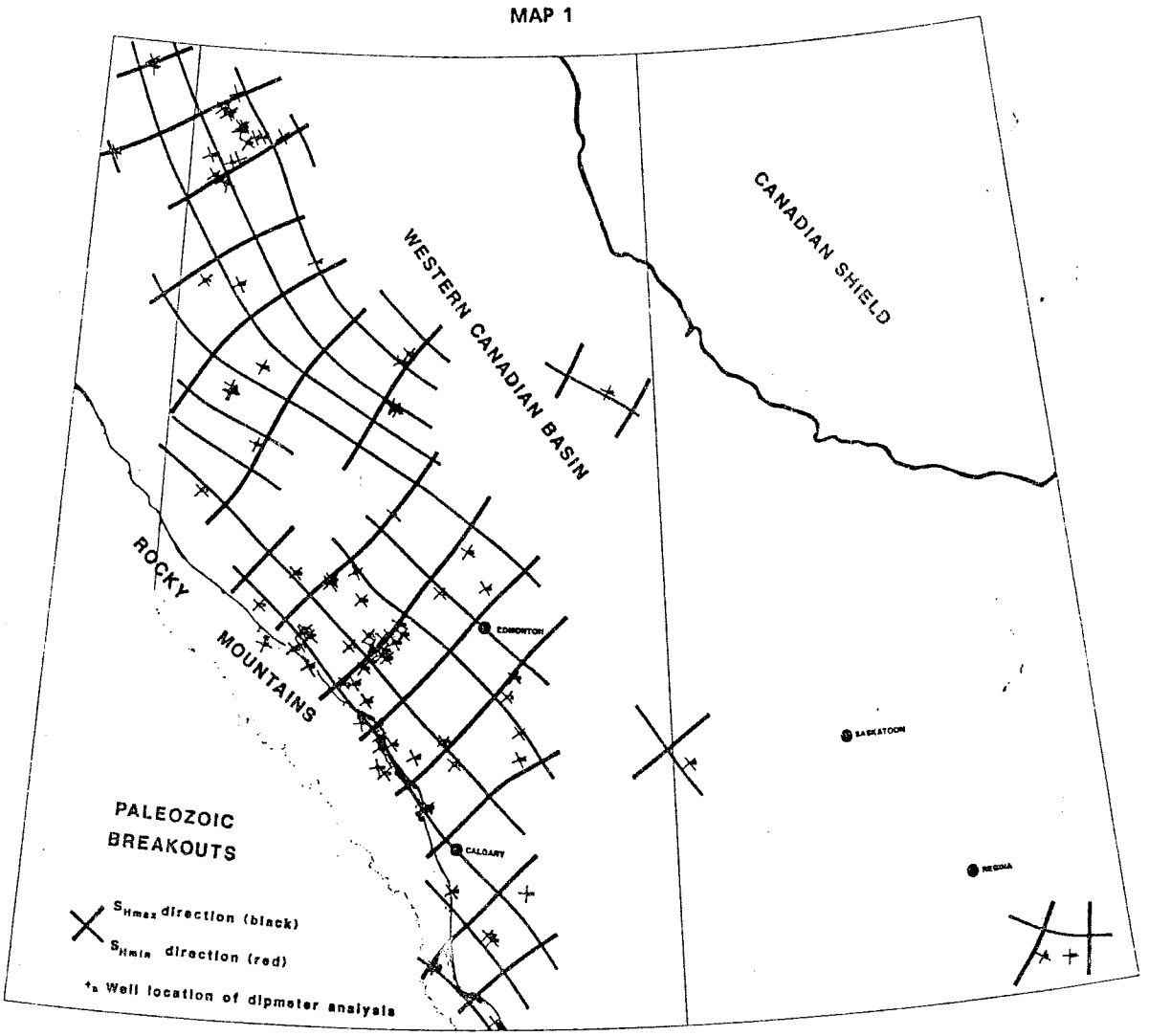

Fig. 43. Stress trajectories in Paleozoic rocks of the Western Canadian Basin as revealed by borehole breakouts. The SHmax orientations can be used to predict the directions of propagation of hydraulic fractures that are induced in Paleozoic rocks (Bell and Price, 1989).

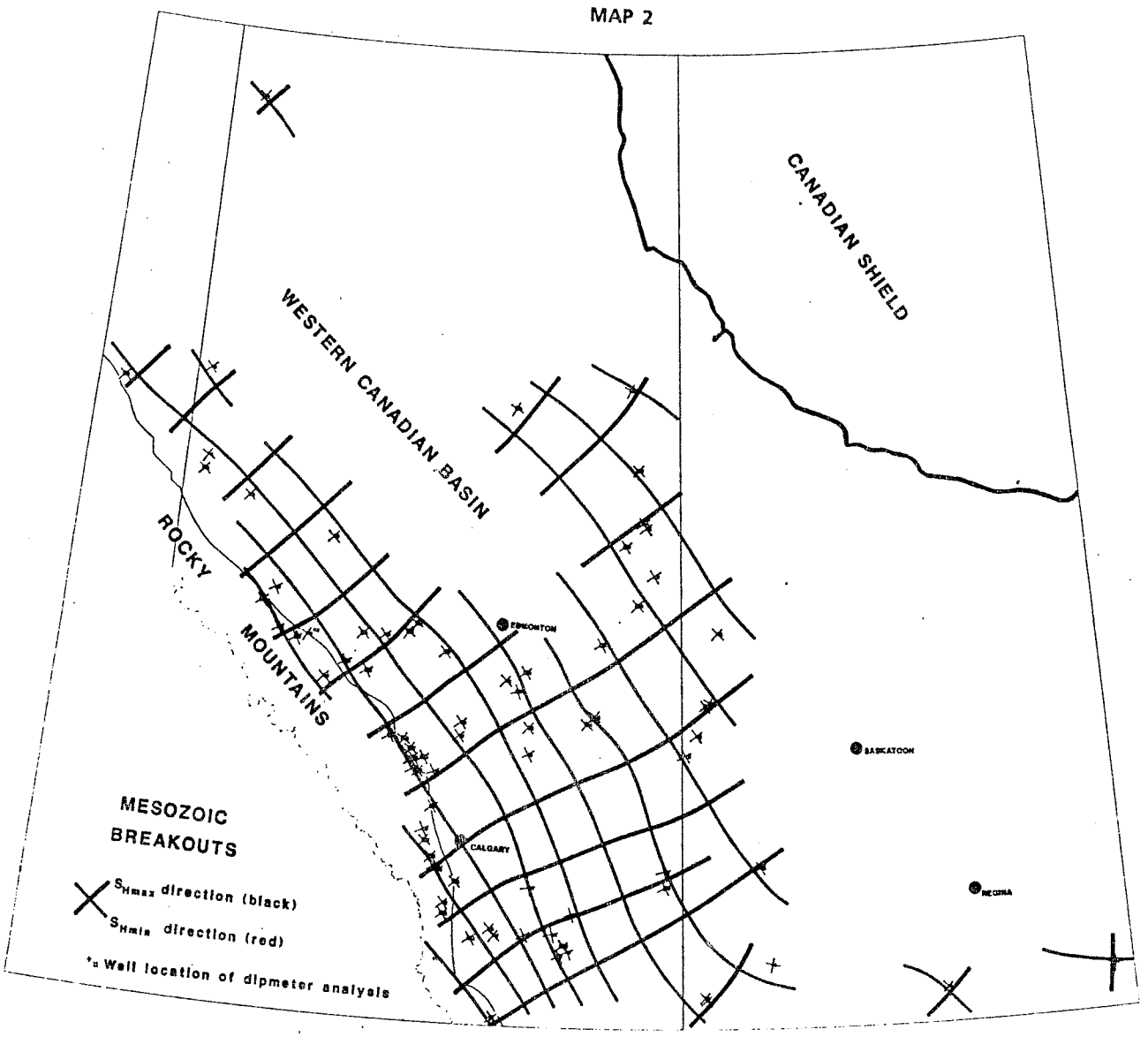

Fig. 44. Stress trajectories in Mesozoic rocks of the Western Canadian Basin as revealed by breakouts. As discussed for Fig. 43, this map is useful for predicting hydraulic fracture orientations in Mesozoic rocks (Bell and Price, 1989).

INCLINED AND HORIZONTAL WELLS

Where there are thick pay sections in "tight" reservoirs, drilling inclined or horizontal wells, and spacing a series of fractures along them, will very often result in significantly improved flow rates. For good results, the inclined or horizontal well should be directed at a high angle to the predicted hydraulic fracture planes. One needs to know the local principal stress orientations to aim such a well appropriately.

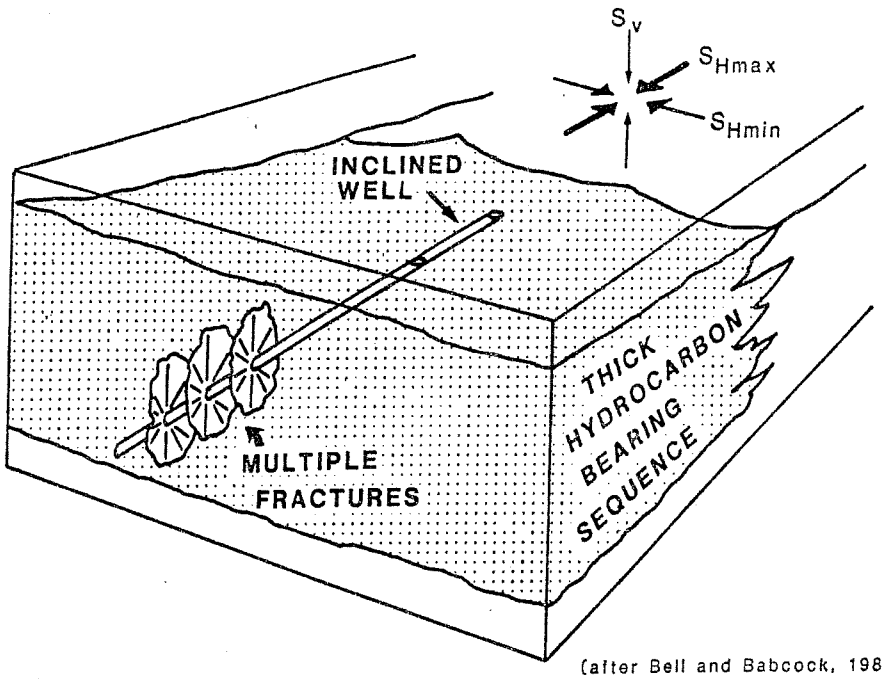

Fig. 45. Schematic block diagram of a multiply fractured inclined well drilled into a thick hydrocarbon-bearing sequence at approximately 45° to SHmin. The multiple fractures feeding such a well would provide greater drainage and higher flow rates than one could expect to obtain from a vertical well with a single fracture feeding it.

In Western Canada, such wells may augment the production of gas from areas like the Deep Basin.

SECONDARY RECOVERY

Secondary recovery programs can benefit from controlled hydraulic fracturing, whereas inadvertent fracturing can reduce their efficiency. In either case, it can be of great assistance to understand the stress regime well enough to be able to predict what pressures will be required to initiate and advance hydraulic fractures and to know what direction they will follow.

The situation at Pembina in Western Canada has been discussed briefly as an example of "mapping" hydraulic fractures to determine stress orientations. In the Pembina field, most of the oil is trapped stratigraphically in Cretaceous sandstones at depths of 1500 to 2000 m. Waterflooding has been employed since 1956 and is responsible for more than 80% of the total procduction. Some of the early waterfloods were injected at pressures well above the smaller principal stress, which is horizontal and oriented NW-SE in the Pembina area (Gough and Bell, 1981). As a result, some water injection wells propagated induced hydraulic fractures northeastwards and southwestwards, and the fractures connected the injection wells to adjacent production wells that were offset in these directions. McLeod (1977) and Hassan (1982) have described the consequences. Initially, oil production increased markedly at wells adjacent to, and southwest or northeast of,the injection wells. However, within four months the increaased flow of oil was replaced almost completely by water, as water-filled propagating fractures, which initially had swept oil ahead of them, intersected the production wells. Once the connecting fractures became established as fluid conduits, they induced a "preferred permeability" in the sandstones and prevented the waterfloods from achieving optimum recovery.

An idealised oil field, based on the Pembina example, is illustrated in Fig. 46 (Bell and Babcock, 1986). It is located in a stress regime where hydraulic fractures will be vertical and propagate northeastwards and southwestwards away from water injection wells. Two waterflood configurations are shown. In the "bad" array, injection and production wells become linked by hydraulic fractures so that water is pumped into one well and flows out of another without sweeping much oil to any production well bores. In the "good" array, injection and production wells are so spaced that induced hydraulic fractures will not connect any wells, and they will actually help distribute the waterflood so that it can sweep oil towards many production wells.

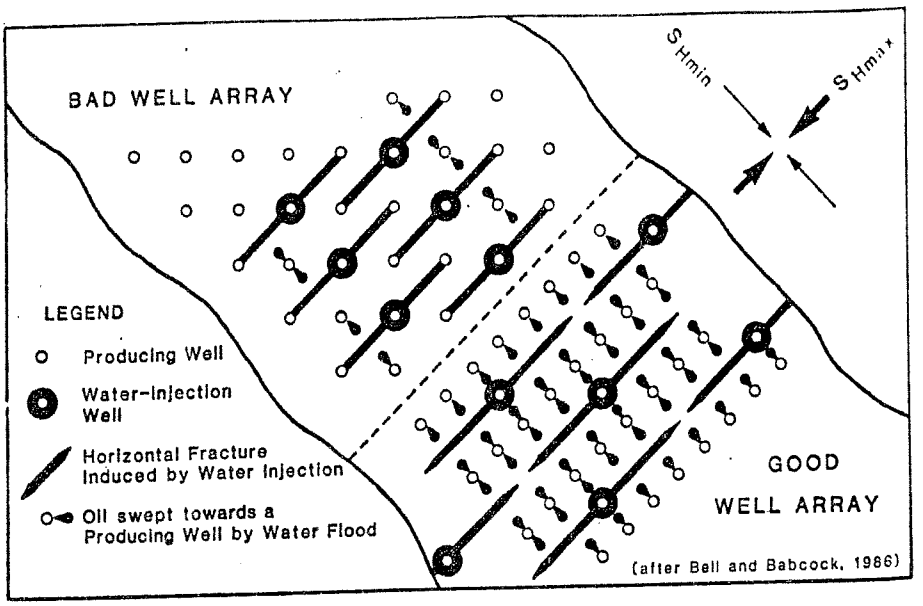

Fig. 46. Map of well arrays in an oilfield where water flooding promotes hydraulic fracturing. An explanation is given in the text (Bell and Babcock, 1986).

The Wattenberg field in the western United States is produced using this approach. The gas-bearing sands there are tight and they require massive hydraulic fracturing to become productive at economic rates. The induced fractures propagate in the 340-160° azimuth (Smith et al., 1978) and simulation studies suggest that their optimum length is 1200 m (Roberts, 1981). Field monitoring has documented gas drainage into these fractures from axially-aligned ellipsoidal zones around them, and the most productive gas wells are those that are located so as to exploit the optimum fracture length and preferred orientation (Smith, 1979).

There are other cases where it is important to prevent inadvertent hydraulic fracturing, as the Norman Wells case history demonstrates (Kempthorne and Irish, 1981; Gronseth and Kry, 1987). Oil occurs here in the Devonian Kee Scarp limestone reef complex which averages 110 m in thickness. The beds dip to the southwest and are between 300 and 600 m deep. The limestone is naturally fractured and the fractures do not penetrate the overlying shale seal. The natural fractures trend NE-SW and give the reservoir a directional permeability parallel to the fracture trend. Breakouts do not occur in the fractured limestones (probably because the fractures effectively dissipate amplified shear stresses), but they are present in the overlying, unfractured shales (Gough and Bell, 1982) and indicate that SHmax is today oriented NE-SW.

Esso's original depletion plan involved waterflooding from the start, perforating new wells in the lower part of the reservoir and hydraulically fracturing them. This strategy was based on the assumption that the smallest principal stress was horizontal and oriented NW-SE, so that the fractures would be vertical and extend parallel to the preexisting natural fractures. It was also assumed that such induced fractures would extend through the reservoir limestone and could be confined within it. However, an extensive in-situ stress determination program proved otherwise. Mini-frac determinations and anelastic strain recovery measurements showed that, even at 600 m, the minimum principal stress was oriented vertically (Gronseth and Kry, 1987). Induced hydraulic fractures would be horizontal and vertical conformance could not be achieved by augmenting the natural fracture system with hydraulic fractures. Because of this, Esso's completion plans were changed to include multiple perforated intervals in wells based on natural permeability variations in the reservoir and the proposed waterflood injection pressures were reduced to prevent inducing any hydraulic fractures.

BOREHOLE STABILITY

Over the years, many suggestions have been advanced as to how caving in wells can be minimised. Changing the drilling rate, changing the chemistry of the mud system, using different bits, firing the drilling foreman, retiring the Production manager, blaming partners and various other methods of improving borehole stability have been tried. The problem is still very much with us and would seem to be related to shape of the borehole, the effective shear strength of the rocks surrounding it and the stress regime. At the present time, there is considerable geomechanical research being directed at borehole stability, so we can expect useful insights to emerge. The discussion here is very cursory.

Zoback et al. (1985) have simulated what happens around a borehole when variations are made in the horizontal stress magnitude contrast, the rock shear strength, its coefficient of friction and the mudweight pressure. They use the Mohr-Coulomb fracture criterion in which the failure envelope has a slope equal to the coefficient of sliding friction, μ , and an intercept, τ_o , equal to the shear strength of the rock. Their analysis is two-dimensional and involves a single cycle of failure. The results are shown below:

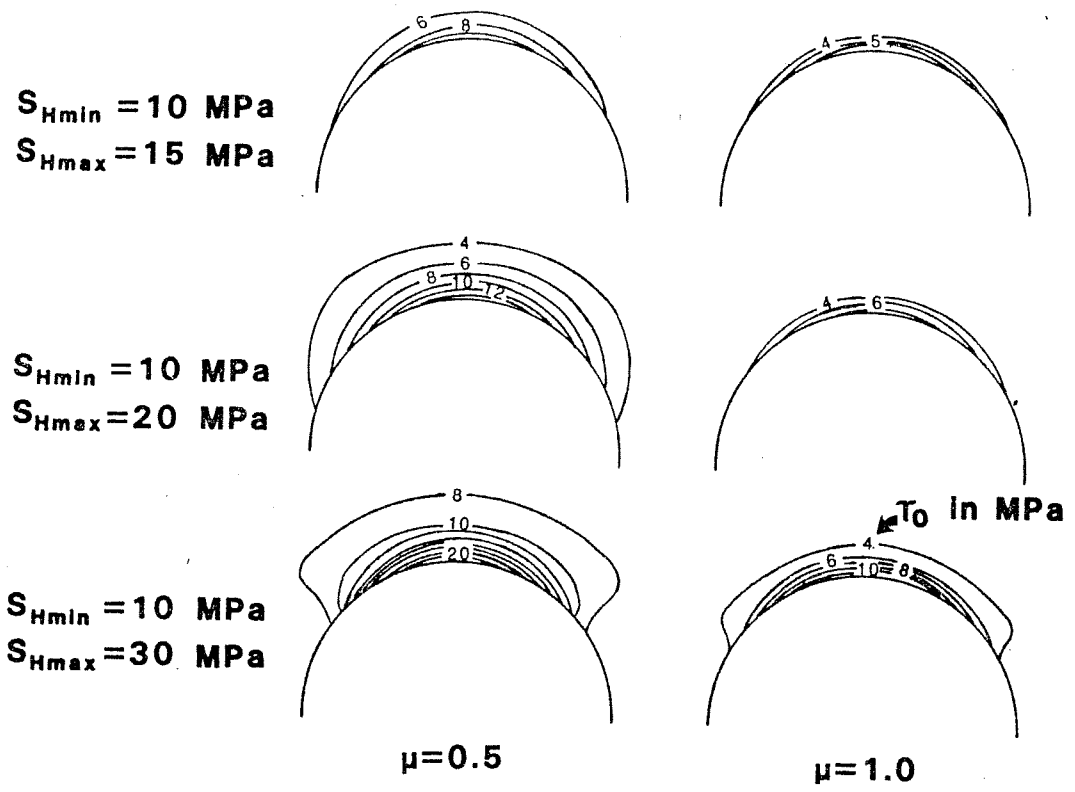

Fig. 47. The predicted effects in terms of borehole stability of varying the stress contrast, changing the shear strength of the rocks and altering their coefficient of friction. The boundaries of the zones in which caving is predicted to occur are labelled with values of rock strength in megapascals. Rocks with lower strengths cave more, as do rocks with a lower coefficient of friction. Increasing the stress contrast also increases caving and vice versa (after Zoback et al., 1985).

These simulations give breakouts of various shapes and sizes that are formed by caving, but they show that the lower the shear strength of the rock, the greater will be the amount of wall caving. More caving occurs if the farfield stress contrast is high than if it is low. The lower the rock's coefficient of friction, the greater will be the amount of caving. Suppose, we now vary the mudweight, and keep all the other parameters constant.

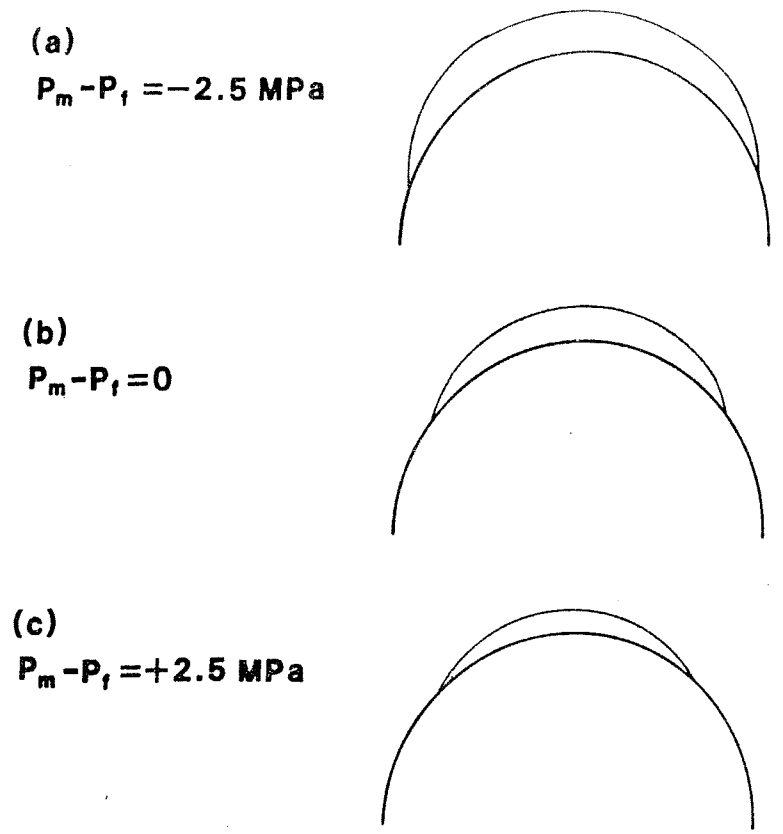

Fig. 48. In this simulation of caving, the model is an isotropic rock with shear strength of 7.5 MPa, μ of 0.6, surrounding a hole drilled in a location where SHmax is 22 MPa and SHmin is 11 MPa. The mudweight is varied between (a) 2.5 MPa below formation pressure, (b) equivalent to formation pressure and (c) 2.5 MPa above formation pressure. Note that caving decreases as the mudweight is raised (after Zoback et al., 1985).

Caving will be suppressed by increasing the mudweight so that it exceeds the formation pressure.

These simulations are simple, but they show that the stress regime and the physical properties of the rocks being drilled have a significant impact on borehole stability. What can be done? We cannot change the rock properties or the stress regime, but we may be able to mitigate their effects. Cooling the mud can improve stability, as can raising the mudweight by a conservative amount (Woodland, 1987). Drilling a smaller hole will also limit caving (Gough and Bell, 1982), but this is rarely practical in oilfield operations. Tunnellers and mine shaft borers face the same problems and control them by lagging their excavations. Is it possible that some kind of mud can be developed which spreads a skin on the side of a wellbore as the well is drilled? Whether or not an exotic technique like this is developed, knowing the basic causes

of the caving can save drillers paying for expensive remedies that are not likely to be effective.

EXPLORING FOR FRACTURED RESERVOIRS

Books have been written and many papers published on how best to explore for fractured reservoirs and it is not my intention to review all the suggestions and case histories here. What may have been overlooked is, if fractures are present and contributing to reservoir performance, where are they most likely to be doing this most effectively? It is suspected that, all other factors being equal, this will be in areas where the minimum principal stress, at a given depth, is smallest. This is because in-situ stresses keep natural fractures closed. If this is true, it is one more reason why we should have a long-term goal of mapping regional variations in SHmin magnitudes. Such work is presently underway in Western Canada (Bell and Price, 1989) and preliminary results should be available shortly.

DIRECTIONAL PERMEABILITY

Does the stress regime in a region affect the development of permeability in reservoir rocks there? At this time we have no answers to this intriguing question, but it would seem to be possible, especially in the Western Canadian Basin.

The stress trajectory maps of the Western Canadian Basin show a horizontal principal stress configuration that appears to be geometrically related to thrust faulting in the Foothills and Rocky Mountains. Regionally speaking SHmax is oriented perpendicular to the traces of these faults. Stauffer and Gendzwill (1987) cite geological evidence that supports the existence of similarly oriented horizontal principal stresses during much of Mesozoic and Cenozoic time. In other words, SHmax has probably had a generally NE-SW orientation for at least the last100 million years. Therefore, the younger Mesozoic sediments are likely to have spent most of their burial life under anisotropic horizontal stress. What might the consequence be? Could this produce preferentially-oriented pressure solution cementation of quartz sand grains, for example? And, if so, could this lead to the growth of a directional permeability fabric in sandstones? And what about the development of natural fractures that formed in an anisotropic stress field? Could they give rise to a component of directional permeability?

The answer is: we do not know. Permeability anisotropy is widely documented, but only by measuring the permeability through a vertically-oriented plug and comparing this to the permeabilty of a horizontal plug of random orientation. As a rule, we do not take two orthogonal plugs in the horizontal plane, and we collect very few oriented cores. It would seem that out of curiosity alone, it would be worth exploring the possibility that some of our reservoirs flow better in one horizontal direction than another, as a consequence of rock fabric. If this occurs, knowledge of such preferred permeability will be very valuable, and it may well be that its development can be related to former stress regimes.

BIBLIOGRAPHY

Adams, J., 1982. Stress-relief buckles in McFarland Quarry, Ottawa. Canadian Jornal of Earth Sciences, v.19, p.1883-1887.

Adams, J. 1987. Canadian crustal stress database - a compilation to 1987. Geological Survey of Canada Open File Report 1622, 130p.

Barton, C. A., and Zoback, M. D., 1988. Determination of in situ stress orientation from borehole guided waves. Journal of Geophysical Research, v. 93, p. 7834-7844.

Bell, J. S., 1985. Offset boreholes in the Rocky Mountains of Alberta, Canada. Geology, v.13, p.734-737.

Bell, J. S., in press. Investigating stress regimes in sedimentary basins using information from oil industry wireline logs and drilling records. Special Publication, Geological Society of London.

Bell, J. S., and Babcock, E. A., 1986. The stress regime of the Western Canadian Basin and implications for hydrocarbon production. Bulletin of Canadian Petroleum Geology, v.34, p. 364-378.

Bell, J. S. and Price, P. R., 1989. In-situ stresses in Western Canada: Implications for the Oil Industry. Poster presented at Forum '89 - Oil and Gas Activities in Canada, Geological Survey of Canada, February 27-28, Calgary.

Blanton, T. L., 1983. The relation between recovery deformation and in situ stress magnitudes. SPE Paper 11624, SPE/DOE Symposium on Low Permeability Gass Reservoirs, Denver, Colorado, March 14-16, 1983.

Blanton, T. L., and Teufel, L. W., 1983. A field test of the strain recovery method of stress determination in Devonian shale. SPE Paper 12304, Eastern Regional Meeting, Society of Petroleum Engineers of AIME, Champion, Pennsylvania, November 9-11, 1983.

Brace, W. F., and Kohlstedt, D L., 1980. Limits on lithospheric stress imposed by laboratory experiments. Journal of Geophysical Research, v. 85, p. 6248-6252.

Breckels, I. M., and Van Eekelen, H. A. M., 1981. Relationship between horizontal stress and depth in sedimentary basins. Paper SPE10336, 56th Annual Fall Technical Conference, Society of Petroleum Engineers of AIME, San Antonio, Texas, October 5-7, 1981.

Bredehoeft, J. D., Wolff, R. G., Keys, W. S., and Shuter, E., 1976. Hydraulic fracturing to determine the regional in-situ stress field, Piceance Basin, Colorado. Geological Society of America Bulletin, v. 87, p. 250-280.

Brereton, N. R., and Evans, C. J., 1987. Rock stress orientations in the United Kingdom from borehole breakouts. Report RG 87/14, British Geological Survey, 36p.

Brown, R. O., 1979. Fracture Identification Log use in Cretaceous of N. Louisiana, Mississippi. Oil and Gas Journal, v.77, no. 18, p.350-355.

Crampin, S., 1987. Geological and industrial implications of extensive-dilatancy anisotropy. Nature, v. 328, p. 491-496.

Daneshy, A. A., Slusher, G. L., Chisholm, P. T., and Magee, D. A., 1986. In-Situ Stress Measurements During Drilling. Journal of Petroleum Technology, August 1986, p. 891-898.

Dickey, P. A., 1986. Petroleum Development Geology, 3rd Edition. Penwell Books, Oklahoma, 530 p.

Ervine, W. B., and Bell, J. S., 1987. Subsurface in-situ stress magnitudes from oil well drilling records: an example from the Venture area, offshore Eastern Canada. Canadian Journal of Earth Sciences, v. 24, p. 1748-1759.

Fordjor, C. K., Bell, J. S., and Gough, D. I., 1983. Breakouts in Alberta and stress in the North American plate. Canadian Journal of Earth Sciences, v. 20, p. 1445-1455.

Gough, D. I., and Bell, J. S., 1981. Stress orientations from oil well fractures in Alberta nd Texas. Canadian Journal of Earth Sciences, v. 18, p. 638-645.

Gough, D. I., and Bell, J. S., 1982. Stress orientations from borehole wall fractures with examples from Colorado, east Texas and

northern Canada. Canadian Journal of Earth Sciences, v. 19, p. 1358-1370.

Gough, D. I., and Gough, W. I., 1987. Stress near the surface of the Earth. Annual Review of Earth and Planetary Sciences, v.15, p. 545-566.

Gronseth, J. M., and Kry, P. R., 1987. In-situ stresses and the Norman Wells expansion project. Paper 87-38-57, 38th Annual Technical Meeting, Petroleum Society of CIMM, Calgary, June 7-10, 1987.

Haimson, B. C., and Fairhurst, C., 1970, *In-situ* stress determination at great depth by means of hydraulic fracturing. *In* Rock Mechanics - theory and practice. Proceedings of the 11th Symposium on Rock Mechanics edited by W. Somerton, American Institute of Mining Engineers, New York, NY, p. 559-584.

Haimson, B. C., and Herrick, C. G., 1986. Borehole breakouts - a new tool for estimating in situ stress? Proceedings, International Symposium on Rock Stress and Rock Stress Measurements, Stockholm, 1-3 September, 1986. Editor: O. Stephansson. p. 271-280.

Hassan, D., 1982. A method for predicting hydraulic fracture azimuth and the implication thereof to improve hydrocarbon recovery. Paper 82-33-19, 33rd Annual Technical Meeting, Petroleum Society of CIMM, Calgary, June 6-9, 1982.

Hoek, E., and Brown, E. T., 1980. Underground Excavations in Rock. Institute of Mining and Metallurgy, London, 527 p.

Hubbert, M. K., and Willis, D. G., 1957. Mechanics of hydraulic fracturing. AIME Petroleum Transactions, v. 210, p. 153-166.

Kempthorne, R. H., and Irish, J. P. R., 1981. Norman Wells - a new look at one of Canada's largest oil fields. Journal of Petroleum Technology, v. 33, p. 985-991.

Kry, P. R., and Gronseth, J. M., 1982. In-situ stresses and hydraulic frcturing in the Deep Basin. Paper 88-33-21, 33rd Annual Tachnical Meeting, Petroleum Society of CIMM, Calgary, June 6-9, 1982.

Mardia, K. V., 1972. Statistics of directional data: probability and mathematical statistics. Academic Press, London and New York, 357 p.

McGarr, A., and Gay, N. C., 1978. State of stress in the Earth's crust. Annual Review of Earth and Planetary Sciences, v. 6, p. 405-436.

McKenzie, D. P., 1969. The relation between fault plane solutions for earthquakes and the directions of the principal stresses. Bulletin of the Seismological Society of America, v. 59, p. 591-601.

McLellan, P., 1988. In situ stress prediction and measurement by hydraulic fracturing, Wapiti, Alberta. Journal of Canadian Petroleum Technology, v. 27, no. 2, p. 85-95.

McLennan, J. D., and Roegiers, J-C., 1982. How instantaneous are instantaneous shut in pressures? SPE Paper 11064, 57th Annual Technical Conference and Exhibition of SPE, New Orleans, Louisiana.

McLeod, J. G. F., 1977. Successful injection pattern alteration, Pembina J Lease, Alberta. Paper presented at 28th Annual Meeting, Petroleum Society of CIMM, Edmonton.

Montgomery, C. T., and Ren, N-K., 1983. Differential strain curve analysis: does it work? *in* M. D. Zoback and B. C. Haimson (editors),Hydraulic Fracture Stress Measurements. National Academy Press, Washington, D. C. , p. 239-245.

Nakamura, K., Jacob, K. H., and Davies, J. N., 1977. Volcanoes as possible indicators of tectonic stress orientation: Aleutians and Alaska. *in* Wyss, M. (editor) Stress in the Earth, Special issue of Pure and Applied Geophysics, v. 115.

Newmark, R. L., Zoback, M. D., and Anderson, R. N., 1984. Orientation of in-situ stresses in oceanic crust. Nature, v. 311, p. 424-428.

Nolte, K. G., 1982. Determination of fracture parameters from fracturing pressure decline. SPE Paper 10911, SPE Cotton Valley Symposium, Tyler, Texas.

Nur, A., and Simmons, G., 1969. The effect of saturation on velocity in low porosity rocks. Earth and Planetary Science Letters, v. 7, p.183-193.

Paillet, F. L., and Kim, K., 1987. Character and distribution of borehole breakouts and their relationship to in situ stresses in deep Columbia River basalts. Journal of Geophysical Research, v. 92, p. 6223-6234.

Podrouzek, A. J., and Bell, J. S., 1985. Stress orientations from wellbore breakouts on the Scotian Shelf. *in* Current Research Part B, Geological Survey of Canada, Paper 85-1B, p. 59-62.

Roberts, C. N., 1981. Fracture optimization in a tight gas play: Muddy "J" Formation, Wattenberg field, Colorado. Paper SPE-DOE 9851, Low Permeability Symposium, Denver, Colorado, May 27-29, 1981.

Schmitt, D. R., 1989. Consequences of crustal stresses and their quantitative measurement. p. 30-31 *in* Scientific Drilling: Sedimentary Basins, M. J. Drury (editor), Canadian Continental Drilling Program Report 89-3, Carleton University, Ottawa, 40 p.

Smith, M. B., 1979. Effect of fracture azimuth on production with application to the Wattenberg gas field. SPE Paper 8298, 54th Annula Fall Conference, Society of Petroleum Engineers of AIME, Las Vegas, Nevada, September 23-26, 1979.

Smith, M. B., Holman G. B., Fast C. R., and Corlin, R. J., 1978. The azimuth of deep, penetrating fractures in the Wattenberg field. Journal of Petroleum Technology, v. 30, p. 185-193.

Stauffer, M. R., and Gendzwill, D. J. 1987. Fractures in the northern plains, stream patterns, and the midcontinent stress field. Canadian Journal of Earth Sciences, v. 24, p. 1086-1097.

Strickland, F. G., and Ren, N-K., 1980. Predicting the in-situ stress state for deep wells using differential strain curve analysis. Paper 80-31-33, 31st Annual Technical Meeting, Petroleum Society of CIM, Calgary, May 25-28, 1980.

Teufel, L. W., 1982. Prediction of Hydraulic Fracture Azimuth from Anelastic Strain Recovery Measurements of Oriented Core. Paper presented at 23rd U. S. Symposium on Rock Mechanics, Berkeley, California, 1982.

Teufel, L. W., and Warpinski, N. R., 1984. Determination of in situ stress from anelastic strain recovery measurements of oriented core: comparison to hydraulic fracture stress measurements in the Piceance Basin, Colorado. Paper presented at 25th U. S. Symposium on Rock Mechanics, Evanston, Illinois, June 1984.

Tittman, J., and Wahl., 1965. The physical foundations of formation density logging (gamma-gamma). Geophysics, v. 30, no. 2, p. 284-294.

Voight, B.., 1968. Determination of the virgin state of stress in the vicinity of a borehole from measurements of the partial anelastic strain tensor in drill cores. Felsmechanik, U. Ingeniergeol., v. 6, p. 201-215.

Wiley, R., 1981. The borehole televiewer: An update on application. World Oil, March 1981, p. 47-53.

Wood, M. D., 1978. Fracture Mapping - Tilt Method - Progress Report. Paper presented at 4th Annual DOE Symposium, Tulsa Oklahoma, 1978.

Woodland, D. C., 1987. Borehole stability in western Canada foothills. Poster presented at 38th annual Technical Meeting, Petroleum Society of CIMM, Calgary, June 7-10, 1987.

Woodland, D. C., and Bell, J. S., 1988. In-situ stress magnitudes from mini-frac records in western Canada. Paper 88-39-67, 39th Annual Technical Meeting, Petroleum Society of CIM, Calgary, June 12-16, 1988.

Zoback, M. D., Moos, D., Mastin, L., and Anderson, R. N., 1985. Wellbore breakouts and in-situ stress. Journal of Geophysical Research, v. 90, p. 5523-5530.

Zoback, M. L., and 22 co-authors, 1989. Global patterns of intraplate stress: a status report on the World Stress Map Project of the International Lithosphere Program. Nature (Fall 1989).

STRESS IN SEDIMENTARY BASINS SEMINAR

presented to Petro Canada Resources Inc.

May 12th, 1989, 1.30 - 4.30 pm.

by

Sebastian Bell and Paul Price

Institute of Sedimentary and Petroleum Geology,
3303 33rd St. N .W., Calgary, Alberta T2L 2A7.
Telephone: 403-284-0110

PROGRAM

1.30	Bell	Introduction	Slides 1,2,3 Viewgraph 1
1.37	Price	Sv calculation	Viewgraph 2 Slide 4 Viewgraph 3 Slide 5
1.45	Bell	Hydraulic fracturing	Viewgraphs 4,5,6 Slides 6,7,8 Viewgraph 7
		SHmax det'n, Pembina	Slides 9, 10, 10a, 10b
2.05	Bell and Price	HYDRAULIC FRACTURE EXERCISE	
2.25	Bell	Leak-off tests	Slides 11,12 Viewgraphs 8,9 Slides 13,14,15,16,17 Viewgraph 10
		Scotian sh. rock strength	Slides 18,19,20,21 Viewgraphs 11,12
2.55		COFFEE BREAK	
3.15	Price	Breakouts	Slides 22,23,24,25,26 Viewgraph 13

			Slides 27,28,29,30,31, 32,33,34,35,36,37,38
3.45	Price and Bell	BOREHOLE BREAKOUT EXERCISE	
4.05	Bell	Other stress direction indicators	Viewgraphs 14,15,16 Slides 39,40,41,42,43,44
4.15	Price	Earthquake focal mechanisms	Viewgraphs 17,18,19 Slide 45
4.20	Bell	Applications	Slides 46,47,48,49,50,51, 52,53,54,55
4.30		End of seminar	

HYDRAULIC FRACTURE ANALYSIS - STRESS MAGNITUDES

Purpose

To use industrial hydraulic fracture records to estimate the magnitude of the smallest principal stress and, by estimating the vertical stress, determine the in-situ stress regime at the fracture depth. The pressure/time record comes from a fracture treatment applied to a Mesozoic sandstone interval in western Canada (T 36-38, R 6-10W5).

Method

1. Note the fluid column pressure at fracture depth.
2. Examine the pressure/time record. Label it with fracture breakdown, fracture propagation and the pressure at which you think the fracture closed (Instantaneous shut in pressure). Measure the ISIP, using the digital printout if necessary.
3. Add the fluid column pressure to the ISIP; this equates to the smallest principal stress. Note its value.
4. Multiply the fracture depth (mid-point true depth) by an assigned density (2.4 - 2.5 is suitable) to obtain the vertical principal stress. Compare it to the ISIP. If Sv > ISIP, then Sv > SHmin, and the ISIP measures SHmin.
5. If ISIP > Sv, there may be a problem with the interpretation. If this proves to be a valid solution, it means that Sv < SHmin < SHmax. If Sv > SHmin, SHmax can be estimated from the equation:

$$SHmax = 3\ SHmin - Pb - Pp + T$$

where Pb is the breakdown pressure, Pp is the pore fluid pressure and T is the tensile strength. To use this equation with this type of fracture record, we have to make the approximation that: Pb - T = Pfp, the fracture propagation pressure. So, if we can estimate pore pressure, we can use the expression:

$$SHmax = 3\ SHmin - Pfp - Pp$$

6. Solve the above equation for SHmax using the given Reservoir Pressure. If the pressure is not known, assume it is hydrostatic.
7. Report estimated stress magnitudes for fracture depth.

Application

Stress magnitude estimates can be used to help assess the potential for fracture containment. The values of SHmin can be

normalised to depth to give the stress gradient. If this procedure is followed for several wells in an area, regional variations in stress can be mapped. This can be done for SHmax gradients as well, but is likely to be less reliable. Such maps can aid exploration and exploitation.

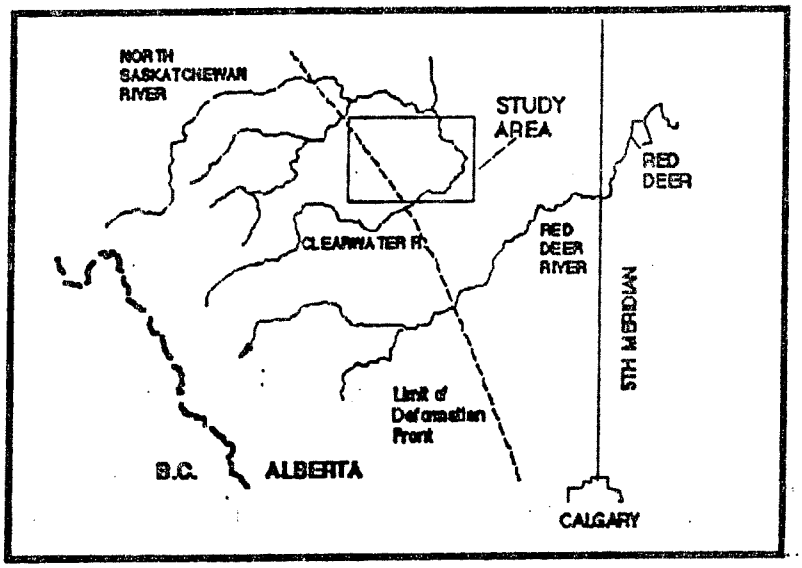

Location Map

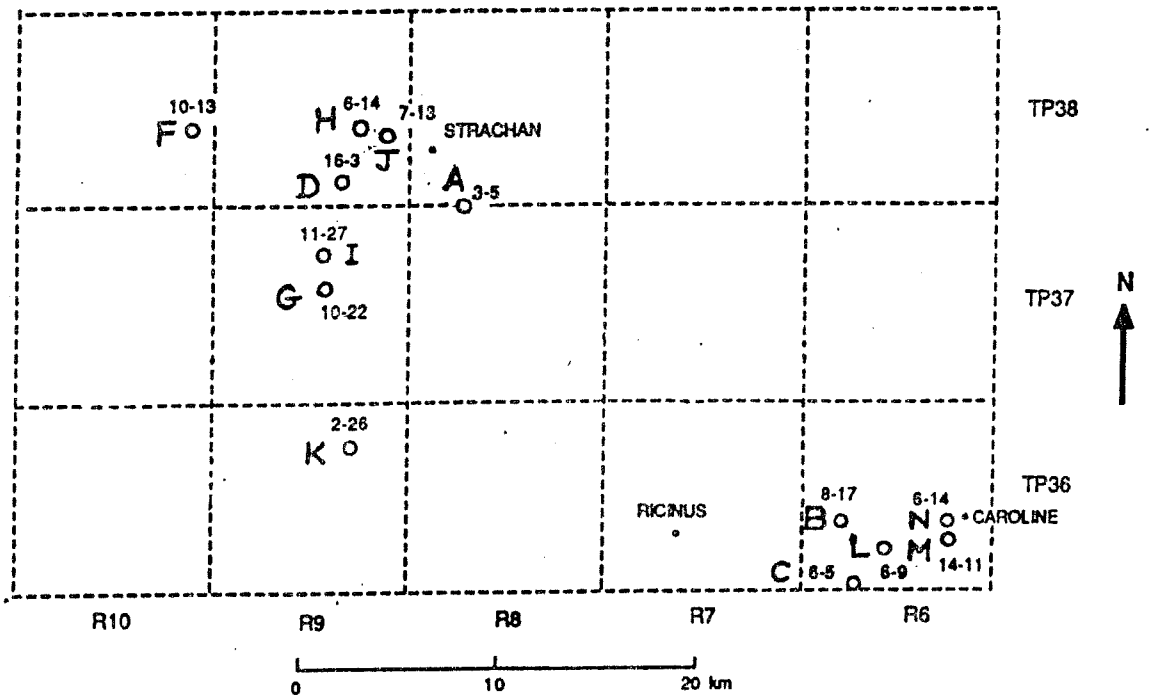

Wells with hydraulic fracture treatments studied in this exercise.

Well: **2-26-36-9W5** **WELL K-a**
Fracture type: Mini-frac.
Mid-point true depth: 2883.4 m.
Fluid column pressure: 25.4 MPa.
Reservoir pressure: 26.3 MPa.

FIGURE A.22: GULF et al. RICINUS 2-26-36-9-W5M (Cardium Fm)

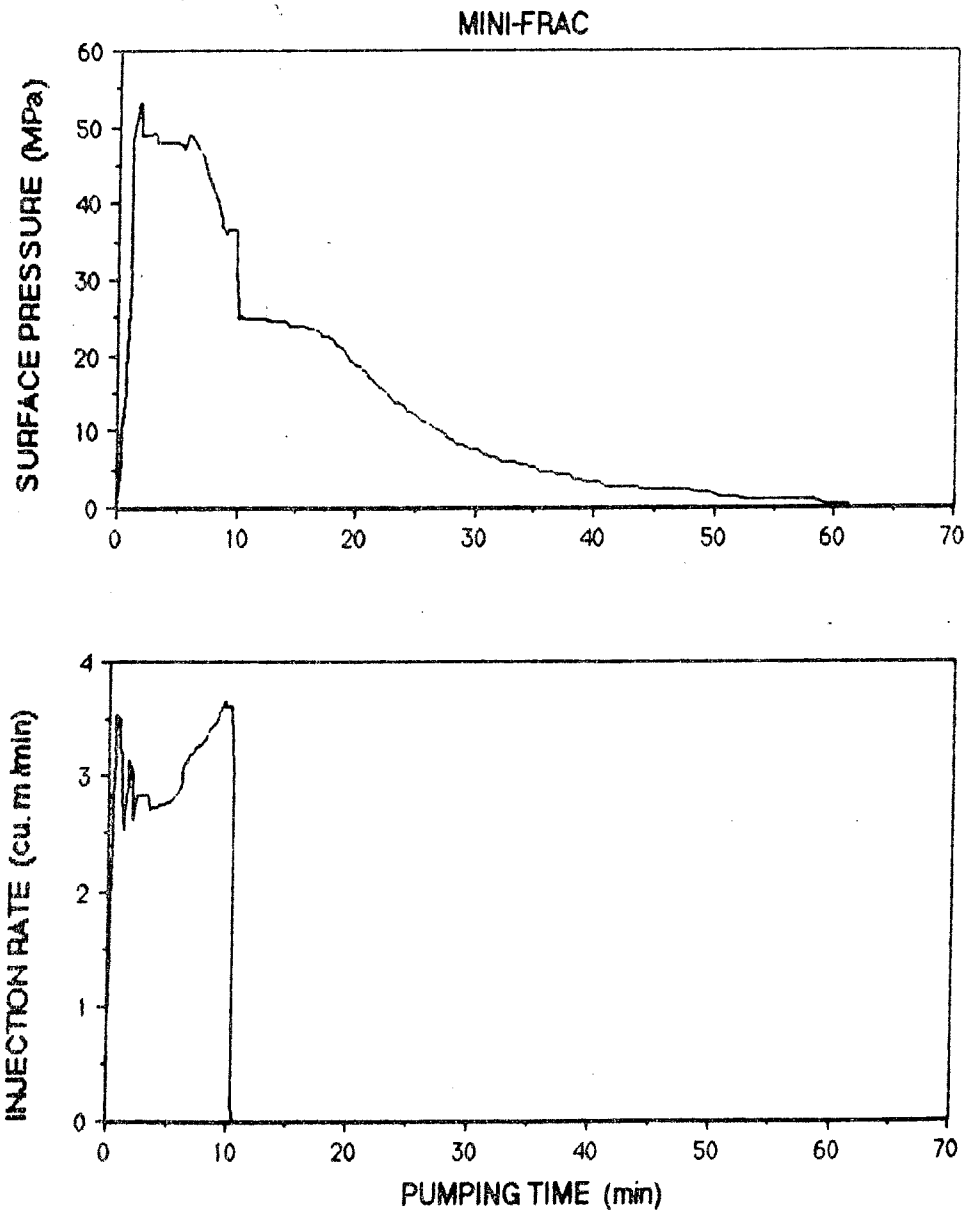

TABLE B.22 : GULF ET AL RICINUS 2-26-36-9W5 (CARDIUN FM) MINI-FRAC

TIME (min)	SURFACE PRESSURE (MPa)	TIME (min)	INJECTION RATE (cu.m /min)	TIME (min)	BOTTOMHOLE PRESSURE (MPa)
0.00	0.0	0.00	0.00	0.00	20.9
0.29	6.0	0.01	0.75	0.18	20.3
0.43	10.1	0.12	1.50	0.36	21.2
0.57	12.4	0.23	1.83	0.45	23.3
0.72	15.2	0.28	2.47	0.73	25.9
0.72	17.5	0.44	2.77	0.82	29.5
0.86	23.5	0.60	3.16	0.82	32.5
1.00	29.0	0.60	3.54	1.09	38.8
1.00	35.0	0.82	3.51	1.18	44.7
1.00	38.3	0.84	3.39	1.18	54.9
1.00	44.2	0.93	3.27	1.27	59.9
1.14	48.4	1.04	3.18	1.36	64.1
1.31	49.8	1.09	2.99	1.45	66.5
1.37	51.1	1.14	2.81	1.54	66.8
1.43	51.6	1.25	2.52	1.63	68.0
1.57	53.0	1.31	2.62	1.82	68.3
1.72	53.0	1.41	2.79	2.00	66.2
1.72	49.3	1.47	2.83	2.00	64.7
1.86	48.9	1.58	2.89	2.36	64.7
2.15	48.9	1.68	3.00	2.91	65.3
2.57	48.9	1.68	3.04	3.27	65.0
2.86	49.3	1.68	3.14	3.27	64.4
3.00	48.9	1.90	3.04	3.81	64.1
3.15	47.9	1.90	2.93	4.54	64.1
3.72	47.9	1.95	2.62	4.72	64.1
4.29	47.9	2.06	2.72	4.99	63.8
4.43	47.9	2.28	2.83	5.54	62.9
4.86	47.9	2.49	2.83	5.72	63.8
5.15	47.5	3.25	2.83	5.81	64.7
5.43	47.0	3.35	2.70	6.08	64.7
5.43	47.0	3.46	2.72	6.45	63.8
5.58	47.9	3.68	2.74	6.72	62.0
5.72	48.9	4.11	2.75	7.36	60.2
5.86	48.9	4.86	2.77	7.63	58.8
6.29	47.9	5.19	2.79	7.90	56.4
7.01	46.1	5.67	2.85	8.35	54.3
7.29	43.8	5.94	2.87	8.72	52.5
7.72	42.4	6.00	2.95	8.99	51.3
8.29	40.1	6.05	3.02	9.17	49.8
8.58	37.8	6.21	3.12	9.44	50.7
8.72	36.9	6.48	3.12	9.90	50.4

TABLE B.22 : GULF ET AL RICINUS 2-26-36-9W5 (CARDIUN FM) MINI-FRAC

TIME (min)	SURFACE PRESSURE (MPa)	TIME (min)	INJECTION RATE (cu.m /min)	TIME (min)	BOTTOMHOLE PRESSURE (MPa)
9.01	35.9	6.59	3.18	9.90	46.8
9.15	36.4	6.97	3.20	10.08	50.4
9.87	36.4	7.34	3.27	10.53	51.0
9.87	30.9	7.67	3.29	10.90	50.7
10.01	26.3	8.04	3.33	11.44	50.4
10.15	24.9	8.48	3.41	11.90	50.4
10.58	24.9	8.91	3.49	12.44	50.1
11.43	24.8	9.18	3.54	12.99	50.7
12.18	24.7	9.66	3.66	13.44	50.4
12.87	24.4	9.66	3.62	13.98	49.8
13.16	24.4	10.09	3.60	14.44	49.8
14.01	24.4	10.25	3.58	14.89	49.5
14.44	24.0	10.31	3.02	15.44	49.5
14.73	24.0	10.36	0.14	15.98	49.5
15.30	24.0	10.47	0.00	16.44	48.6
15.73	24.0			17.07	48.3
16.02	23.5			17.53	48.0
16.30	23.5			18.16	47.4
16.44	23.5			18.61	46.8
16.87	23.0			19.07	46.2
17.16	22.6			19.52	45.6
17.59	22.6			19.89	45.0
17.73	22.1			20.34	44.1
18.02	22.1			20.88	43.2
18.16	21.7			21.43	42.4
18.45	21.2			21.97	41.8
18.45	21.2			22.52	41.2
18.88	20.7			22.79	40.3
19.16	20.3			23.34	39.7
19.30	19.8			23.88	39.1
19.45	19.4			24.43	38.2
19.59	19.4			24.97	37.6
19.88	18.9			25.61	37.0
20.16	18.4			25.88	36.7
20.31	18.4			26.24	36.1
20.59	18.0			26.79	35.8
20.73	18.0			27.33	35.2
20.88	17.5			27.88	34.6
21.02	17.1			28.69	34.0
21.31	17.1			29.33	33.4
21.45	16.6			29.78	33.1

TABLE B.22 : GULF ET AL RICINUS 2-26-36-9W5 (CARDIUN FM) MINI-FRAC

TIME (min)	SURFACE PRESSURE (MPa)	TIME (min)	INJECTION RATE (cu.m /min)	TIME (min)	BOTTOMHOLE PRESSURE (MPa)
21.74	16.1			30.51	32.5
22.16	15.7			30.87	31.9
22.31	15.2			31.51	31.9
22.59	14.7			32.05	31.6
22.88	14.3			32.51	31.3
23.16	13.8			33.05	31.0
23.59	13.8			33.78	31.0
24.02	13.4			34.14	30.7
24.31	12.4			34.60	30.4
24.59	12.4			35.05	30.1
25.02	12.0			35.69	30.1
25.45	11.5			36.41	29.5
25.88	11.1			37.05	29.2
26.31	10.6			38.23	28.9
26.88	10.1			39.14	28.9
27.31	9.7			40.13	28.3
27.60	9.2			41.32	28.0
28.03	8.8			42.50	27.7
28.46	8.3			43.77	27.4
28.88	8.3			44.95	27.1
29.31	7.8			46.04	27.1
29.74	7.4			47.85	26.8
30.17	7.4			49.85	26.8
30.74	6.9			51.85	26.5
31.03	6.9			54.39	26.2
31.32	6.5			56.93	26.2
31.74	6.5			59.84	25.7
32.32	6.0			61.20	25.7
32.75	6.0				
33.32	6.0				
33.75	5.5				
34.03	5.5				
34.32	5.5				
34.60	5.1				
35.03	5.1				
35.46	4.6				
35.89	4.6				
36.18	4.6				
36.46	4.6				
37.04	4.1				
37.46	4.1				

TABLE B.22 : GULF ET AL RICINUS 2-26-36-9W5 (CARDIUM FM) MINI-FRAC

TIME (min)	SURFACE PRESSURE (MPa)
37.89	4.1
38.32	3.7
38.89	3.7
39.47	3.2
39.89	3.2
40.47	3.2
41.04	2.8
41.90	2.8
42.33	2.8
43.04	2.8
43.61	2.8
44.33	2.3
45.19	2.3
45.90	2.3
46.76	2.3
47.62	2.3
48.62	1.8
49.62	1.8
50.62	1.4
51.76	1.4
52.76	0.9
53.91	0.9
55.48	0.9
56.77	0.9
57.48	0.9
58.34	0.9
59.34	0.5
60.20	0.5
61.20	0.5

Well: **14-11-36-6W5** **WELL M**
Fracture type: Main frac.
Mid-point true depth: 2670.6 m.
Fluid column pressure: 21.9 MPa.
Reservoir pressure: 24.0 MPa.

FIGURE A.31. GULF GARRINGTON 14-11-36-6W5 (Glauconite Frn)

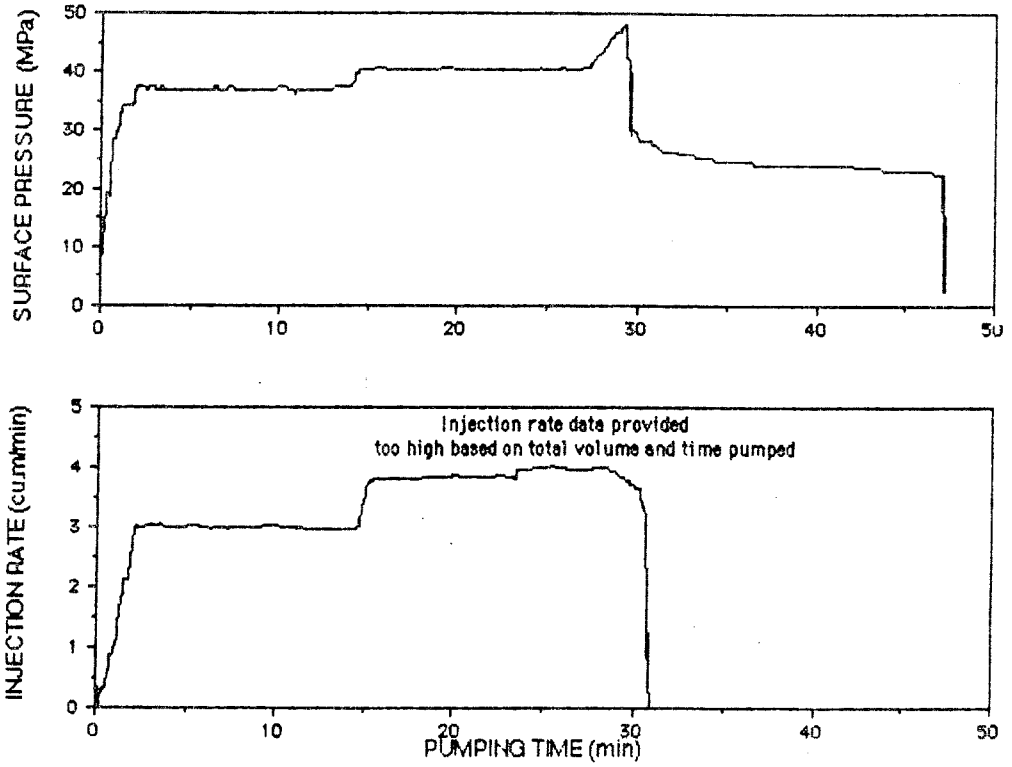

TABLE B.31 : GULF GARRINGTON 14-11-36-6W5 (GLAUCONITE FM)

TIME (min)	SURFACE PRESSURE (MPa)	TIME (min)	SURFACE PRESSURE (MPa)	TIME (min)	INJECTION RATE (cu.m /min)	TIME (min)	INJECTION RATE (cu.m /min)
0.00	2.0	0.47	23.1	0.00	0.00	0.70	0.67
0.00	2.6	0.47	24.2	0.08	0.00	0.70	0.64
0.00	3.1	0.58	24.7	0.08	0.04	0.70	0.67
0.00	3.7	0.58	25.3	0.00	0.04	0.70	0.71
0.00	4.2	0.58	25.8	0.00	0.07	0.70	0.74
0.00	4.8	0.58	26.4	0.00	0.11	0.70	0.78
0.00	5.3	0.58	26.9	0.00	0.14	0.70	0.81
0.00	5.9	0.58	27.5	0.00	0.21	0.70	0.85
0.00	6.4	0.58	28.1	0.00	0.25	0.70	0.88
0.00	7.0	0.58	28.6	0.00	0.28	0.77	0.88
0.00	7.5	0.70	28.6	0.00	0.32	0.85	0.88
0.00	8.1	0.81	28.6	0.00	0.35	0.93	0.92
0.12	8.7	0.81	29.2	0.08	0.35	0.93	0.95
0.12	9.2	0.81	29.7	0.08	0.32	0.93	0.99
0.12	9.8	0.93	29.7	0.08	0.25	1.00	1.03
0.12	10.3	0.93	30.3	0.08	0.21	1.00	1.06
0.12	10.9	1.05	30.8	0.08	0.18	1.08	1.13
0.12	11.4	1.05	31.9	0.08	0.14	1.08	1.20
0.12	12.0	1.05	32.5	0.15	0.14	1.08	1.24
0.23	12.5	1.05	33.0	0.15	0.07	1.16	1.27
0.23	13.1	1.16	33.0	0.15	0.11	1.16	1.34
0.23	13.6	1.16	33.6	0.23	0.14	1.16	1.41
0.23	14.2	1.28	34.1	0.23	0.21	1.16	1.45
0.23	14.8	1.40	34.1	0.31	0.25	1.24	1.52
0.35	15.3	1.51	34.1	0.31	0.28	1.24	1.56
0.35	16.4	1.63	34.1	0.31	0.32	1.24	1.59
0.35	17.0	1.75	34.1	0.39	0.32	1.24	1.63
0.35	17.5	1.75	34.7	0.39	0.35	1.24	1.66
0.35	18.1	1.86	34.7	0.46	0.35	1.31	1.73
0.35	18.6	1.86	35.3	0.46	0.39	1.31	1.80
0.47	18.6	1.86	35.8	0.46	0.42	1.31	1.84
0.35	18.6	1.86	36.9	0.54	0.42	1.39	1.87
0.47	18.6	1.98	36.9	0.54	0.46	1.39	1.94
0.47	19.2	1.98	37.5	0.62	0.49	1.39	1.98
0.35	19.2	2.09	37.5	0.62	0.53	1.39	2.01
0.47	19.7	2.21	37.5	0.62	0.57	1.39	2.05
0.47	20.3	2.33	37.5	0.62	0.60	1.47	2.09
0.47	20.8	2.44	36.9	0.62	0.64	1.47	2.12
0.47	21.4	2.56	36.9	0.62	0.60	1.55	2.12
0.47	22.0	2.68	37.5	0.62	0.64	1.62	2.12
0.47	22.5	2.79	37.5	0.70	0.64	1.70	2.12

TABLE B.31 : GULF GARRINGTON 14-11-36-6W5 (GLAUCONITE FM)

TIME (min)	SURFACE PRESSURE (MPa)	TIME (min)	SURFACE PRESSURE (MPa)	TIME (min)	INJECTION RATE (cu.m /min)	TIME (min)	INJECTION RATE (cu.m /min)
2.91	37.5	7.21	37.5	1.78	2.16	4.17	3.00
3.02	37.5	7.33	37.5	1.78	2.19	4.25	3.00
3.02	36.9	7.45	36.9	1.78	2.23	4.48	3.00
3.14	36.9	7.56	36.9	1.78	2.26	4.72	3.00
3.26	36.9	7.68	36.9	1.78	2.30	4.87	3.00
3.26	37.5	7.79	36.9	1.86	2.30	5.02	3.04
3.37	37.5	7.91	36.9	1.86	2.40	5.26	3.04
3.37	36.9	8.03	36.9	1.86	2.51	5.41	3.04
3.49	36.9	8.14	36.9	1.86	2.55	5.49	3.04
3.61	36.9	8.26	36.9	1.93	2.58	5.57	3.04
3.72	36.9	8.38	36.9	1.93	2.62	5.64	3.04
3.84	36.9	8.49	36.9	1.93	2.69	5.64	3.00
3.96	36.9	8.61	36.9	1.93	2.79	5.88	3.00
4.07	36.9	8.73	36.9	1.93	2.83	6.18	3.00
4.19	36.9	8.84	36.9	2.01	2.86	6.42	2.97
4.30	36.9	8.96	36.9	2.01	2.90	6.49	3.00
4.42	36.9	9.19	36.9	2.01	2.93	6.57	3.00
4.54	36.9	9.31	36.9	2.01	2.97	6.65	3.00
4.65	36.9	9.54	36.9	2.09	2.97	6.80	3.00
4.77	36.9	9.66	36.9	2.09	3.00	7.03	3.00
4.89	36.9	9.77	36.9	2.16	3.00	7.27	2.97
5.00	36.9	9.89	37.5	2.16	3.04	7.34	3.00
5.12	36.9	10.00	37.5	2.16	3.00	7.42	3.00
5.24	36.9	10.12	37.5	2.24	3.00	7.50	3.00
5.35	36.9	10.24	37.5	2.32	3.00	7.58	3.00
5.47	36.9	10.35	36.9	2.40	3.00	7.73	3.00
5.58	36.9	10.47	36.9	2.47	3.00	8.04	3.00
5.70	36.9	10.70	36.9	2.71	3.04	8.35	3.00
5.82	36.9	10.82	36.4	2.86	3.04	8.50	3.00
5.93	36.9	10.94	36.9	2.94	3.08	8.66	3.00
6.05	36.9	11.05	36.9	3.01	3.08	8.89	3.00
6.17	36.9	11.17	36.9	3.01	3.04	9.04	3.00
6.28	36.9	11.28	36.9	3.17	3.04	9.20	3.00
6.28	37.5	11.40	36.9	3.32	3.04	9.28	3.04
6.40	37.5	11.63	36.9	3.40	3.04	9.43	3.04
6.51	37.5	11.75	36.9	3.48	3.08	9.59	3.04
6.51	36.9	11.98	36.9	3.56	3.04	9.74	3.04
6.75	36.9	12.10	36.9	3.79	3.00	9.90	3.04
6.86	36.9	12.33	36.9	3.87	3.00	9.97	3.04
6.98	36.9	12.45	36.9	3.94	3.00	10.05	3.04
7.10	37.5	12.56	36.9	4.10	3.00	10.13	3.04

TABLE B.31 : GULF GARRINGTON 14-11-36-6W5 (GLAUCONITE FM)

TIME (min)	SURFACE PRESSURE (MPa)	TIME (min)	SURFACE PRESSURE (MPa)	TIME (min)	INJECTION RATE (cu.m /min)	TIME (min)	INJECTION RATE (cu.m /min)
12.68	36.9	17.80	40.2	10.20	3.00	14.61	3.15
12.80	36.9	17.92	40.2	10.28	3.00	14.69	3.15
13.03	37.5	18.03	40.2	10.36	3.00	14.69	3.18
13.15	37.5	18.15	40.2	10.44	3.00	14.77	3.22
13.26	37.5	18.38	40.2	10.67	3.00	14.77	3.29
13.38	37.5	18.50	40.2	10.98	3.00	14.84	3.36
13.61	37.5	18.61	40.2	11.13	3.00	14.92	3.43
13.73	37.5	18.73	40.2	11.13	2.97	15.00	3.50
13.84	37.5	19.08	40.8	11.13	3.00	15.00	3.54
13.96	37.5	19.20	40.8	11.21	3.00	15.00	3.57
14.08	38.0	19.31	40.8	11.29	3.00	15.00	3.61
14.19	38.6	19.54	40.8	11.29	2.97	15.00	3.64
14.19	39.1	19.66	40.8	11.36	2.97	15.07	3.71
14.19	39.7	19.78	40.2	11.36	3.00	15.15	3.75
14.31	39.7	20.01	40.2	11.44	3.00	15.23	3.75
14.43	39.7	20.13	40.2	11.60	2.97	15.23	3.78
14.43	40.2	20.24	40.2	11.91	2.97	15.31	3.78
14.54	40.2	20.36	40.2	12.06	2.97	15.38	3.78
14.77	40.2	20.48	40.2	12.29	2.97	15.46	3.82
14.89	40.2	20.71	40.2	12.45	2.97	15.69	3.82
15.01	40.2	20.82	40.2	12.52	2.97	16.00	3.82
15.12	40.2	20.94	40.2	12.60	2.97	16.16	3.82
15.24	40.2	21.06	40.2	12.76	2.97	16.23	3.82
15.36	40.8	21.17	40.2	12.99	2.97	16.31	3.82
15.47	40.8	21.52	40.2	13.06	2.97	16.39	3.82
15.59	40.8	21.64	40.2	13.14	2.97	16.62	3.82
15.71	40.8	21.87	40.2	13.37	2.97	17.01	3.82
15.82	40.8	21.99	40.2	13.53	2.97	17.24	3.82
16.05	40.2	22.10	40.2	13.76	2.97	17.55	3.82
16.29	40.2	22.22	40.2	13.92	2.97	17.63	3.82
16.40	40.2	22.34	40.2	13.99	2.97	17.70	3.82
16.52	40.2	22.45	40.2	14.07	2.97	17.78	3.82
16.64	40.2	22.69	40.2	14.15	2.97	18.01	3.82
16.75	40.2	22.80	40.2	14.22	2.97	18.24	3.85
16.87	40.2	22.92	40.2	14.30	2.97	18.48	3.85
16.99	40.2	23.03	40.2	14.38	2.97	18.79	3.85
17.10	40.2	23.15	40.2	14.46	2.97	18.86	3.85
17.22	40.2	23.27	40.2	14.53	2.97	19.09	3.85
17.33	40.2	23.38	40.2	14.69	3.00	19.33	3.85
17.45	40.2	23.62	40.2	14.69	3.04	19.64	3.85
17.68	40.2	23.73	40.2	14.61	3.08	19.79	3.85

TABLE B.31 : GULF GARRINGTON 14-11-36-6W5 (GLAUCONITE FM)

TIME (min)	SURFACE PRESSURE (MPa)	TIME (min)	SURFACE PRESSURE (MPa)	TIME (min)	INJECTION RATE (cu.m /min)	TIME (min)	INJECTION RATE (cu.m /min)
23.85	40.2	29.20	48.0	19.87	3.85	25.90	3.99
23.97	40.2	29.32	48.0	19.87	3.89	26.05	3.99
24.20	40.2	29.32	47.5	19.94	3.89	26.21	3.99
24.31	40.2	29.32	46.9	20.02	3.89	26.28	3.99
24.55	40.8	29.32	46.3	20.41	3.85	26.28	3.96
24.66	40.2	29.32	45.8	20.64	3.85	26.36	3.96
24.90	40.2	29.32	45.2	20.95	3.85	26.52	3.96
25.01	40.2	29.32	44.7	21.26	3.85	26.59	3.96
25.13	40.2	29.32	44.1	21.49	3.85	26.75	3.96
25.36	40.2	29.32	43.6	21.65	3.85	26.83	3.96
25.48	40.2	29.32	43.0	21.80	3.85	27.06	3.96
25.59	40.2	29.32	42.5	22.03	3.85	27.29	3.96
25.71	40.2	29.43	42.5	22.11	3.85	27.52	3.96
25.71	40.8	29.43	41.9	22.34	3.89	27.60	3.96
25.94	40.8	29.55	41.9	22.57	3.89	27.68	3.96
26.06	40.2	29.55	41.4	22.73	3.89	27.68	3.99
26.29	40.2	29.55	40.8	22.81	3.85	27.83	3.99
26.41	40.2	29.55	40.2	22.88	3.85	27.98	3.99
26.52	40.2	29.67	39.7	23.04	3.85	28.06	3.99
26.64	40.2	29.67	39.1	23.19	3.85	28.22	3.99
26.76	40.2	29.55	39.1	23.35	3.85	28.37	3.99
26.99	40.8	29.55	38.6	23.35	3.82	28.45	3.99
27.22	40.8	29.55	38.0	23.42	3.82	28.60	3.96
27.34	40.8	29.55	37.5	23.42	3.85	28.76	3.92
27.34	41.4	29.55	36.9	23.50	3.85	28.84	3.92
27.46	41.4	29.55	36.4	23.50	3.89	28.91	3.92
27.57	41.9	29.67	35.8	23.50	3.92	29.14	3.89
27.69	42.5	29.67	35.3	23.50	3.96	29.22	3.85
27.80	43.0	29.67	34.7	23.58	3.96	29.30	3.85
27.92	43.0	29.55	34.7	23.66	3.96	29.38	3.85
28.04	43.6	29.55	34.1	23.89	3.96	29.45	3.82
28.15	44.1	29.55	33.6	23.96	3.96	29.53	3.78
28.27	44.7	29.55	33.0	24.20	3.96	29.61	3.78
28.39	45.2	29.55	32.5	24.43	3.99	29.69	3.78
28.50	45.8	29.55	31.9	24.58	3.99	29.76	3.71
28.62	45.8	29.55	31.4	24.82	3.99	29.84	3.71
28.74	46.3	29.55	30.8	25.05	3.99	29.92	3.71
28.74	46.9	29.55	30.3	25.28	3.99	29.99	3.68
28.97	46.9	29.67	29.7	25.43	4.03	30.07	3.68
28.97	47.5	29.67	29.2	25.51	4.03	30.07	3.64
29.08	47.5	29.67	29.7	25.74	3.99	30.15	3.64

TABLE B.31 : GULF GARRINGTON 14-11-36-6W5 (GLAUCONITE FM)

TIME (min)	SURFACE PRESSURE (MPa)	TIME (min)	SURFACE PRESSURE (MPa)	TIME (min)	INJECTION RATE (cu.m /min)	TIME (min)	INJECTION RATE (cu.m /min)
29.67	30.3	34.32	24.7	30.23	3.64	30.77	1.70
29.67	30.8	34.55	24.7	30.30	3.64	30.77	1.63
29.67	30.3	34.78	24.7	30.30	3.61	30.77	1.56
29.78	30.3	34.90	24.7	30.38	3.61	30.77	1.48
29.90	29.7	35.02	24.7	30.38	3.57	30.77	1.45
29.90	29.2	35.13	24.7	30.38	3.54	30.77	1.41
30.01	28.6	35.37	24.7	30.38	3.50	30.77	1.34
30.01	28.1	35.48	24.7	30.38	3.46	30.85	1.24
30.13	28.1	35.60	24.7	30.46	3.43	30.85	1.17
30.25	28.1	35.72	24.7	30.46	3.36	30.85	1.10
30.36	28.1	35.83	24.7	30.54	3.36	30.85	1.06
30.48	28.1	36.06	24.7	30.54	3.29	30.85	0.99
30.60	28.1	36.30	24.7	30.61	3.22	30.77	0.92
30.71	28.1	36.41	24.2	30.61	3.15	30.77	0.85
30.71	27.5	36.65	24.2	30.61	3.08	30.85	0.74
30.83	27.5	36.76	24.2	30.61	3.00	30.85	0.64
30.95	27.5	36.88	24.2	30.61	2.97	30.85	0.53
31.06	26.9	37.00	24.2	30.61	2.93	30.85	0.46
31.18	26.9	37.11	24.2	30.61	2.90	30.85	0.39
31.41	26.4	37.34	24.2	30.61	2.83	30.85	0.32
31.53	26.4	37.58	24.2	30.61	2.79	30.85	0.28
31.64	26.4	37.69	24.2	30.61	2.76	30.92	0.25
31.76	26.4	37.81	24.2	30.61	2.72	30.92	0.21
31.88	26.4	38.04	24.2	30.61	2.65	30.92	0.14
31.99	26.4	38.16	24.2	30.69	2.58	30.92	0.07
32.23	26.4	38.39	24.2	30.69	2.55	30.92	0.04
32.23	25.8	38.62	24.2	30.69	2.51	30.92	0.00
32.34	25.8	38.74	24.2	30.69	2.44	30.92	0.04
32.46	25.8	38.86	24.2	30.69	2.40	31.00	0.04
32.57	25.8	38.97	24.2	30.69	2.37	30.92	0.00
32.69	25.8	39.21	24.2	30.69	2.33		
32.81	25.8	39.44	24.2	30.77	2.30		
32.92	25.8	39.55	24.2	30.77	2.26		
33.04	25.8	39.67	24.2	30.77	2.23		
33.16	25.3	39.90	24.2	30.77	2.19		
33.39	25.3	40.25	24.2	30.77	2.16		
33.50	25.3	40.37	24.2	30.77	2.09		
33.62	25.3	40.60	24.2	30.77	1.98		
33.74	25.3	40.72	24.2	30.77	1.94		
33.97	25.3	40.83	24.2	30.77	1.87		
34.09	25.3	41.18	24.2	30.77	1.80		

TABLE B.31 : GULF GARRINGTON 14-11-36-6W5 (GLAUCONITE FM)

TIME (min)	SURFACE PRESSURE (MPa)	TIME (min)	SURFACE PRESSURE (MPa)	TIME (min)	INJECTION RATE (cu.m /min)	TIME (min)	INJECTION RATE (cu.m /min)
41.30	24.2	47.00	20.3				
41.42	24.2	47.00	19.7				
41.53	24.2	47.00	19.2				
41.76	24.2	47.00	18.6				
41.88	24.2	47.00	18.1				
42.00	24.2	47.00	17.5				
42.11	23.6	47.00	17.0				
42.23	23.6	47.00	16.4				
42.35	23.6	47.12	16.4				
42.46	23.6	47.12	15.9				
42.58	23.6	47.23	15.3				
42.81	23.6	47.23	14.8				
43.04	23.6	47.23	14.2				
43.16	23.6	47.23	13.6				
43.28	23.6	47.23	13.1				
43.39	23.6	47.23	12.5				
43.51	23.6	47.23	12.0				
43.74	23.1	47.23	11.4				
43.98	23.1	47.23	10.9				
44.21	23.1	47.23	10.3				
44.44	23.1	47.23	9.8				
44.56	23.1	47.23	9.2				
44.67	23.1	47.23	8.7				
44.91	23.1	47.23	8.1				
45.02	23.1	47.23	7.5				
45.14	23.1	47.23	7.0				
45.37	23.1	47.23	6.4				
45.60	23.1	47.23	5.9				
45.72	23.1	47.23	5.3				
45.84	23.1	47.12	4.8				
46.07	23.1	47.12	4.2				
46.42	23.1	47.23	4.2				
46.65	22.5	47.23	3.7				
46.77	22.5	47.23	3.1				
46.88	22.5	47.23	2.6				
47.00	22.5	47.12	2.6				
47.12	22.5	47.12	3.1				
47.12	22.0	0.00	2.0				
47.12	21.4						
47.12	20.8						
47.00	20.8						

BREAKOUT ANALYSIS EXERCISE - STRESS DIRECTIONS.

Purpose

To obtain in-situ stress orientations of the principal horizontal stresses at the well location by interpreting a four arm dipmeter log. The logged section traverses Devonian carbonates in the West Pembina area of Alberta.

Method

1. Check the caliper record for differential extension. Note the zones where this occurs and label them with the caliper set that is recording the largest diameter. Is it 1 - 3 or 2 - 4?
2. Check the Caliper 1 azimuth orientation record to determine the intervals over which tool rotation has ceased. The azimuth for Caliper 1 is recorded by the solid line.
3. Identify breakout intervals from the Caliper No 1 azimuth log as those intervals where no tool rotation is occurring which, more or less, coincide with the assymetrically elongated intervals on the caliper log.
4. For each breakout, measure the orientation of Caliper 1 using the scale provided. Make measurements at intervals (say every 10 ft or 5 m) over each breakout. Average the orientation data.
5. Add the magnetic declination (25° E, given on the log header) to the average orientation and this will give the direction in which Caliper 1 was pointing when the tool "locked into" the breakout.
6. Report the breakout long axis in the 90° -180° quadrant. If the 1 - 3 caliper records the long axis of the breakout, you may need to subtract 180° . If the 2 - 4 caliper records the long axis of the breakout, you may need to add or subtract 90° .

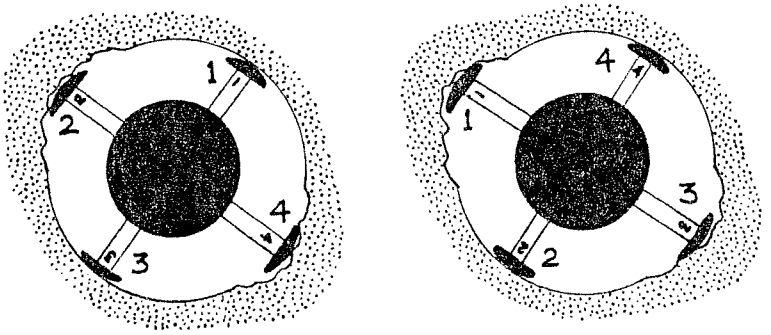

Left Margi

0
4
8
1
1
2
2
2
3
3

Application

Applying this method to all the breakouts and averaging their azimuths gives the mean breakout azimuth for a well. This is interpreted as SHmin, perpendicular to the direction that induced hydraulic fractures will follow.

Locations of the five wells used in the Dipmeter Analysis Exercise. The numbers refer to individual sections of the logs that are examined. For example, Well 1 (1-9-50-12W5) has four intervals (1 - 4) that are analysed.

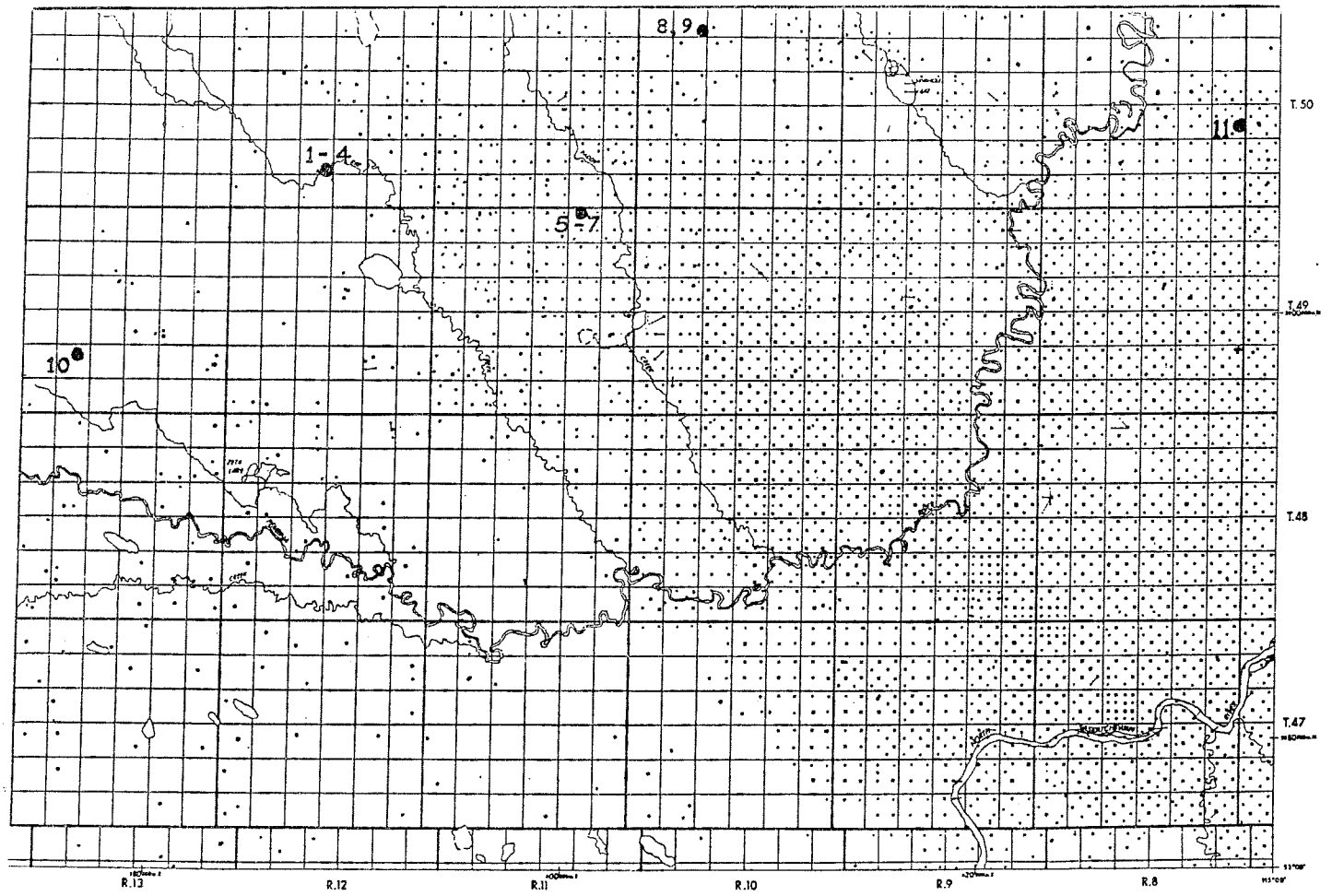

95

Bit size:
152 mm

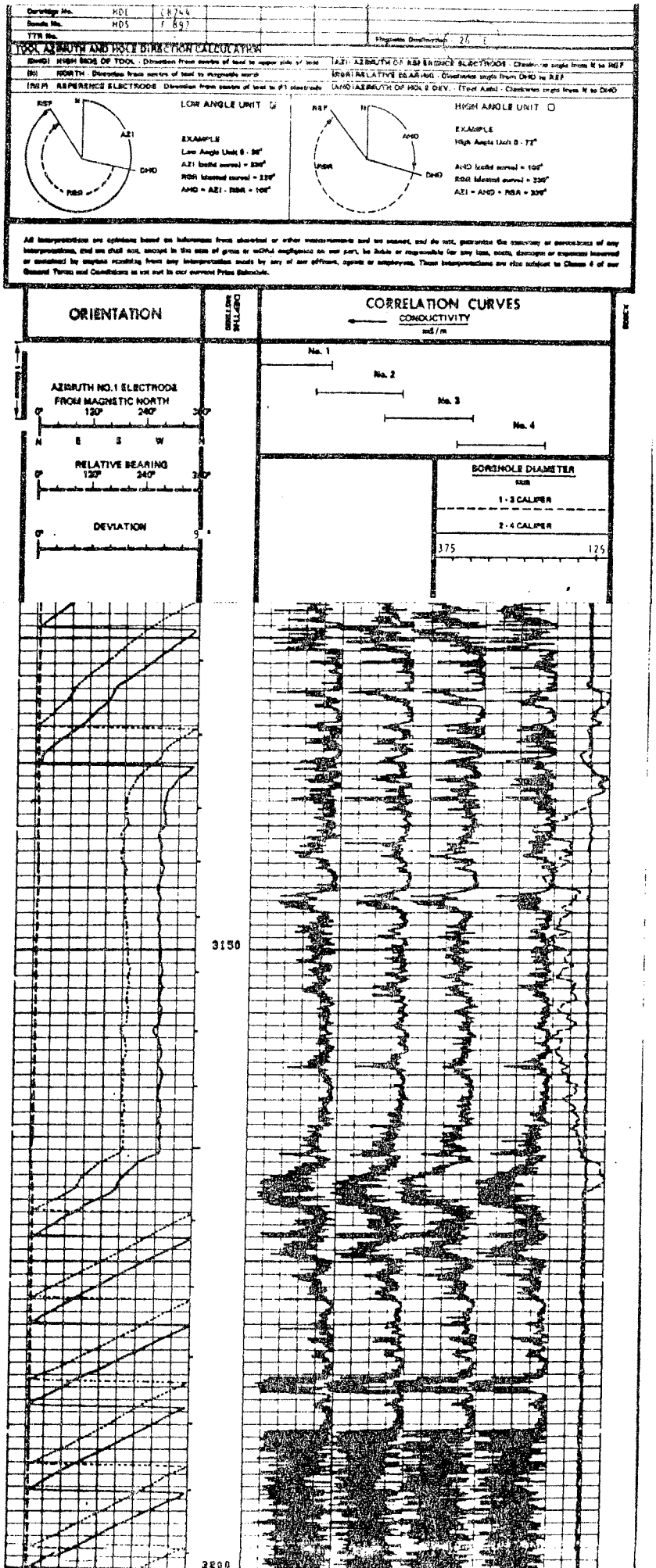

Bit size:
222 mm